Solar Power and Chemical Energy Systems
IEA Technology Collaboration Programme

Documentation of Meteorological Data Sets

delivered together with the
SolarPACES Guideline for Bankable STE Yield Assessment

January, 2017

Edited by Richard Meyer & Marko Schwandt

Intentionally left blank

Acknowledgments

The data sets provided by Suntrace GmbH are co-funded by the BMWi project CSP Bankability (No. 0325293). The data is based on the satellite-derived radiation product Solemi from DLR e.V. and on-site measurements from:

- DLR e.V. high precision meteorological station at the Plataforma Solar de Almería in Spain (Dr. Stefan Wilbert)
- station number 42 (TAM) of the BSRN network
  Mimouni, Mohamed (2016): Basic measurements of radiation at station Tamanrasset (2001-01 to 2015-06), reference list of 174 datasets. National Meteorological Office of Algeria. doi:10.1594/PANGAEA.859963
- station number 41 (SOV) of the BSRN network
  Al-Abbadi, Naif (2016): Basic measurements of radiation at station Solar Village (1998-09 to 2002-12), reference list of 52 datasets. King Abdulaziz City for Science and Technology. doi:10.1594/PANGAEA.860279
- station number 40 (DAA) of the BSRN network
  Esterhuyse, Danie (2008): Basic measurements of radiation at station De Aar (2000-06 to 2000-12 and 2001-07 to 2004-12), reference list of 48 datasets. South African Weather Service, Pretoria. doi:10.1594/PANGAEA.860278

Disclaimer

This report and relate data sets are free to use for scientific purposes. If referring to the report it should be cited as

> Meyer & Schwandt (2017): *Documentation of Meteorological Data Sets* delivered together with the *SolarPACES Guideline for Bankable STE Yield Assessment*, Version 2017, www.solarpaces.org/yield-analysis-guideline

If applying the related data set (or parts of it). always this report shall be cited as above and the respective BSRN-data sources as cited in Chapter 2.1.2. In the acknowledgments the following text shall always be given:

> "Data set provided by Suntrace GmbH co-funded by the BMWi project CSPBankability (No. 0325293). The data is based on the satellite-derived radiation product Solemi from DLR e.V. and on measurements from MEASUREMENTDATASUPPLIER"

where MEASUREMENTDATASUPPLIER shall be one or several of the station-specific texts as defined above in Chapter Acknowledgements.

This project has been funded by the German Federal Ministry Economic Affairs and Energy under contract No. 0325293.

Gefördert durch:
Bundesministerium für Wirtschaft und Energie
aufgrund eines Beschlusses des Deutschen Bundestages

Table of contents

Abbreviations

Name	Description
AOD	Aerosol Optical Depth
CSP	Concentrating Solar Power
DHI	Diffuse Horizontal Irradiance
DLR	Deutsches Zentrum für Luft- und Raumfahrt (German Aerospace Center)
DNI	Direct Normal Irradiance
DZTAM	Example site Tamanrasset, Algeria
ESPSA	Example site Plata Forma Solar de Almería, Spain
GHI	Global Horizontal Irradiance
IEC	International Electrotechnical Commission
MERRA-2	Modern-Era Retrospective analysis for Research and Applications version 2
MFG	Meteosat First Generation
MSG	Meteosat Second Generation
MY	Meteorological Year
NREL	National Renewable Energy Laboratory, USA
SASVO	Example site Solar Village, Saudi Arabia
SOLEMI	Solar Energy Mining
TMY	Typical Meteorological Year
WGS84	World Geodetic System 1984 reference
ZADAA	Example site De Aar, South Africa

1. Introduction

Most important to reach good estimates on electricity yields of a CSP plant is the knowledge on Direct Normal Irradiance (DNI) conditions, as this component of solar irradiance is the one which can be concentrated by mirrors. In the frame of the elaboration of the 'guideline for standardized yields analysis of solar thermal power plants' (guiSmo) and the BMWi founded project CSP Bankability, the irradiance conditions for four considered demo sites are analysed. Based on the results various Typical Meteorological Year (TMY) and Meteorological Year (MY) data sets in different time resolutions are created. These datasets serve as input of the solar radiation and meteorological conditions for the yield simulations performed during the elaboration of the guideline for standardized yields analysis of solar thermal power plants.

The four demo sites are:

Site 1) **ESPSA**: Plataforma Solar de Almería (PSA), located around 30km in North of Almería, Spain

Site 2) **DZTAM:** Tamanrasset, located in Tamanrasset, Algeria

Site 3) **SASO**V: Solar Village, located around 40km in the North West from the centre of, Riyadh, Saudi Arabia

Site 4) **ZADAA:** De Aar, located In the South East outside De Aar, South Africa

The geographical coordinates of the sites, for which this assessment is conducted, are given in Table 1-1. All coordinates are given according to WGS84 geodetic system. In the following the sites will be referred to by the assigned site codes **ESPSA**, **DZTAM**, **SASOV** and **ZADAA**. The locations of the sites are shown in Figure 1-1.

This document describes the content and creation of Typical Meteorological Year (TMY) and Meteorological Year (MY) data sets for each of the four demo sites created and submitted by Suntrace GmbH. The results for the sites, which include the long-term characteristics of solar irradiance conditions along with the data sources used, are described in the report. As these TMYs and MYs are optimized for solar thermal Concentrating Solar Power (CSP) applications it mainly focuses on the available Direct Normal Irradiance (DNI), which is closely related to CSP power plant energy yield. The analysis is based on ground-based data sources. The TMY that has been created is suitable for energy yield calculation.

Demo site No	Site code	Site name	Country	Latitude [°N]	Longitude [°E]	Elevation [m]
1	ESPSA	PSA	Spain	37.0909	-2.3581	492
2	DZTAM	Tamanrasset	Algeria	22.7903	5.5292	1385
3	SASOV	Solar Village	Saudi Arabia	24.9100	46.4100	650
4	ZADAA	De Aar	South Africa	-30.6667	23.9930	1287

Table 1-1: Overview of the four demo sites including coordinates

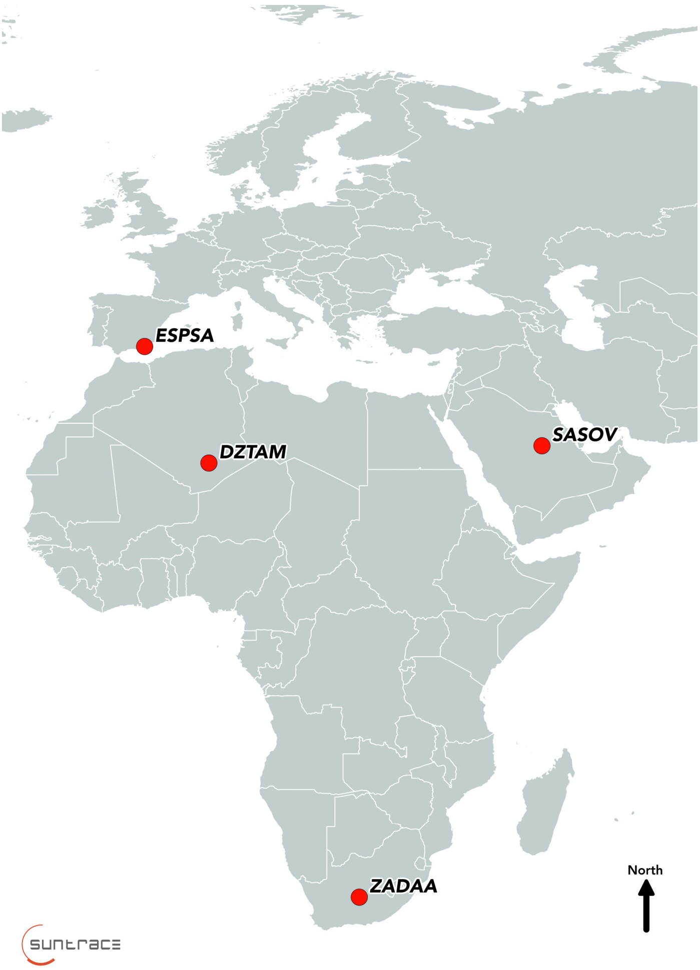

Figure 1-1: Map showing the location of the four demo sites ESPSA, DZTAM, SASOV and ZADAA.

The long-term average of DNI for the demo sites shall be derived from a combination of local measurements with site-specific long-term time series based on satellite data. Therefor, the long-term satellite time series are adjusted by the on-site measurements.

For CSP performance simulations a representative annual data set in 10-minute, 15-minute, 30-minute and hourly time resolution (Typical Meteorological Year-TMY) shall be given. The average of this TMY shall closely meet the long-term average DNI. To derive these values an analysis of uncertainties has to be undertaken. This shall take into account the accuracy of the underlying data sets, the period of record and also the inter-annual variability of DNI.

The annual 10-minute, 15-minute, 30-minute and hourly data sets shall be accompanied by auxiliary meteorological data, which are also required for executing realistic performance calculations of CSP plants. For parabolic trough (PT) plants, which is the considered technology of “guiSmo” and of the BMWi founded project “CSP Bankability”, temperature and humidity of ambient air and wind speed and direction are recommended with these datasets. For risk assessment of the solar power project, Meteorological Years representing P75, P90 and P95 value of DNI with respect to multiple and single year uncertainty are also provided as part of this assessment. Additional data sets in higher time resolution (1min or 5min) and representing any PXY (e.g. P70 or P99) are not requested for the project at that time and hence are not delivered, but could also be created without difficulty.

This report first assesses the available input data sets. The methodology followed to derive long-term average of DNI and the corresponding uncertainty is explained in brief. The following chapter then reports the main results including long-term average of DNI and analysis of corresponding uncertainty, properties of DNI and ambient air conditions at the sites. Besides main findings the conclusion gives advice on how to further improve these results.

2. Description of the available input data sets

For all four demo sites several independent DNI data sets are available. In this study the following data sets are considered

- For deriving the long–term DNI averages: on-site measurements covering periods with different lengths as well as satellite-derived data from the DLR-SOLEMI data set of the German Aerospace Center (DLR).
- For creating the TMY and MY data sets: on-site measurements and for the cases when important measurands (like wind speed, barometric pressure, etc.) are not available these measurands are obtained by synthetically generated data sets from MERRA2.

To compare the results of the long–term DNI averages with a third independent data set, satellite derived DNI data from DLR-ISIS are used. However, the uncertainty of this data set is considered with around 15% as too high and is therefore not considered for determining the long-term DNI average.

2.1. On-site measurements

2.1.1. ESPSA

The German Aerospace Center (DLR) is operating a high precision meteorological measurement station at the Plataforma Solar de Almería in Spain. This is equipped with a first class thermopile pyrheliometer mounted on a 2-axis automatic sun tracker, which measures Direct Normal Irradiance (DNI). A secondary standard thermopile pyranometer (ISO 9060, 1990) measures Global Horizontal Irradiance (GHI) and a shaded thermopile pyranometer (ISO 9060, 1990) measures Diffuse Horizontal Irradiance (DHI). In addition, the station also measures air temperature, humidity, pressure, wind speed and direction. All data streams are logged in 1-minute time resolution. This station is running properly, is very well maintained and the data obtained is without major errors. Measurements are of similar intensity when compared to other measurements in the region. Maxima of DNI in each measured month seems realistic.

2.1.2. BSRN stations DZTAM, SASOV and ZADAA

For three stations, all members of the BSRN network, data have been provided for this study. These stations are also equipped with a first class thermopile pyrheliometer mounted on a 2-axis automatic sun tracker measuring DNI and two secondary standard thermopile pyranometer (ISO 9060, 1990) measuring GHI and DHI. In addition (except DZTAM) the stations also measure various auxiliary measurements of the ambient conditions like air temperature, humidity and pressure. Table 3-1 gives an overview of the on-site measurements available for each site. All data streams are logged in 1-minute time resolution. Since these three stations are members of the BSRN network it is assumed that they are running properly and are well maintained. For these stations the measurements show a similar intensity when compared to other measurements in the region. Maxima of DNI in each measured month seems realistic.

In the following more detailed information with DOI by PANGEA of the available data for these three stations is given, see also Figure 2-1, Figure 2-2 and Figure 2-3.

<u>DZTAM</u>

web page: https://doi.pangaea.de/10.1594/PANGAEA.859963

citation: Mimouni, Mohamed (2016): Basic measurements of radiation at station Tamanrasset (2001-01 to 2015-06), reference list of 174 datasets. National Meteorological Office of Algeria. doi:10.1594/PANGAEA.859963.

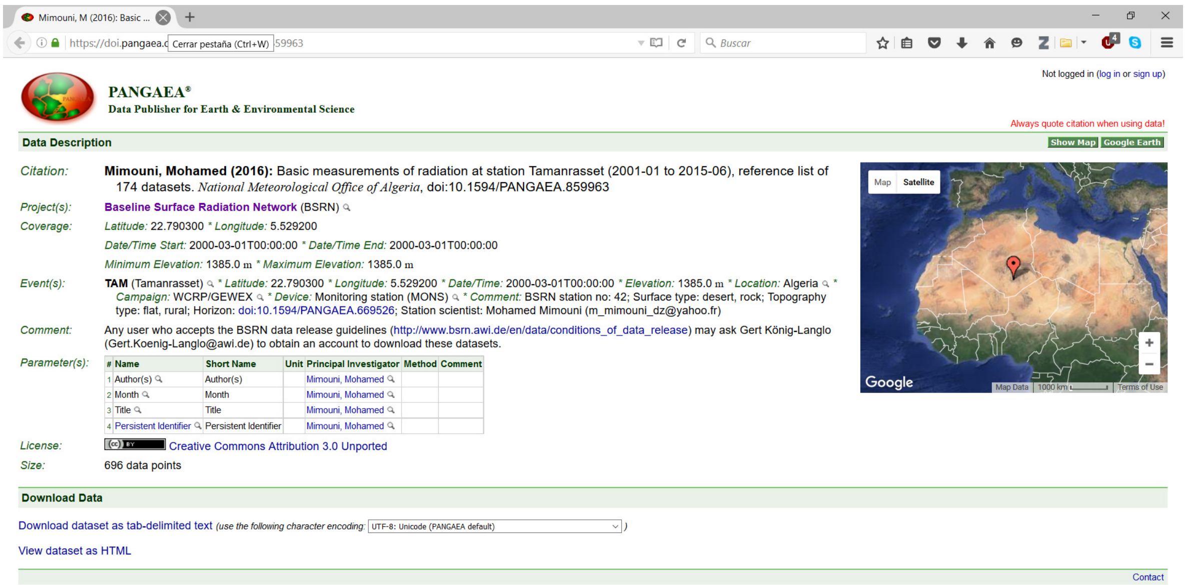

Figure 2-1: Screenshot of Pangaea web page for DZTAM with detailed information about used data.

<u>SASOV</u>

web page: https://doi.pangaea.de/10.1594/PANGAEA.860279

citation: Al-Abbadi, Naif (2016): Basic measurements of radiation at station Solar Village (1998-09 to 2002-12), reference list of 52 datasets. King Abdulaziz City for Science and Technology. doi:10.1594/PANGAEA.860279.

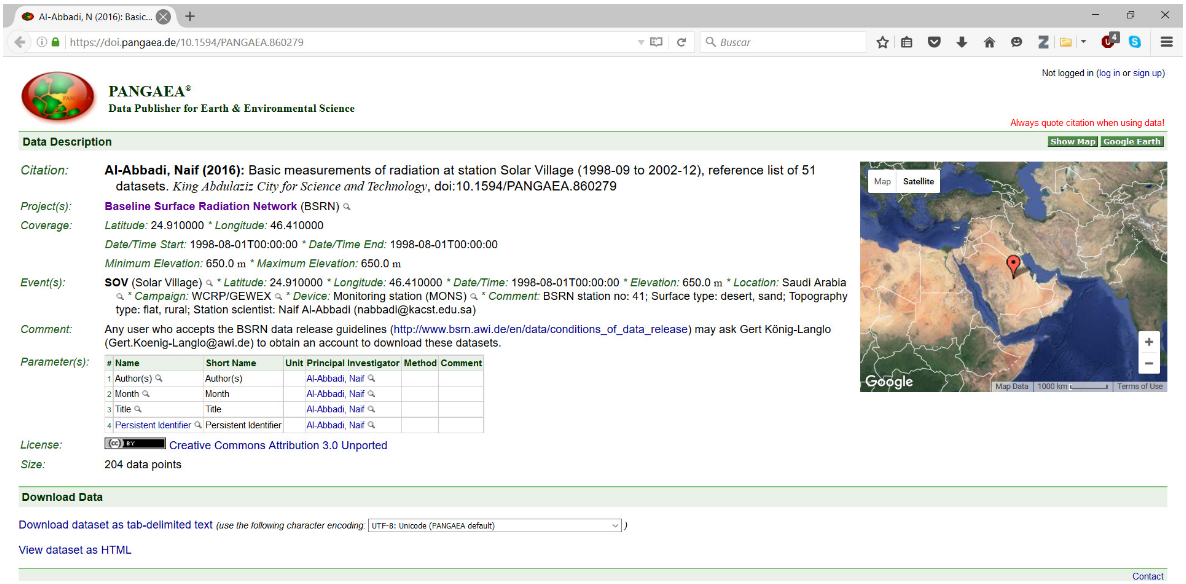

Figure 2-2: Screenshot of Pangaea web page for SASOV with detailed information about used data.

<u>ZADAA</u>

web page: https://doi.pangaea.de/10.1594/PANGAEA.860278

citation: Esterhuyse, Danie (2016): Basic measurements of radiation at station De Aar (2000-06 to 2000-12 and 2001-07 to 2004-12), reference list of 51 datasets. South African Weather Service, Pretoria. doi:10.1594/PANGAEA.860278.

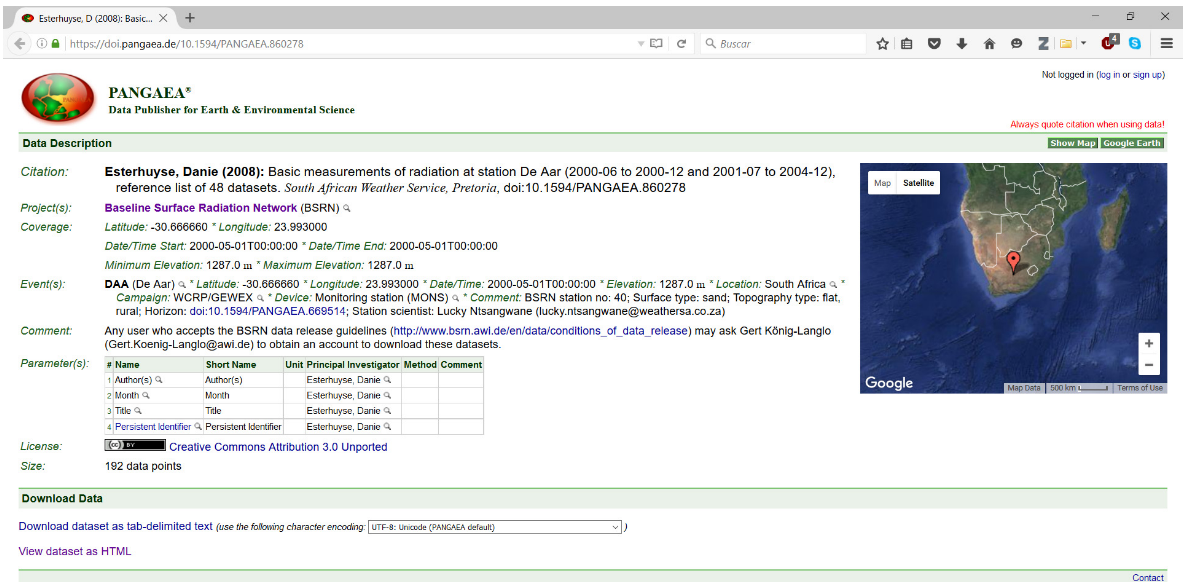

Figure 2-3: Screenshot of Pangaea web page for ZADAA with detailed information about used data.

2.2. DLR-SOLEMI satellite derived data sets

Solar Energy Mining (SOLEMI) is a service providing irradiance data set up by DLR. The service is mainly based on METEOSAT-data with a nominal resolution of 2.5 km in the visible channel and 5 km in the infrared channel and half-hourly temporal resolution using data from both Meteosat positions at 0° and 63°East. From dates of 2004 onwards the service uses also Meteosat Second Generation imagery with a nominal spatial resolution of 1 km (in the high resolution visible channel) and 15 minutes time resolution.

The transfer of the extra-terrestrial solar irradiance to the Earth's surface is influenced by various constituents of the atmosphere. Ozone, aerosol and water vapour are modelled with long time climatological and reanalysis data sets. Clouds which have the largest influence and highest variability are determined from the half hourly Meteosat images. Both visible and infrared channels are used to improve the detection at sunrise and sunset and of high cirrus clouds.

The method applied to retrieve solar irradiance data is based on method of Schillings et al. (2004a) with improvements from the Heliosat-method similar as described by Betcke et al. (2006) . The basic idea of the method is a two-step approach. In the first step, a relative normalised cloud reflectivity - the cloud index - is derived from Meteosat data. The derived cloud index is correlated to the clear-sky index k, which relates the actual ground irradiance G to the irradiance of the cloud-free case G_{clearsky}. Consequently, in addition to the cloud index derived from the satellite signal, a clear-sky model, providing G_{clearsky}, is necessary for the estimation of the actual ground irradiance. This clear sky model includes knowledge on the sun geometry and atmospheric turbidity to describe aerosol and water extinction. The n-k relation is powerful, validated, and leads to small root mean square deviations (RMSD) between measured and calculated solar irradiance for almost homogenous cloud situations. The RMSD for hourly global irradiance values is typically in the order of 13-15%, while for DNI it rather is in the order of 40 % (Schillings et al., 2004b).

The ENVISOLAR science review (A. Zelenka, 2004) states, that the RMSD observed is mainly due to misfit between ground measurement (point) and satellite measurement (pixel average). For DNI the random contributions caused by this 'parallax error' are much more pronounced as the virtual location of the clouds in satellite images differs from the position of the cloud shadows. For GHI due to the smoothing behaviour of the diffuse radiation component this jitter is much less intense and thus RSMD on hourly base substantially lower.

2.3. MERRA-2

The Modern-Era Retrospective analysis for Research and Applications version 2 (MERRA-2) is a NASA atmospheric reanalysis for the satellite era using the Goddard Earth Observing System Model, Version 5 (GEOS-5) with its Atmospheric Data Assimilation System (ADAS), version 5.12.4. The MERRA project focuses on historical climate analyses for a broad range of weather and climate time scales and places the NASA EOS suite of observations in a climate context.

MERRA-2 was initiated as an intermediate project between the aging MERRA data and the next generation of Earth system analysis envisioned for the future coupled reanalysis. Without a substantial investment to update MERRA's data assimilation routines, the system lacked the capability to analyse the latest observations. In addition, numerous advances to the GEOS5 system had been implemented since freezing the MERRA system in 2008. Therefore, a new full reanalysis integration was undertaken. MERRA-2 covers the period 1980 to present.

3. Methodology for generation

In the following it is briefly described how the site-specific satellite data from DLR-SOLEMI are adjusted by the on-site measured data at the four project sites and how the long-term average is calculated in this assessment. Further it explains how the site-specific TMY is created in this case based on the available data.

3.1. QC of on-site measurement data

For the four demo sites on-site measurements of GHI, DNI and DHI as well as various auxiliary measurements are available in 1 minute time resolution covering different time periods. These measurements are from DLR for ESPSA and from the BSRN network for DZTAM, SASOV and ZADAA. Table 3-1 gives an overview of the available on-site measurements. At all four sites DNI is measured with a first class Pyrheliometer and GHI & DHI are measured with two secondary standard Pyranometer.

Site code	GHI, DNI, DHI	Air temp.	Rel. Humidity	Barom. pressure	Wind speed	Wind direction	period	source
ESPSA	●	●	●	●	●	●	2002-06-26 to 2011-04-30	DLR
DZTAM	●	○	○	○	○	○	2000-03-01 to 2015-06-30	BSRN
SASOV	●	●	●	○	○	○	1998-09-11 to 2002-12-31	BSRN
ZADAA	●	●	●	●	○	○	2001-07-01 to 31-12-2004	BSRN

●: available ○: not available

Table 3-1: Overview available on-site measurements for the four demo sites.

To check the quality of data, various quality control tests are applied to the on-site measurement data. These tests check the plausibility of the data following best practices like those recommended by BSRN (Long and Dutton, 2002 and Long and Shi, 2008) and NREL-SERI QC (NREL 1993). For this study only data that have passed QC test are used. In addition the quality-controlled data have been visually checked.

3.2. Analysis of satellite-derived data

Long-term satellite-derived time series obtained from DLR-SOLEMI from 1st January 1991 up to 31st December 2013 (ESPSA, DZTAM, SASOV) or up to 31st December 2009 (ZADAA) in hourly time resolution are available. These datasets have been checked for completeness, accuracy and plausibility. Various statistical characteristics of the data are analysed like long-term annual average, yearly averages, inter-annual variability, monthly averages over every single year, long-term monthly averages and frequency distribution. This analysis is done to better understand the characteristics and occurrence of solar radiation at the particular sites under consideration.

Due to the volcanic eruption of Mount Pinatubo in 1991 causing high stratospheric disturbance (largest since Krakatoa eruption in 1883) up to 1993, the years from 1991 to 1993 are discarded for determining the long-term average of DNI. Hence, only DLR-SOLEMI from 1st January 1994 up to 31st December 2013 (ESPSA, DZTAM, SASOV) or up to 31st December 2009 (ZADAA) are used for this study for the four demo sites.

3.3. Comparison of satellite-derived data with on-site measurement data

The DNI on-site measured data is compared for each station with parallel period of satellite-derived DNI data obtained from DLR-SOLEMI. In the following only data pairs are inter-compared when both measured and satellite data are available and have passed QC. The inter-comparison is done with respect to various parameters like average, minimum, maximum, standard deviation, frequency distribution, monthly averages and values under different solar radiation conditions like clear-sky and cloudy-sky situations, different seasons of the year etc.

3.4. Site-specific Adjustment of satellite-derived DNI data

Following the approach of (Mieslinger et al. 2014), the satellite-derived DNI values of DLR-SOLEMI at the four demo sites are adjusted by the more accurate on-site measured values. The DNI values measured by ground-based solar radiation measurement stations are taken as the reference in this procedure. The main aim of Mieslinger-method is to reduce the mean bias of satellite data with respect to the measured data and to improve the frequency distribution of satellite data. The frequency distribution of measured data is taken as reference, with respect to which the frequency distribution of satellite data is characterized and adjusted. In this manner the satellite data is adjusted to the reference data in terms of the irradiation distribution and its annual mean.

(Mieslinger et al. 2014) method makes use of a regression analysis in which a regression model is fitted to the correlation of the time-series of ground-measured and satellite-derived datasets. A 3rd degree polynomial is used in the regression model.

$$y(x) = p_1x^3 + p_2x^2 + p_3x + p_4$$

Two conditions are used in this regression model: a) the intercept *p4* should be zero because when ground-measured values are zero (at night), the satellite-derived values should also be zero and b) the modified time series shall be free of bias or at least be within the average level of uncertainty of the measurements. Hence, the degrees of freedom of this function are reduced to 2 (by writing p1 in terms of p2 and p3). Finally, a cost function that respects these 2 conditions is optimized in order to determine the values of the coefficients of the regression model *p2* and *p3*.

After the adjustment of the satellite-derived data, the mean of DNI for the overlapping period should be equal to the mean of the on-site measured DNI during overlapping period. Moreover, there is the additional condition that the maximum of the top 5 percentile adjusted satellite-derived DNI must also be equal to the maximum of the top 5 percentile ground-measured DNI during overlapping period.

This method is applied to the data at the test sites for the individual overlapping period between measured solar radiation stations and DLR-SOLEMI. After applying this correction to the satellite data, the statistical characteristics such as minimum, maximum, standard deviation, etc. of adjusted DLR-SOLEMI data is checked and compared with that of on-site measurement data. It is found that applying this process, the adjusted DLR-SOLEMI data gives more realistic results compared to the original dataset. The results are very promising and fulfil the aim of giving the more precise characteristic of the on-site measurement data to the satellite-derived data. This method is applied to the whole DLR-SOLEMI time series from January 1994 up to December 2013 (2009 for ZADAA).

3.5. Analysis of the long-term average of DNI

The long-term average of DNI from DLR-SOLEMI datasets is determined from the time-series covering 20 years (16 years for ZADAA), which are then adjusted using the ground-based measurements. Frequency distribution of DNI is also a factor that indirectly determines the long-term average of DNI.

During the overlapping period the bias of DLR-SOLEMI datasets with respect to the on-site measurement data is quite different for the four sites and hence the resulting corrections applied to the long-term datasets are also different for each site. Also the inter-annual variability and the frequency distribution of satellite derived DNI at the four sites are quite different compared to the DNI of the ground-based measurements.

3.6. Determination of long term best estimate of DNI

To determine the long-term best estimate of Direct Norma Irradiance (DNI) the recommendations from the International Electrotechnical Commission (IEC) documented in (IEC TC117 2016, 62862-1-2): '*Solar thermal electric plants - Part 1-2: Creation of annual solar radiation data set for solar thermal electric plant simulation'* are followed. This are in particular for this assessment of the four demo sites the in chapter 5.2.1 in (IEC TC117 2016, 62862-1-2) given recommendations for determining the long term best estimate based on a single data solar radiation data source for an overall period of ten or more years.

The representative long-term best estimate of DNI for each month is calculated by the sum of the daily values of the adjusted satellite data for the specific month of all available years. Following the Sandia National Laboratories Method [4], a weighted mean (WM) is evaluated using the Finkelstein-Schafer statistic (FS) for each month available in the data source. This statistic considers the distance between the distribution functions (CDF or cumulative density function) of the daily data for DNI in a specific month and the CDF for daily data in that month in all the years available.

$$FS_{jk} = \sum_{r=1}^{n_r} \left| FDA_j(r) - FDA_{jk}(r) \right|$$

where:

r:	values of each of the ranges (abscissas) the daily values are distributed in, where the distribution function is evaluated
nr:	number of ranges (abscissas) in the distribution functions
$FDA_{jk}(r)$:	value of the distribution function of the daily data evaluated in range ***r***, in the daily data sample in month ***j*** and year ***k***
$FDA_j(r)$:	value of the distribution function of the daily data evaluated in range ***r***, in the daily data sample in month ***j*** of all the years

The specific month for determining the representative long-term best estimate is selected according to the following procedure. First, the 5 months with lower FS statistic value are chosen. Second, from these 5 months, the one with the most similar monthly mean value compared to the whole data set monthly mean for the specific month (e.g. January) is chosen.

3.7. Analysis of the uncertainty of long-term DNI

The goal of the uncertainty analysis is to determine the uncertainty of the best estimate of DNI, which is in most cases the dominating source of uncertainty for calculating potential yields. This overall uncertainty of the long-term average depends on the one side on methodological shortcomings like uncertainty of measurements, satellite data and of the adjustment methodology. On the other side the uncertainty is also caused by the inter-annual variability and the limited number of years taken into account to derive the long-term average.

The uncertainty of the measured data depends on

a) the uncertainty of the instrument measuring DNI,

b) the uncertainty related to the calibration and maintenance of the instrument measuring DNI

c) the uncertainty due to temporal coverage taking into account the inter-annual variability and the limited number of years for calculating the long-term average.

These three uncertainties together give the total measurement uncertainty.

The Adjustment methodology of (Mieslinger et al. 2014) eliminates the bias of satellite-derived irradiance data against measured values during the overlap period. As it can be assumed that the systematic deviations of the satellite data are similar during earlier or later times, applying this method to long-term satellite-derived data strongly reduces the systematic error of the satellite-derived data. However, some additional errors are caused by changes in the quality of the satellite data when extrapolating the adjustment to times outside the overlap period. A reason for not using the complete period of available measurements for the adjustment can be low data quality. Although during the overlap the bias can be zeroed out, the method leaves a methodological uncertainty, which is estimated based on the results of (Mieslinger et al. 2014). The uncertainty due to the variability of the solar resource and the limited length of the observation period is calculated from the standard deviation of the yearly averages over the period for which the measurement adjusted satellite-derived data are available.

In summary, the uncertainty of long-term data depends on the uncertainty of satellite-derived data, the uncertainty of the adjustment methodology and the uncertainty caused by inter-annual variability and the limited number of years taken to derive the long-term average. Since the aim of the adjustment methodology mentioned in 3.4 is to remove the mean bias and improve the frequency distribution during the overlapping period, applying this method to long-term satellite-derived data tends to remove the uncertainty of the satellite-derived data. Therefore, the resulting uncertainty of the long-term data depends then on

a) the uncertainty of the adjustment methodology,

b) the uncertainty of the measured data and

c) the uncertainty due to temporal coverage.

Hence, the total uncertainty is calculated by taking into consideration uncertainties of measured data, long-term data and the inter-annual variability. The combined uncertainties for each of the four data sets is calculated by following the Gaussian law of error propagation by quadratically adding the three sources of uncertainties. Therefore, this uncertainty, shortly named 'multiple year uncertainty', refers to multiple year inter-annual variability. To calculate the 'single year uncertainty', which refers to single year inter-annual variability, the Gaussian law of error propagation is followed by quadratically adding the multiple year uncertainty and the standard deviation of the inter-annual variation.

3.8. Generation of Typical Meteorological Year (P50) Data Set

Commonly, energy performance calculations to predict potential energy production of a solar power plant use a Typical Meteorological Year (TMY) data set as input. TMYs need to cover a full year and shall provide the most relevant meteorological parameters for the technology to be evaluated. For CSP plants this is DNI, ambient air temperature, relative humidity and wind speed among other auxiliary meteorological parameters, which help to simulate energy losses more realistically and which may influence design parameters of the plant. A TMY shall well represent the characteristic meteorological conditions of average years at a site. The annual average DNI in a TMY shall represent the average or P50 case of the long-term DNI within a certain tolerance. At the P50 level of exceedance, the probability that the actual long-term average is exceeded is equal to the probability that it will be lower to this P50, in relation to uncertainty effects.

Concerning inter-annual variability, the P50 also expresses the value, which is exceeded in 50% of all years (hence 50% of all years show lower irradiance) assuming the long-term average value was correctly determined and neither over- or underestimated.

Extreme weather events, which are not typical for a site, are filtered out for the TMY. Hence, a TMY is not suitable as the only base for system or component design with respect to the robustness to resist extreme weather events such as very high wind speeds, precipitations, high/low temperatures, hazards, etc.

The typical meteorological year (TMY) generally includes DNI, GHI and DHI values of solar radiation and also other meteorological parameters like ambient temperature, relative humidity, pressure, wind speed and wind direction. Preferably, a TMY should be created from a multi-year data set of ground-based meteorological measurement data, with sufficient quality. For generating the TMYs for the 4 tests sites the values of DNI, GHI, DHI as well as the auxiliary meteorological data like ambient air temperature, wind speed and wind direction are obtained from the measurements on site if available or by modelled data from MERRA2 when not measured on site.

The annual DNI cycle is also important for yield prediction of CSP plants. Thus, the values of the TMY should well represent the annual DNI cycle. The TMY shall also have a frequency distribution, especially for DNI, which matches the one from the site measurements. Therefore, a TMY is built in such a way that it represents the long-term average value of DNI.

Typical meteorological years can be created by several procedures. In the context of the present work an improved concatenating method as described by Hoyer-Klick et al. (2009) is used to create the TMY under consideration to fulfil the criteria given by the International Electrotechnical Commission in (IEC TC117 2016, 62862-1-2).

These criteria are:

- The difference between monthly irradiance of the TMY (for each month) and the corresponding representative long-term best estimate for each month must not be higher than the 2% of the twelfth part of the annual representative long-term best estimate: $TMY_{month} – P50_{month} < 0.02 \times P50_{year}/12$.
- Substitution of days with other day of the same month must be done within a range of ±5 days
- In a generated dataset, the same day (from the original dataset) must not appear more than 4 times.
- A generated dataset must not contain more than a 50% substituted dates per month.
- The result has to be an annual dataset found by concatenation of 365 days of complete valid days, which includes all the simultaneous variables

As mentioned above, here an improved concatenating method as described by Hoyer-Klick et al. (2009) is used to create the TMY. The original method uses only one complete year of ground-based measurements, because often not more than one year of measurements are available at a site. The monthly averages of each month in this case are adjusted by replacing sunny days with cloudy days and vice-versa as required, until the monthly average of DNI matches with the long-term monthly average of DNI. One drawback of using only one year of data is that the frequency distribution can be changed because of the frequent synthesizing of days. By copying many days with similar irradiance conditions as sometimes needed when the single measured year in a month has larger deviations the natural variability is flattened out. Using a longer measured data set improves these shortcomings substantially. Therefore, a slight modification is applied here: In this improved methodology, when available, the use of more than one year of ground-based measurements is allowed. Individual months from different years are selected which are closest to the long-term monthly averages of DNI. If the difference in the monthly average of DNI of the month selected as compared to the long-term monthly average of DNI is more than the allowed tolerance, only then the monthly averages are adjusted by replacing sunny days with cloudy days or vice-versa. This method leads to more realistic TMYs as the number of shifting days is reduced. After adjusting the data of the individual months to represent the long-term monthly averages, individual months of the year are selected and concatenated to create a representative year. In case it is not possible to reach the allowed difference between the monthly DNI average and the long-term monthly DNI average by concatenating of complete days, a constant factor is applied to some selected days. These selected days are all the days of the month excluding the four days with the two highest and the two lowest daily averages in the month and excluding the days of the month which were replaced before. For time stamps for which a factor is applied to DNI, GHI is recalculated by DNI and DHI. The DNI values on which the factor is applied and the corresponding recalculated GHI values are flagged as “synthetic”.

In the case of the four test sites on-site measurement data in 1-minute time resolution is used, which also includes auxiliary meteorological parameters. Depending on the site not all necessary auxiliary parameters are measured (refer to Table 3-1 for the available on-site measurements at each site). Missing parameters are substituted by modelled data from MERRA2 taking the real location and real time into account.

The auxiliary meteorological parameters used in the TMY are coherent with DNI values selected for the TMY. Thus, a complete TMY is created in 1-minute resolution, which not only matches the average of DNI within the acceptable tolerance, but also well represents the annual DNI cycle. Using measured data instead of model-derived data as far as possible has the advantage that the resulting TMY and MY-data sets represent well the ambient meteorological conditions at the site. Also the DNI data are more realistic because ground-corrected satellite-derived irradiance data does not show the same temporal patterns as measurements. This is especially valid for 1 min data, which today can only be derived from satellite using interpolation techniques, because the maximum temporal resolution of the used satellites is 15 min. For satellite data before 2004 only 30 min resolution is available.

From this TMY data set in 1min time resolution the requested TMY data sets with lower time resolutions (10min, 15min, 30min, 60min) are created by temporal averaging. The calculation of the sun elevation angels of the TMY data sets is done in a different way for high and low time resolutions, see chapter 3.10 for more details.

Since the on-site measurements of DNI, GHI and DHI are measured at all four stations with three different instruments having their proper uncertainty, commonly, the correlation (GHI = DHI + cos(sun zenith)) between the three components is not completely fulfilled. As will be shown in chapter 5, the coherence test between DNI, GHI and DHI is also not always passed. To create completely coherent TMY data sets for all four time resolutions, the GHI of the TMY data sets is recalculated by DNI, DHI and sun elevation taken also from the corresponding TMY data set. For the cases when DNI and GHI are direct measurements (labelled with 2) the recalculated GHI is labelled as "indirect measurement data" (label 3).

3.9. Determination of P90 (PXY) value of DNI and creation of MYP90 (PXY) Data Sets

P90 value of DNI means that this DNI value would be exceeded in 90% of the cases. These values are necessary for risk assessment of solar power plants during due diligence. Assuming normal probability distribution and taking into consideration P50 value and associated uncertainty, the P90 DNI value is derived. In this case two P90 values are derived, wherein two different types of uncertainties are considered.

There is a difference between a Meteorological Year (MY) considering single year inter-annual variability and a Meteorological Year (MY) considering multiple year inter-annual variability. The distinction consists in the underlying overall uncertainty of the P50 value which is used to calculate the P90 value. If the 90% probability of exceedance is requested for each single year, single year uncertainty is applied, which takes the extend of inter-annual variation into account. When the overall uncertainty considers single year inter-annual variability this uncertainty is applied for the predicted annual power production of only on single year. When the overall uncertainty of the predicted power production is applied for the whole planed production time of the power plant this uncertainty considers multiple year inter-annual variability. Hence, the multiple year uncertainty is lower than the single year uncertainty and thus the P90 values considering multiple year uncertainty are higher than the P90 values considering single year uncertainty. As a result, one P90 value of DNI is derived from the uncertainty considering inter-annual variability of DNI related to multiple years and the other P90 value of DNI is derived from the uncertainty considering inter-annual variability of DNI related to single year.

For risk assessment of the solar power project, two Meteorological Years data sets representing P90 values of DNI are derived based on the P50 value and the associated uncertainties using a procedure similar for creating a TMY as mentioned in 3.8. Here also on-site measurement data is used to create the MY90s related to single year and multiple years. The long-term monthly averages of DNI of the two MY90s are determined based on the ratio P90 value of DNI/long-term P50 value of DNI. Individual months from different years are selected which are closest to the long-term monthly P90 averages of DNI. When necessary, monthly averages are adjusted by replacing sunny days with cloudy days and vice-versa until the difference in the monthly average of DNI of the month selected as compared to the long-term monthly P90 average of DNI is below the allowed tolerance. After adjusting the data of the individual months to represent the long-term monthly averages, individual months of the year are selected and concatenated to create a representative year. In case it is not possible to reach the allowed difference between the monthly DNI average and the P90 value for DNI by concatenating, a constant factor is applied as described above in chapter 3.8. Correspondingly to the TMY data sets the MY90 data sets are created in 1min time resolution, from which the requested TMY data sets with lower time resolutions (10min, 15min, 30min, 60min) are created by temporal averaging. The calculation of the sun position angles as well as the calculation of the GHI by measured DNI and DHI is done just as for the TMY data sets.

In the same way, the P75 and P95 values for single year and multiple year uncertainty are calculated and the corresponding MYs created in 10min, 15min and 60min time resolution.

3.10. Temporal resolution and sun position of TMY & MY data sets

As explained before, in a first step the TMY and MY data sets are created in 1min time resolution. Then, by temporal averaging, the TMY and MY data sets are created in the requested lower time resolutions, which are 10min, 15min, 30min and 60min.

The calculation of the sun elevation angels of the TMY data sets is done in a different way for high and low time resolutions. For time resolutions up to 15min the sun position is directly calculated from the centre of the averaging interval using the SG2 algorithm (Philippe Blanc, Lucien Wald 2012), in which also the atmospheric pressure and air temperature of the TMY data sets are taken into account as input parameters. For the data sets in 30min and 60min time resolution the so called “effective” sun elevation is calculated following a suggested methodology from Philippe Blanc. In this methodology the sun elevation is calculated by clear sky DNI and clear sky Direct Horizontal Irradiance not considering negative values during sun rise/set. Thus, sun elevations during night hours are 0. The clear sky DNI and clear sky Direct Horizontal Irradiance are calculated by a clear sky model for 1min time resolution and averaged to the necessary time resolution (30min or 60min). The here used clear sky model is (Bird, R. E., and R. L. Hulstrom 1981). The sun azimuth is for all time resolutions directly calculated from the centre of the averaging interval using the SG2 algorithm (Philippe Blanc, Lucien Wald 2012), in which also the atmospheric pressure and air temperature of the TMY data sets are taken into account as input parameters.

4. TMY and MY data format and definitions

Following International Electrotechnical Commission (IEC) the annual series are formatted according to the draft document (Carsten Hoyer-Klick, et al. 2016). The format is based on the standard ASCII character set. The field *#characterset* is mandatory as a second line of the file to ease interpretation of the remaining text fields. Time stamps follow ISO 8601. YYYY-MM-DDTHH:MM:SS.ssss with leading zeros. Time stamps for temporally averaged data refer to the end of the integration period as it is the convention in meteorology. Integration and averaging always refers to the complete time interval. This is especially important at sunrise and sunset, as it should also include the time frame when the sun is still or already below the horizon. Limiting such intervals only to the time when the sun is above the horizon is not allowed. The only exception is the sun elevation or sun zenith angle. During the sun rise or sun set these values are calculated in a way that allows calculating the DNI from direct horizontal irradiance using the averaged sun elevation angle.

Following (Carsten Hoyer-Klick, et al. 2016). the WGS84 geodetic system standard is taken as the reference ellipsoid to define the geographical location on lambertian coordinates. The geographic identification of the place to which the data set refers to is determined by the geodetic latitude and longitude coordinates and the elevation above mean sea level. For each individual data point in the TMY two timestamps are given. One time stamp indicates the time of the value within the TMY (functional date). The other timestamp corresponds to the time to which the original data value belongs to (original date). The time in the TMY cannot be completely defined without stating the year. In order to avoid errors and ambiguities the year of the TMY data set is set to 2015. This way the solar position can be calculated in the same way by all users and it is clear that the TMY is no leap year. The record date corresponds to the UTC referencing system.

A label which gives information on the origin or type of data of the minimum variable (direct normal irradiance) is included in the data set. Depending on the origin, values of this label will vary from 2 to 7, reserving 1 for “unknown”. Possible label values are summarized in Table 4-1. Two label columns should be provided for each record, one associated with the original date (“label_orig”) and the other associated with the functional date (“label_func”). Any data point of the data set in which the functional date and the original date are not identical (excluding years) is considered synthetic, whatever its origin.

In Figure 4-1 used data format is exemplary shown for the TMY data set for ESPSA in 60min time resolution (guiSmo_ESPSA_TMY_P50_60min_2207kWh_DNI_mltyear_20160823.txt).

Data from	Label
Unknown	1
Direct measurement data	2
Indirect measurement data	3
Derived data	4
Synthetic data	5
Satellite data	6
Meteorological model data	7

Table 4-1: Direct normal irradiance place label values

guiSmo_ESPSA_TMY_P50_60min_2207kWh_DNI_mltyear_20160823.txt

```
#MET_IEC.v1.0 headerlines:91
#characterset ISO-8859-1
#delimiter \t
#endofline \n
#title TMY/MY - CSP Bankability - PSA: guiSmo_ESPSA_TMY_P50_60min_2207kWh_DNI_mltyear_20160823.txt
#history.2016-08-23T11:35 created
#comment The yearly sum of each radiation component corresponds to the meteorological year (MY) P50 value considerung multiple-y
#comment Time stamps refer to the end of the averaging period.
#comment Sun height angles are calculated as "effective" sun height angles by clear sky DNI and clear sky Direct Horizontal Irra
#comment This data set is free to use for scientific purposes. The following text shall always be given in the Acknowledgements:
#comment "Data set provided by Suntrace GmbH co-funded by the BMWi project CSP Bankability (No. 0325293). The data is based on t
#comment used convention for data labeling:
#comment 1: unknown
#comment 2: direct measurement data
#comment 3: indirect measurement data
#comment 4: derived data
#comment 5: synthetic data
#comment 6: satellite data
#comment 7: meteorological model data
#datasource mixed
#IPR.institution.1.name DLR/CIEMAT/Plataforma Solar de Almeria (PSA)
#IPR.source.1.name DLR_PSA_HP
#IPR.source.1.URL psa.es
#IPR.institution.2.name DLR
#IPR.source.2.name DLR Solemi
#IPR.source.2.URL http://www.dlr.de/tt/desktopdefault.aspx/tabid-2885/4422_read-6581
#IPR.provider.name Suntrace GmbH
#IPR.provider.URL http://www.suntrace.de
#IPR.provider.copyrightText Copyright (C) 2016 by Suntrace GmbH
#location.latitudeDegrN 37.090
#location.longitudeDegrE -2.360
#location.elevationMAMSL 492
#time.timezone UTC+00:00
#time.resolutiontype fixed
#time.resolutionSec 3600
#time.averaging yes
#time.completeness yes
#time.calender.leap_years no
#gap.notanumber NaN
#gap.treatment interpolated
#QC.type.1 Suntrace
#channel.time.name time
#channel.time.units YYYY-MM-DDThh:mm
#channel.solar_elevation_angle.name solar elevation angle
#channel.solar_elevation_angle.units degrees
#channel.solar_azimuth_angle.name solarazimuth angle
#channel.solar_azimuth_angle.units degrees
#channel.time_orig.name original time from which the data has been taken
#channel.time_orig.units YYYY-MM-DDThh:mm
#channel.dni.name direct normal irradiance
#channel.dni.units w.m-2
#channel.dni_label.name label for direct normal irradiance
#channel.dni_label.units -
#channel.ghi.name global horizontal irradiance
#channel.ghi.units w.m-2
#channel.ghi_label.name label for global horizontal irradiance
#channel.ghi_label.units -
#channel.dhi.name diffuse horizontal irradiance
#channel.dhi.units w.m-2
#channel.dhi_label.name label for diffuse horizontal irradiance
#channel.dhi_label.units -
#channel.wind_speed.name wind speed
#channel.wind_speed.units m.s-1
#channel.wind_speed_label.name label for wind speed
#channel.wind_speed_label.units -
#channel.wind_from_direction.name wind direction
#channel.wind_from_direction.units degrees
#channel.wind_from_direction_label.name label for wind direction
#channel.wind_from_direction_label.units -
#channel.air_temperature.name air temperature
#channel.air_temperature.units degrC
#channel.air_temperature_label.name label for air temperature
#channel.air_temperature_label.units -
#channel.wet_bulb_temperature.name wet bulb temperature
#channel.wet_bulb_temperature.units degrC
#channel.wet_bulb_temperature_label.name label for wet bulb temperature
#channel.wet_bulb_temperature_label.units -
#channel.dew_point_temperature.name dew point temperature
#channel.dew_point_temperature.units degrC
#channel.dew_point_temperature_label.name label for dew point temperature
#channel.dew_point_temperature_label.units -
#channel.relative_humidity.name relative humidity
#channel.relative_humidity.units percent
#channel.relative_humidity_label.name label for relative humidity
#channel.relative_humidity_label.units -
#channel.air_pressure.name barometric pressure
#channel.air_pressure.units hPa
#channel.air_pressure_label.name label for barometric pressure
#channel.air_pressure_label.units -
#begindata
time    solar_elevation_angle   solar_azimuth_angle time_orig   dni dni_label   ghi ghi_label   dhi dhi_label   wind_speed  wind
2015-01-01T01:00      0.0    -164    2011-01-01T01:00   0   5   0   5   0   2   0.3   2    32   2   8.2   2   8.0   3
2015-01-01T02:00      0.0    -125    2011-01-01T02:00   0   5   0   5   0   2   0.5   2    45   2   7.9   2   7.8   3
2015-01-01T03:00      0.0    -106    2011-01-01T03:00   0   5   0   5   0   2   0.8   2    52   2   7.5   2   7.3   3
2015-01-01T04:00      0.0     -94    2011-01-01T04:00   0   5   0   5   0   2   0.9   2   353   2   8.2   2   8.0   3
2015-01-01T05:00      0.0     -85    2011-01-01T05:00   0   5   0   5   0   2   0.2   2     8   2   7.8   2   7.6   3
2015-01-01T06:00      0.0     -77    2011-01-01T06:00   0   5   0   5   0   2   0.1   2   350   2   8.3   2   8.1   3
2015-01-01T07:00      0.0     -69    2011-01-01T07:00   0   5   0   5   0   2   0.5   2    35   2   8.7   2   8.3   3
2015-01-01T08:00      3.0     -60    2011-01-01T08:00   5   5   10  5   10  2   0.7   2    22   2   8.6   2   8.0   3
2015-01-01T09:00     10.6     -51    2011-01-01T09:00   183 5   98  5   64  2   1.4   2    26   2   9.6   2   8.7   3
```

Figure 4-1: First 100 lines of TMY data set for ESPSA in 60min time resolution (guiSmo_ESPSA_TMY_P50_60min_2207kWh_DNI_mltyear_20160823.txt).

5. Summary of Results

5.1. Analysis of measurements

As mentioned in Chapter 3.1, only quality-controlled data has been used for analysis. In addition a visual check of the valid quality-controlled data is done. The results of the quality assessed data for all four demo sites can be seen in Table 5-1 and Figure 5-1. The most observed not passed test is the coherence test (flag 5), which checks the correlation between DNI, GHI and DHI (GHI = DHI + cos(sun zenith)) allowing a certain tolerance between calculated and measured GHI (8% for sun elevations > 15º, else 15%). This is for ESPSA 0.1%, for DZTAM 3.9%, for SASOV 0.7% and for ZADAA 3.2%. This is probably caused by soiling. Missing values for DNI are caused by breaks in station operation or maintenance or simply by limited availability in the moment of the processing. However, the quality of the available DNI measurements is qualified to be very high for the four stations. The proportion of the available DNI measurements (without missing values, including night values) which are not flagged as erroneous or potential erroneous is for ESPSA 99.9%, for DZTAM 96.1%, for SASOV 99.3% and for ZADAA 96.5%.

Site code	Overall average [W/m^2]	Missing values (flag 0,10) [%]	Correct (flag 1) [%]	Rare observation (flag 9) [%]	Potential erroneous (flag 4) [%]	Erroneous (flag 2,3,5,6,8) [%]
ESPSA	242	26.6	73.3	0	0	0.1
DZTAM	271	0	96.1	0	0	3.9
SASOV	268	2	97.3	0	0	0.7
ZADAA	303	3.6	93.1	0	0.1	3.3

Table 5-1: Overview results of quality control of on-site measurements for the four demo sites. See Figure 5-1 for description of flag numbers.

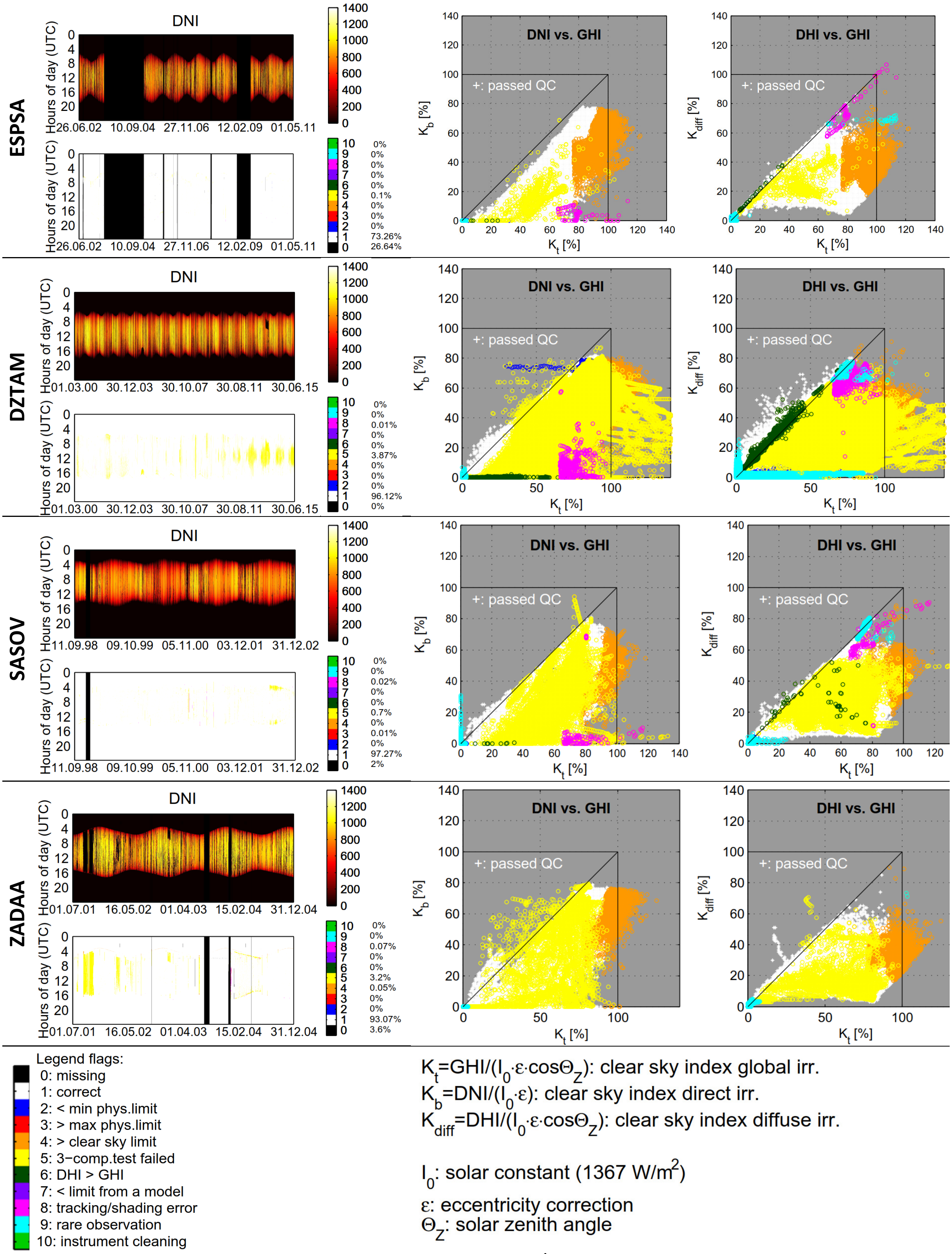

Figure 5-1: QC output for DNI for the four demos sites. 2nd column: DNI (top) / flags (below) for each minute of the day throughout the complete time period. 3rd column: on ordinate clear sky index of direct (left) / diffuse (right) against clear sky index of global irradiance (abscissas).

5.2. Long-term average of DNI

5.2.1. Adjustment of satellite-derived DNI values by on-site measurement data

The method of (Mieslinger et al. 2014) is applied for the overlapping time period to adjust the satellite derived DNI values from DLR-SOLEMI by on-site measurements. After applying this method it is found for all four demo sites that the mean of the adjusted satellite-derived datasets is equal to that of on-site measurement data used for training (qc-filtered) during the overlapping period. Training here is the determination process of the adjustment function for which just qc-filtered on-site measurements inside the overlapping period are applied. Frequency distribution of the adjusted-satellite derived datasets is different than that of the original satellite data and matches quite well with on-site measurement data. Figure 5-2 shows for the four sites the scatter plot of original DNI values (quality controlled, visually detected and excluded) in hourly time resolution obtained from the measurements and satellite for the overlapping period. Table 5-2 compares the averaged DNI of the on-site measurements against the satellite derived data before and after adjustment during the overlapping period with on-site measurements for the four demo sites.

Based on the results of adjustment of satellite-derived data for the overlapping period, the site-specific long-term solar radiation time series from DLR-SOLEMI covering 20 (16 for ZADAA) years are adjusted at the four demos sites. For DZTAM and SASOV the adjustment results in a noticeable modification of the annual average of DLR-SOLEMI data set. For ESPSA and ZADAA the annual averages of the adjusted DLR-SOLEMI data set are slightly higher in comparison to the original DLR-SOLEMI data sets. Moreover, adjustment of DLR-SOLEMI data set results in slightly improved frequency distribution as can be seen in Figure 5-3. As can be seen in Figure 5-4, the monthly DNI average values of adjusted DLR-SOLEMI dataset matches slightly better with that of ground-based measurements in comparison to the original DLR-SOLEMI data sets. It can be seen that for SASOV the improvement due to adjustment is more important in comparison to the other three sites.

It has to be noted that these four demo sites represent very special cases. For these locations the accuracy of the satellite derived DNI data sets is already exceptionally higher in comparison to other sites, since the available on-site measurements (3 BSRN stations and one station from DLR) for such long periods had already been used to train the corresponding models for deriving DNI from the satellite images. In practice, during the development process of a CSP-project, the access to the on-site measurements, if available, is very restricted and are not used by the providers of satellite derived radiation data sets for training their models. Therefore, in general practice, the improvement by adjusting the satellite derived DNI data sets by on-site measurements is more significant than the one observed for these demos sites.

Site code	Averaged DNI during overlapping period in W/m²						correlation coefficient with on-site measurements during overlapping period		Averaged DNI long term complete period in W/m²	
	on-site measurements		DLR-SOLEMI		DLR-SOLEMI Adjusted		DLR-SOLEMI	DLR-SOLEMI adjusted	DLR-SOLEMI	DLR-SOLEMI adjusted
	all	train	all	train	all	train				
ESPSA	242.8	485.3	243.0	484.5	243.4	485.3	0.9255	0.9258	252.0	252.2
DZTAM	269.6	546.9	262.3	522.6	274.7	546.9	0.9350	0.9355	262.4	274.6
SASOV	268.5	544.8	246.3	501.7	268.4	544.8	0.9424	0.9477	238.5	260.1
ZADAA	302.6	617.9	302.3	614.2	304.3	617.9	0.9480	0.9484	308.5	310.3

Table 5-2: Comparison averaged DNI of on-site measurements against DLR-SOLEMI before and after adjustment during overlapping period with on-site measurements and for complete time period for the four demo sites.

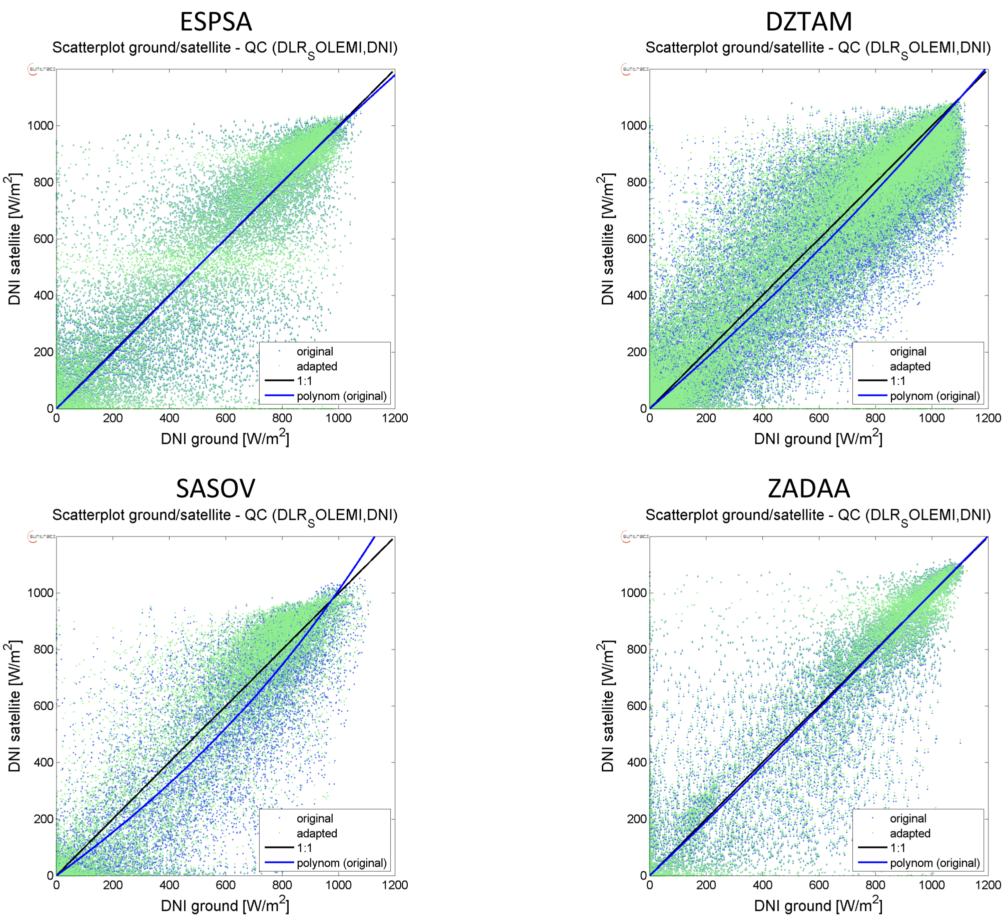

Figure 5-2: Scatter plot of DNI for QC passed values: on-site measurements against original and adjusted satellite derived DNI from DLR-SOLEMI in hourly time resolution for the full overlapping

period for the four demo sites. The dark black line represents the 1:1 relationship. The blue line represents the polynomial fit.

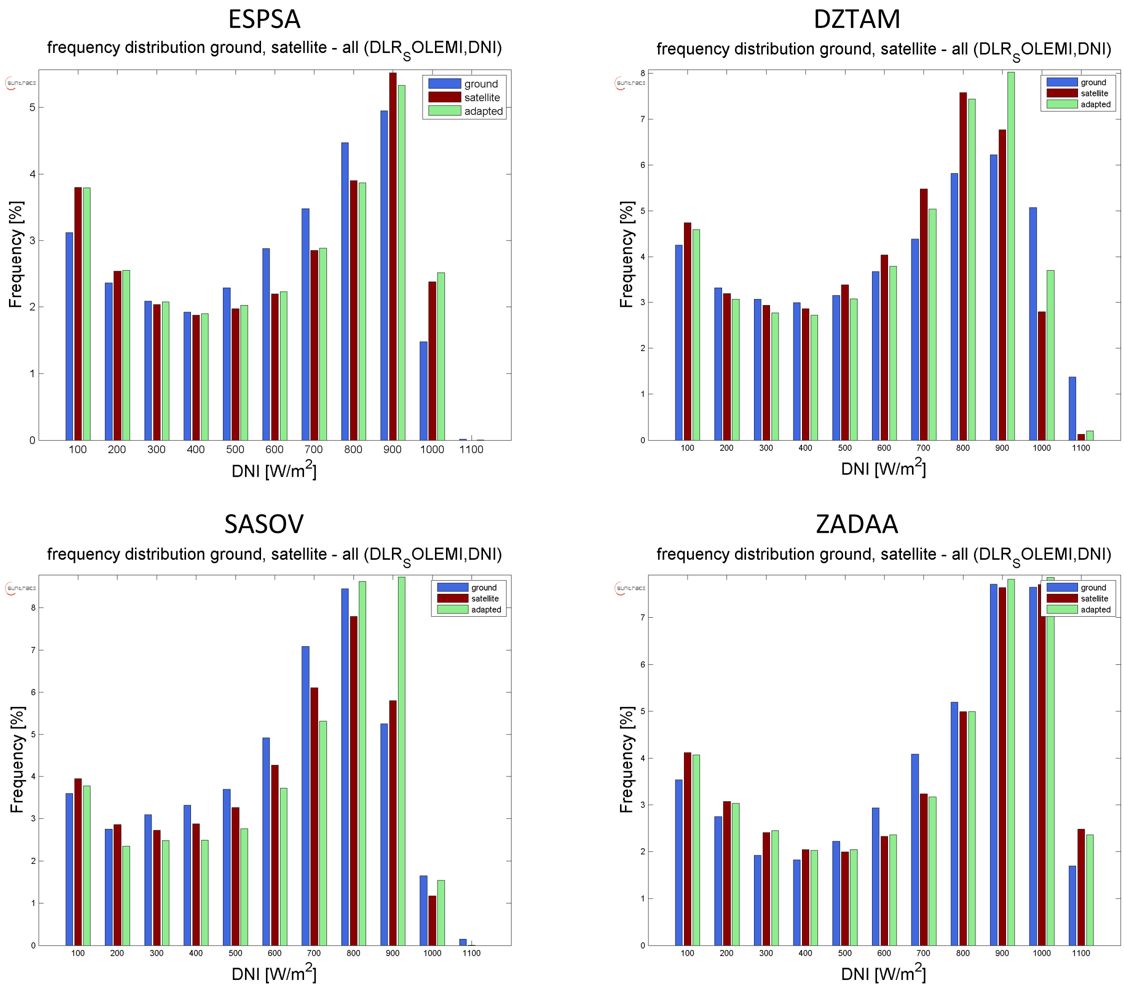

Figure 5-3: Frequency distribution of DNI for all values: on-site measurements against original and adjusted satellite derived DNI from DLR-SOLEMI in hourly time resolution for the full overlapping period for the four demo sites.

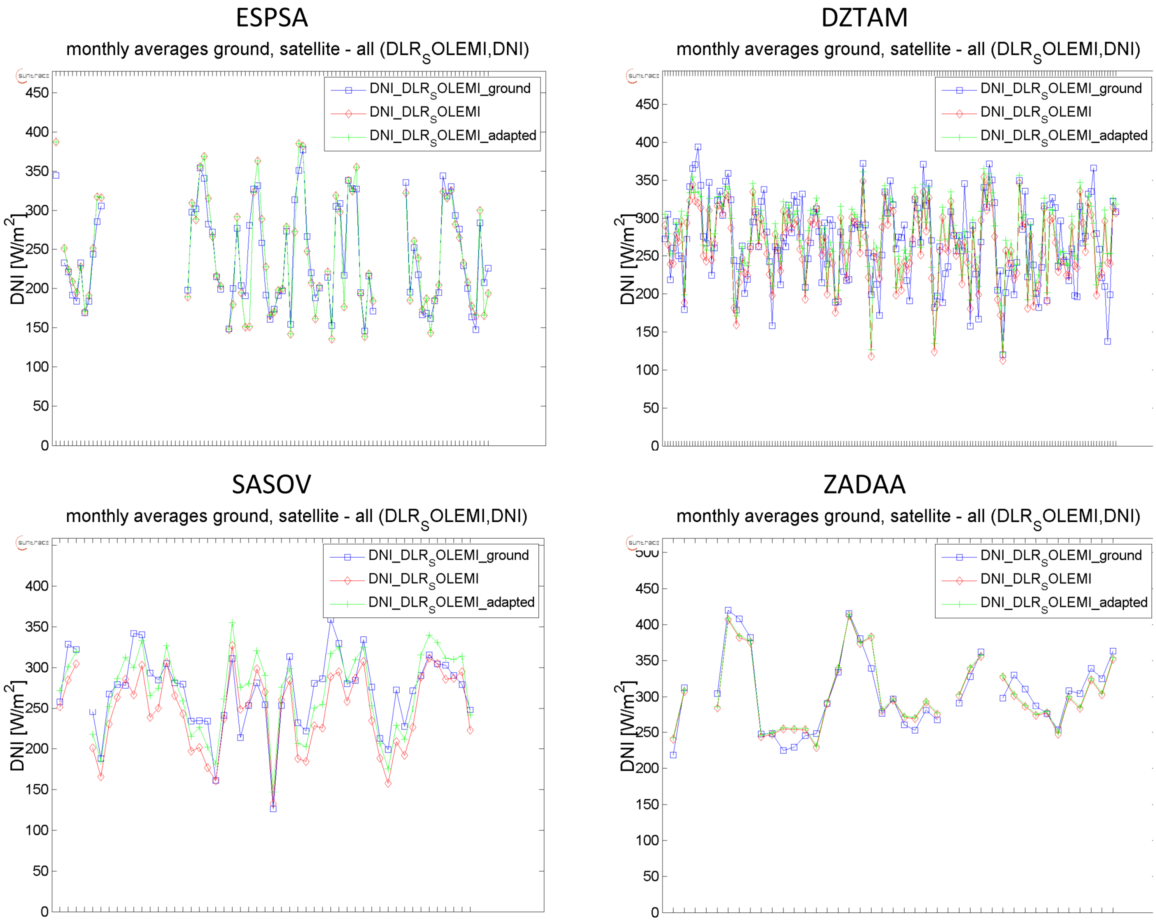

Figure 5-4: DNI monthly averages during the full overlapping period for all values.

5.2.2. Determination of long-term average of DNI

As discussed in 3.6, the best estimate for the long-term annual DNI average expected at the four demo sites is derived following the methodology recommended by the International Electrotechnical Commission in (IEC TC117 2016, 62862-1-2) using on-site measurements adjusted long-term satellite derived DNI data from DLR-SOLEMI.

For the four demo sites three different input data sets have been assessed, each from which finally one data set (on-site measurements adjusted DLR-SOLEMI) is taken into account for determining the long-term annual average of DNI. Although the on-site measurements have a lower uncertainty and are used for the adjustment of the satellite derived DNI, they are not directly used for determining the long term annual average since the time period covered by them is much shorter in comparison to the long-term satellite derived DLR-SOLEMI DNI data set and therefore not as representative.

The main results can be found in Table 5-3 and Figure 5-5, which visualizes the DNI long-term averages for the three data sets with the best estimate (green line) at the four demo sites. For the demo site 1, ESPSA, the long-term average for DNI amounts to 252 W/m^2, which is equivalent to 2212 kWh/m^2 per year or 6.06 kWh/m^2 per day. For the demo site 2, DZTAM, the long-term average for DNI amounts to 273 W/m^2, which is equivalent to 2393 kWh/m^2 per year or 6.55 kWh/m^2 per day. For the demo site 3, SASOV, the long-term average for DNI amounts to 260 W/m^2, which is equivalent to 2275 kWh/m^2 per year or 6.23 kWh/m^2 per day. For the demo site 4, ZADAA, the long-term average for DNI amounts to 310 W/m^2, which is equivalent to 2716 kWh/m^2 per year or 7.43 kWh/m^2 per day.

Site	Source	temporal coverage		no. of years	overall uncertainty multiple year		overall uncertainty single year		annual average DNI	
		Start	End	[years]	abs.[W/ m²]	rel.[%]	abs.[W/ m²]	rel.[%]	[W/m²]	[kWh/m²]
ESPSA	DLR-SOLEMI	1994-01	2013-12	20	6.9	2.7	14.0	5.6	252	2209
	DLR-SOLEMI adjusted	1994-01	2013-12	20	6.9	2.7	14.0	5.6	252	2211
	DLR_ISIS	1983-07	2004-12	21	32.7	15.0	34.3	15.8	217	1904
	on-site	2002-07	2011-04	8	6.4	2.6	13.4	5.6	242	2121
	best estimate	**-**	**-**	**-**	**6.9**	**2.7**	**14.0**	**5.6**	**252**	**2212**
DZTAM	DLR-SOLEMI	1991-01	2013-12	20	6.7	2.5	14.2	5.2	262	2301
	DLR-SOLEMI adjusted	1991-01	2013-12	20	6.7	2.5	14.2	5.2	275	2407
	DLR_ISIS	1983-07	2004-12	21	36.7	15.0	38.4	15.7	244	2141
	on-site	2000-03	2015-06	14	6.3	2.3	13.9	5.1	271	2378
	best estimate	**-**	**-**	-	**6.7**	**2.5**	**14.1**	**5.2**	**273**	**2393**
SASOV	DLR-SOLEMI	1991-01	2013-12	20	7.8	3.0	14.4	5.5	238	2090
	DLR-SOLEMI adjusted	1991-01	2013-12	20	7.8	3.0	14.4	5.5	260	2280
	DLR_ISIS	1983-07	2004-12	21	30.6	15.0	32.0	15.7	203	1783
	on-site	1998-10	2002-12	4	8.2	3.1	14.9	5.5	268	2350
	best estimate	**-**	**-**	**-**	**7.8**	**3.0**	**14.3**	**5.5**	**260**	**2275**
ZADAA	DLR-SOLEMI	1991-01	2005-12	16	9.1	2.9	12.7	4.1	309	2705
	DLR-SOLEMI adjusted	1991-01	2005-12	16	9.1	2.9	12.7	4.1	310	2720
	DLR_ISIS	1983-07	2004-12	21	38.1	15.0	38.8	15.3	254	2225
	on-site	2001-07	2004-12	3	8.0	2.6	11.9	3.9	307	2691
	best estimate	**-**	**-**	**-**	**9.0**	**2.9**	**12.7**	**4.1**	**310**	**2716**

Table 5-3: Overview of long-term averages for the four demo sited from various DNI data sets.

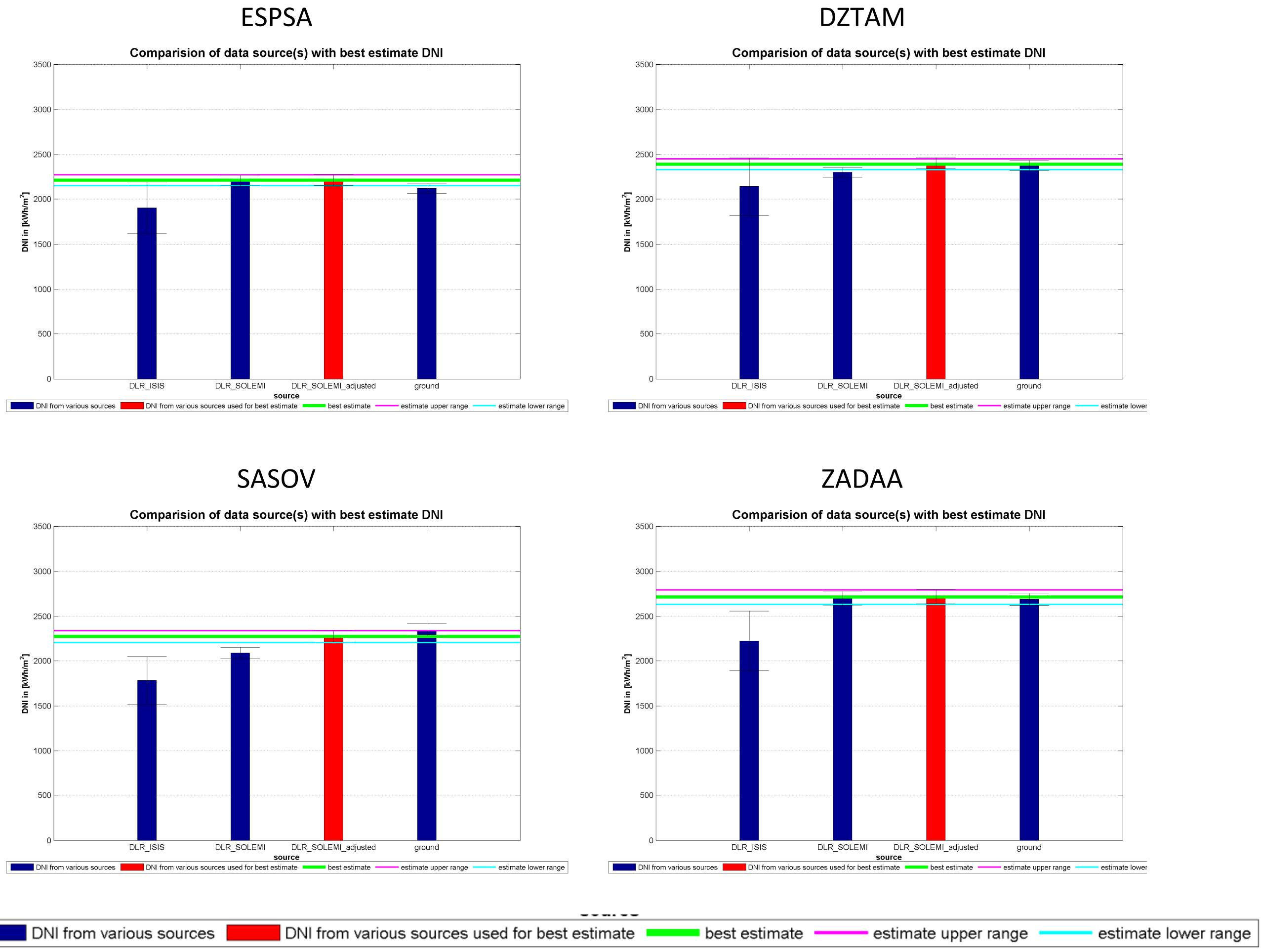

Figure 5-5: Overview of the long-term DNI values from different data sets for the four demos sites (red: used / blue: not used for determination of best estimate) and the best estimate (green line). The lower (cyan) and upper (magenta) lines illustrate the ranges of the best estimate, which are based on the estimated uncertainty of the best estimate.

5.3. Inter-annual variability of DNI

For determining the inter-annual variability of DNI the data set from DLR-SOLEMI is analysed. Figure 5-6 shows the inter-annual variability of DNI as yearly averages of the available datasets for the four sites. The purple line represents the long-term average of DNI at the four demo sites. It is observed that the inter-annual variability for ESPSA, DZTAM and SASOV is with 12 W/m^2 nearly identical.

Based on the DLR-SOLEMI data set, at ESPSA the inter-annual variability of DNI is 12.2 W/m^2, approximately equivalent to ± 4.9%, at DZTAM the inter-annual variability of DNI is 12.4 W/m^2, approximately equivalent to ± 4.5%, at SASOV the inter-annual variability of DNI is 12.0 W/m^2, approximately equivalent to ± 4.6% and at ZADAA the inter-annual variability of DNI is 8.9 W/m^2, approximately equivalent to ± 2.9%.

Following (Meyer et al. 2009) the uncertainty due to considering only a few years reduces with the number of years. In this analysis the main base for fixing the long-term value is the 20 (16 for ZADAA) years data set of DLR-SOLEMI. Thus, the contribution to uncertainty due to inter-annual variations is 1.1% for ESPSA, 1.0% for DZTAM, 1.0% for SASOV and 0.7% for ZADAA. This is taken as an input in chapter 5.4 to derive the overall uncertainty with respect to multiple years and single years.

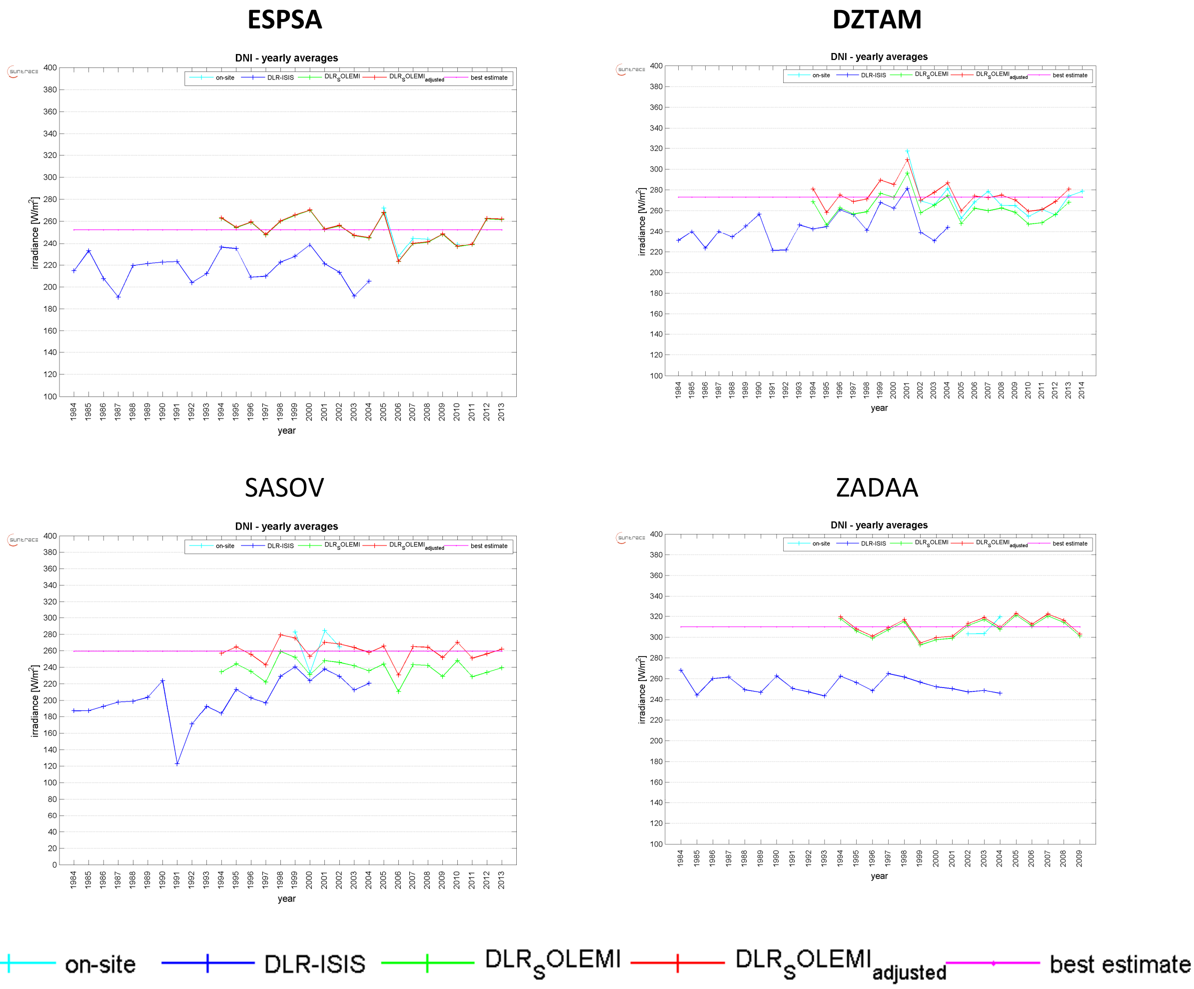

Figure 5-6: Timescale showing the inter-annual variation of DNI obtained from DLR-SOLEMI, adjusted DLR-SOLEMI, DLR-ISIS in comparison to on-site measurement data sets and long term best estimate in terms of yearly averages for the four demo sites.

5.4. Analysis of uncertainty of DNI

As explained in 3.7, the total long-term uncertainty of long-term average of DNI depends on the uncertainty of measurements, uncertainty of long-term data and the inter-annual variability of DNI. The quality of the data measured on the four sites is very high as can be seen in 5.1. Also the maintenance and cleaning of the meteorological measurement stations is supposed to be well done since the station at ESPSA is operated by the DLR and the other three stations are part of BSRN network demanding very high quality of equipment and operation. As a result the total uncertainty of DNI data measured under consideration of the instrument uncertainty and the uncertainty due to calibration and maintenance issues is assumed to be 2%.

DLR-SOLEMI DNI data from January 1994 to December 2013 (or to December 2006 for ZADAA respectively) are used to train the algorithm for adjustment methodology. As explained in 3.7, the uncertainty of satellite data is removed by using the adjustment methodology to the data. According to (Mieslinger et al. 2014), the uncertainty of the adjustment methodology is ca. 2% on an average, which varies depending on the site, the source of data and how long the overlapping period with on-site measurements is.

For the two sites SASOV and ZADAA the uncertainty of the adjustment methodology is assumed to be 2% for DLR-SOLEMI due to the fact that the long-term satellite-derived time-series make use of two different satellite derivation models (MFG from 1994 to 2004 and MSG from 2004 onwards). Although for these two sites the length of the overlapping period with on-site measurements is more than four years (which is more than usual), the overlapping periods with on-site measurements are just during the usage of MFG (for ZADAA just some months of MSG), see Table 3-1: Overview available on-site measurements for the four demo sites. For the two sites ESPSA and DZTAM the measurements took place during the usage of MFG and also MSG. Moreover, the overlapping periods with on-site measurements are with more than 6 years (effectively, excluding the gaps) at ESPSA and with more than 15 years at ZADAA, exceptionally long. This allows reducing the assumed uncertainty of the adjustment methodology to 1.5% for ESPSA and to 1% for ZADAA.

The combined uncertainties considering multiple years ('multiple year uncertainty') for each of the four data sets is calculated by following the Gaussian law of error propagation by quadratically adding the three sources of uncertainties. To calculate the 'single year uncertainty', which refers to single year inter-annual variability, the Gaussian law of error propagation is followed by quadratically adding the multiple year uncertainty and the standard deviation of the inter-annual variation. Table 5-4 below shows the values of uncertainties taken into consideration:

Calculation of long-term uncertainty of long-term average of DNI for multiple year and single year

site	overall uncertainty				adjust-ment uncer-tainty	uncer-tainty on-site meas.	uncertainty due to temporal coverage (multiple year)	uncertainty due to temporal coverage (single year)
	multiple year $U_{my}=\sqrt{(A^2+B^2+C_{my}^2)}$		single year $U_{sy}=\sqrt{(U_{my}^2+C_{sy}^2)}$		A	B	$C_{my}=C_{sy}/\sqrt{n}$	C_{sy}
	abs. [W/m²]	rel.[%]	abs. [W/m²]	rel.[%]	[%]	[%]	[%]	[%]
ESPSA	6.9	2.7	14.1	5.6	1.5	2	1.1	4.9
DZTAM	6.7	2.5	14.1	5.2	1	2	1.0	4.5
SASOV	7.8	3.0	14.3	5.5	2	2	1.0	4.6
ZADAA	9.0	2.9	12.7	4.1	2	2	0.7	2.9

Table 5-4: Explanation of derivation of the total long-term uncertainty of DNI following Meyer et al. (2008).

For ESPSA the total uncertainty of the long-term value of DNI is found to be 2.7% for multiple years and 5.6% for single year. For DZTAM the total uncertainty of the long-term value of DNI is found to be 2.5% for multiple years and 5.2% for single year. For SASOV the total uncertainty of the long-term value of DNI is found to be 3.0% for multiple years and 5.5% for single year. For ZADAA the total uncertainty of the long-term value of DNI is found to be 2.9% for multiple years and 4.1% for single year.

5.5. Annual cycle of DNI

Figure 5-7 and Table 5-5 to Table 5-8 show the long-term annual cycle of DNI of best estimate in comparison to DLR-SOLEMI, adjusted DLR-SOLEMI, on-site measurements and DLR-ISIS. It can be seen from the comparison of annual cycles of measured values and the best estimate that the trend of seasonal variation of DNI matches quite well.

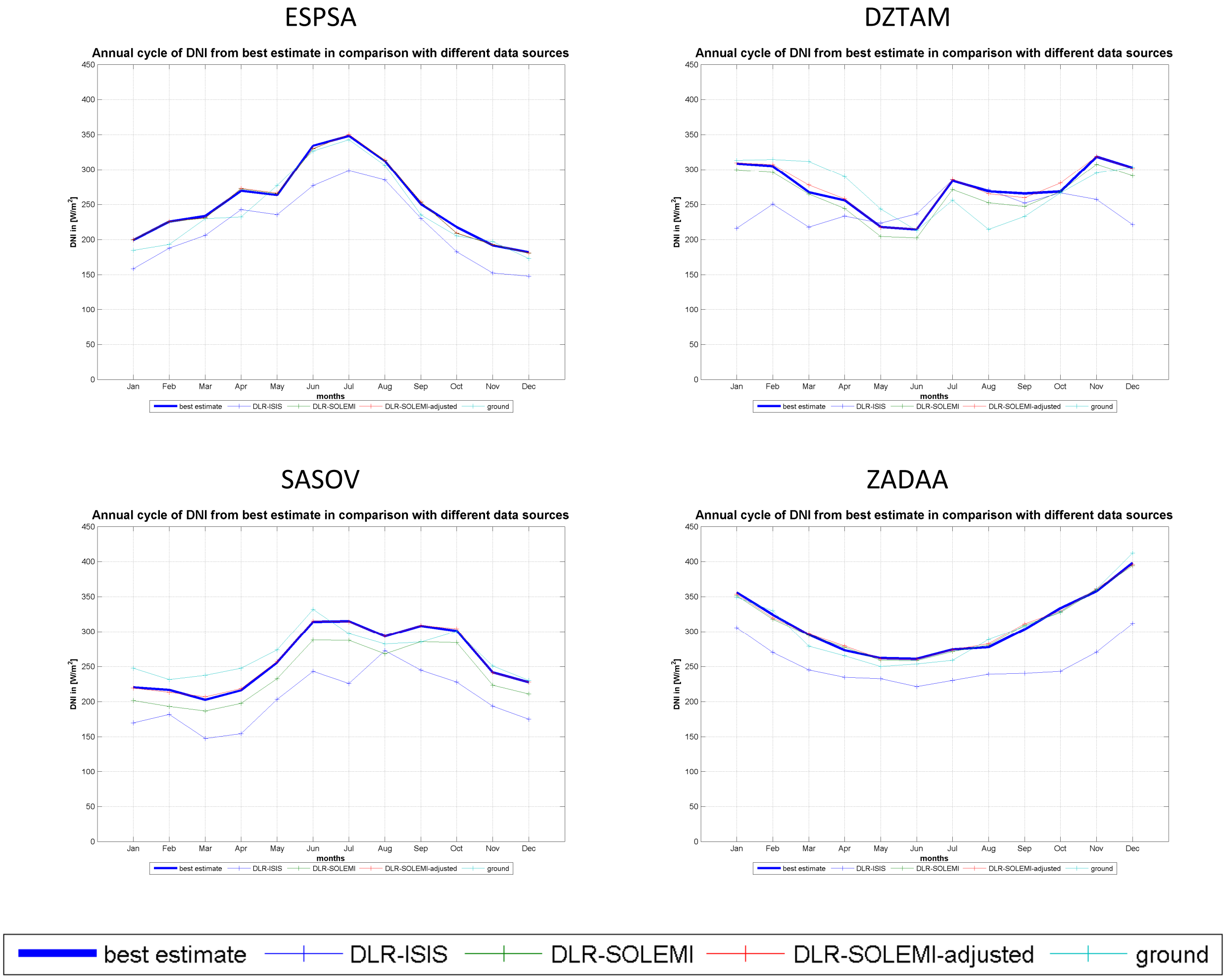

Figure 5-7: Long-term monthly averages of DNI obtained from DLR-SOLEMI, adjusted DLR-SOLEMI, DLR-ISIS in comparison to on-site measurement data sets and long term best estimate for the four demo sites.

5.6. P90 and PXY values of DNI

As mentioned in Chapter 3.9, for risk assessment of the solar power projects, a Meteorological Year representing the P90 value of DNI is derived based on the P50 value and the associated uncertainty.

For the demo site 1, ESPSA, it is found that the P90 values of DNI at this site considering uncertainty associated with inter-annual variability related to single-year and multiple-years differ by 3.8%. The multiple years P90 value of DNI at this site is estimated to be 3.5% below the long-term best estimate (P50). This leads to a long-term average P90 value of DNI based on multiple years uncertainty of 244 W/m^2 or 2135 kWh/m^2 per year or 5.84 kWh/m^2 per day. The single year P90 value of DNI at this site is estimated to be 7.1% below the long-term best estimate (P50). This leads to a long-term average P90 value of DNI based on single year uncertainty of 234 W/m^2 or 2054 kWh/m^2 per year or 5.62 kWh/m^2 per day.

For the demo site 2, DZTAM, it is found that the P90 values of DNI at this site considering uncertainty associated with inter-annual variability related to single-year and multiple-years differ by 3.6%. The multiple years P90 value of DNI at this site is estimated to be 3.2% below the long-term best estimate (P50). This leads to a long-term average P90 value of DNI based on multiple years uncertainty of 264 W/m^2 or 2318 kWh/m^2 per year or 6.35 kWh/m^2 per day. The single year P90 value of DNI at this site is estimated to be 6.6% below the long-term best estimate (P50). This leads to a long-term average P90 value of DNI based on single year uncertainty of 255 W/m^2 or 2235 kWh/m^2 per year or 6.12 kWh/m^2 per day.

For the demo site 3, SASOV, it is found that the P90 values of DNI at this site considering uncertainty associated with inter-annual variability related to single-year and multiple-years differ by 3.3%. The multiple years P90 value of DNI at this site is estimated to be 3.9% below the long-term best estimate (P50). This leads to a long-term average P90 value of DNI based on multiple years uncertainty of 249 W/m^2 or 2187 kWh/m^2 per year or 5.99 kWh/m^2 per day. The single year P90 value of DNI at this site is estimated to be 7.1% below the long-term best estimate (P50). This leads to a long-term average P90 value of DNI based on single year uncertainty of 241 W/m^2 or 2114 kWh/m^2 per year or 5.79 kWh/m^2 per day.

For the demo site 4, ZADAA it is found that the P90 values of DNI at this site considering uncertainty associated with inter-annual variability related to single-year and multiple-years differ by 1.6%. The multiple years P90 value of DNI at this site is estimated to be 3.7% below the long-term best estimate (P50). This leads to a long-term average P90 value of DNI based on multiple years uncertainty of 298 W/m^2 or 2614 kWh/m^2 per year or 7.16 kWh/m^2 per day. The single year P90 value of DNI at this site is estimated to be 5.2% below the long-term best estimate (P50). This leads to a long-term average P90 value of DNI based on single year uncertainty of 294 W/m^2 or 2573 kWh/m^2 per year or 7.05 kWh/m^2 per day.

Table 5-5 to Table **5-8** show for the four demos sites for each month the long term best estimate (P50) in comparison to various PXY cases for multiple and single year uncertainty of DNI. Also the long term averages of DLR-ISIS, DLR-SOLEMI, adjusted DLR-SOLEMI and on-site measurements are listed.

ESPSA																			
	sources / best estimate (P50) [W/m²] for avg. or [kWh/m²] for sums					multiple year [W/m²] for avg. or [kWh/m²] for sums							single year [W/m²] for avg. or [kWh/m²] for sums						
	DLR ISIS	**DLR SOLEMI**	**DLR SOLEMI adapted**	**on site**	**P50**	**P70**	**P75**	**P80**	**P85**	**P90**	**P95**	**P99**	**P70**	**P75**	**P80**	**P85**	**P90**	**P95**	**P99**
Jan	158	200	200	185	199	196	195	194	193	191	189	185	192	190	187	185	181	176	167
Feb	188	217	217	193	221	218	217	215	214	212	210	205	213	211	208	205	202	196	186
Mar	206	227	227	230	233	229	228	227	226	224	221	216	225	222	220	216	213	207	196
Apr	243	274	275	232	269	264	263	262	260	258	255	249	259	256	253	250	245	238	226
May	235	268	268	277	266	262	261	259	258	256	253	247	256	254	251	247	243	236	223
Jun	277	327	327	327	322	317	315	314	312	309	306	299	310	307	303	299	294	285	270
Jul	298	350	350	343	348	342	341	339	337	334	330	323	335	332	328	323	317	308	292
Aug	285	311	311	306	311	306	304	303	301	299	295	288	300	296	293	289	283	276	261
Sep	230	256	257	235	259	255	253	252	251	249	246	240	250	247	244	240	236	230	217
Oct	183	210	211	205	215	212	211	210	208	207	204	200	207	205	203	200	196	191	181
Nov	152	195	195	197	192	189	188	187	185	184	182	178	185	183	181	178	175	170	161
Dec	148	181	181	173	182	179	178	177	176	175	173	169	175	173	171	169	166	161	153
year	217	251	252	242	**252**	247	246	245	243	241	239	233	242	240	237	234	229	223	211
year sum	1904	2204	2206	2121	**2205**	2169	2159	2147	2134	2117	2092	2045	2125	2102	2077	2047	2010	1954	1851
day sum	5.21	6.04	6.04	5.81	**6.04**	5.94	5.91	5.88	5.84	5.80	5.73	5.60	5.82	5.76	5.69	5.60	5.50	5.35	5.07

Table 5-5: For ESPSA: Long term best estimate (P50) in comparison to various PXY cases for multiple and single year uncertainty of DNI as well as long term averages of DLR-ISIS, DLR-SOLEMI, DLR-SOLEMI$_{adjusted}$ and on-site measurements for each month.

DZTAM																			
	sources / best estimate (P50) [W/m²] for avg. or [kWh/m²] for sums					multiple year [W/m²] for avg. or [kWh/m²] for sums							single year [W/m²] for avg. or [kWh/m²] for sums						
	DLR ISIS	**DLR SOLEMI**	**DLR SOLEMI adapted**	**on site**	**P50**	**P70**	**P75**	**P80**	**P85**	**P90**	**P95**	**P99**	**P70**	**P75**	**P80**	**P85**	**P90**	**P95**	**P99**
Jan	216	300	310	314	309	305	304	302	301	299	296	291	300	298	295	292	288	283	272
Feb	251	296	308	315	305	301	300	299	297	295	293	288	297	294	292	289	285	279	268
Mar	218	265	278	312	268	264	263	262	261	259	257	252	260	258	256	253	250	245	236
Apr	233	244	258	290	256	253	252	251	249	248	246	241	249	247	245	242	239	234	225
May	223	204	217	244	218	215	215	214	213	211	209	206	212	211	209	206	204	200	192
Jun	237	202	215	213	214	212	211	210	209	208	206	202	209	207	205	203	200	196	189
Jul	285	272	286	256	284	280	279	278	277	275	272	268	276	274	271	269	265	260	250
Aug	271	252	265	215	269	265	264	263	262	260	258	253	261	259	257	254	251	246	236
Sep	252	247	260	233	266	262	261	260	259	257	255	250	258	256	254	251	248	243	234
Oct	267	269	280	266	268	265	264	263	262	260	258	253	261	259	257	254	251	246	236
Nov	257	308	319	295	319	314	313	312	310	308	306	300	310	307	305	301	297	291	280
Dec	221	291	302	303	303	299	298	296	295	293	290	285	294	292	289	286	283	277	266
year	244	262	275	271	**273**	269	268	267	266	264	262	257	266	264	261	258	255	250	240
year sum	2141	2301	2407	2378	**2393**	2362	2354	2344	2332	2318	2297	2256	2328	2310	2289	2265	2235	2190	2106
day sum	5.86	6.30	6.59	6.51	**6.55**	6.47	6.44	6.42	6.39	6.35	6.29	6.18	6.37	6.32	6.27	6.20	6.12	6.00	5.77

Table 5-6: For DZTAM: Long term best estimate (P50) in comparison to various PXY cases for multiple and single year uncertainty of DNI as well as long term averages of DLR-ISIS, DLR-SOLEMI, DLR-SOLEMI$_{adjusted}$ and on-site measurements for each month.

SASOV																			
	sources / best estimate (P50) [W/m²] for avg. or [kWh/m²] for sums					multiple year [W/m²] for avg. or [kWh/m²] for sums							single year [W/m²] for avg. or [kWh/m²] for sums						
	DLR ISIS	**DLR SOLEMI**	**DLR SOLEMI adapted**	**on site**	**P50**	**P70**	**P75**	**P80**	**P85**	**P90**	**P95**	**P99**	**P70**	**P75**	**P80**	**P85**	**P90**	**P95**	**P99**
Jan	170	202	219	248	220	217	216	215	214	212	210	205	214	212	210	208	205	200	192
Feb	182	193	213	232	217	213	212	211	210	208	206	201	210	208	206	204	201	197	189
Mar	148	187	207	238	202	199	198	197	196	195	192	188	197	195	193	191	188	184	176
Apr	154	197	218	248	216	213	212	210	209	208	205	201	210	208	206	204	201	196	188
May	203	233	257	274	256	252	251	249	248	246	243	238	248	246	244	241	238	233	223
Jun	243	288	315	332	314	309	308	306	304	302	298	292	305	302	299	296	292	286	274
Jul	226	287	314	297	315	310	308	307	305	303	299	293	306	303	300	297	293	286	274
Aug	273	268	294	282	293	289	287	286	284	282	279	273	285	282	280	277	273	267	256
Sep	245	285	309	285	308	303	302	300	299	296	293	287	299	297	294	291	286	280	269
Oct	228	284	304	300	301	296	295	293	292	289	286	280	292	290	287	284	280	274	262
Nov	194	223	241	251	241	238	237	235	234	232	229	224	234	232	230	228	224	219	210
Dec	175	211	228	230	228	224	223	222	220	219	216	212	221	219	217	214	211	207	198
year	203	238	260	268	**260**	255	254	253	251	249	247	241	252	250	247	245	241	236	226
year sum	1783	2090	2280	2350	**2275**	2239	2229	2217	2204	2187	2162	2115	2209	2190	2169	2145	2114	2068	1983
day sum	4.88	5.72	6.24	6.43	**6.23**	6.13	6.10	6.07	6.03	5.99	5.92	5.79	6.05	6.00	5.94	5.87	5.79	5.66	5.43

Table 5-7: For SASOV: Long term best estimate (P50) in comparison to various PXY cases for multiple and single year uncertainty of DNI as well as long term averages of DLR-ISIS, DLR-SOLEMI, DLR-SOLEMI$_{adjusted}$ and on-site measurements for each month.

ZADAA																			
	sources / best estimate (P50) [W/m^2] for avg. or [kWh/m^2] for sums					multiple year [W/m^2] for avg. or [kWh/m^2] for sums							single year [W/m^2] for avg. or [kWh/m^2] for sums						
	DLR ISIS	**DLR SOLEMI**	**DLR SOLEMI adapted**	**on site**	**P50**	**P70**	**P75**	**P80**	**P85**	**P90**	**P95**	**P99**	**P70**	**P75**	**P80**	**P85**	**P90**	**P95**	**P99**
Jan	306	352	354	349	356	351	349	347	345	343	339	332	349	346	344	341	338	332	322
Feb	270	318	320	330	324	319	318	316	315	312	309	302	318	316	313	311	307	303	294
Mar	245	295	297	279	296	291	290	289	287	285	282	276	289	288	286	283	280	276	268
Apr	235	278	280	265	273	269	268	266	265	263	260	255	267	266	264	261	259	255	247
May	233	259	261	250	262	258	257	256	254	252	250	244	256	255	253	251	248	245	237
Jun	222	258	261	254	261	257	256	254	253	251	248	243	255	254	252	250	247	243	236
Jul	230	272	274	259	274	270	269	268	266	264	261	256	268	267	265	263	260	256	248
Aug	239	281	283	289	278	273	272	271	269	267	264	259	272	270	268	266	263	259	251
Sep	241	309	311	307	303	299	297	296	294	292	289	283	297	295	293	290	287	283	274
Oct	243	328	329	329	334	329	327	325	324	321	318	311	327	324	322	320	316	311	302
Nov	271	360	362	361	358	352	351	349	347	344	341	334	350	348	346	343	339	334	324
Dec	312	394	396	412	398	392	390	388	386	383	379	371	390	387	384	381	377	371	360
year	254	309	310	307	**310**	305	304	302	300	298	295	289	303	301	299	297	294	289	280
year sum	2225	2705	2720	2691	**2716**	2674	2662	2649	2633	2614	2585	2531	2657	2641	2622	2601	2573	2533	2458
day sum	6.09	7.40	7.45	7.37	**7.43**	7.32	7.29	7.25	7.21	7.16	7.08	6.93	7.28	7.23	7.18	7.12	7.05	6.94	6.73

Table 5-8: For ZADAA: Long term best estimate (P50) in comparison to various PXY cases for multiple and single year uncertainty of DNI as well as long term averages of DLR-ISIS, DLR-SOLEMI, DLR-SOLEMI$_{adjusted}$ and on-site measurements for each month.

5.7. Frequency distribution of DNI

The frequency distribution of DNI derived from original and adjusted DLR-SOLEMI time series in comparison to on-site measurements as well as TMY, MY75, MY90 and MY95 (multiple year) is shown in Figure 5-8. Figure 5-9 represents the cumulative frequency distribution and duration curve of TMY in comparison to MY75, MY90 and MY95, which is helpful for engineering purpose.

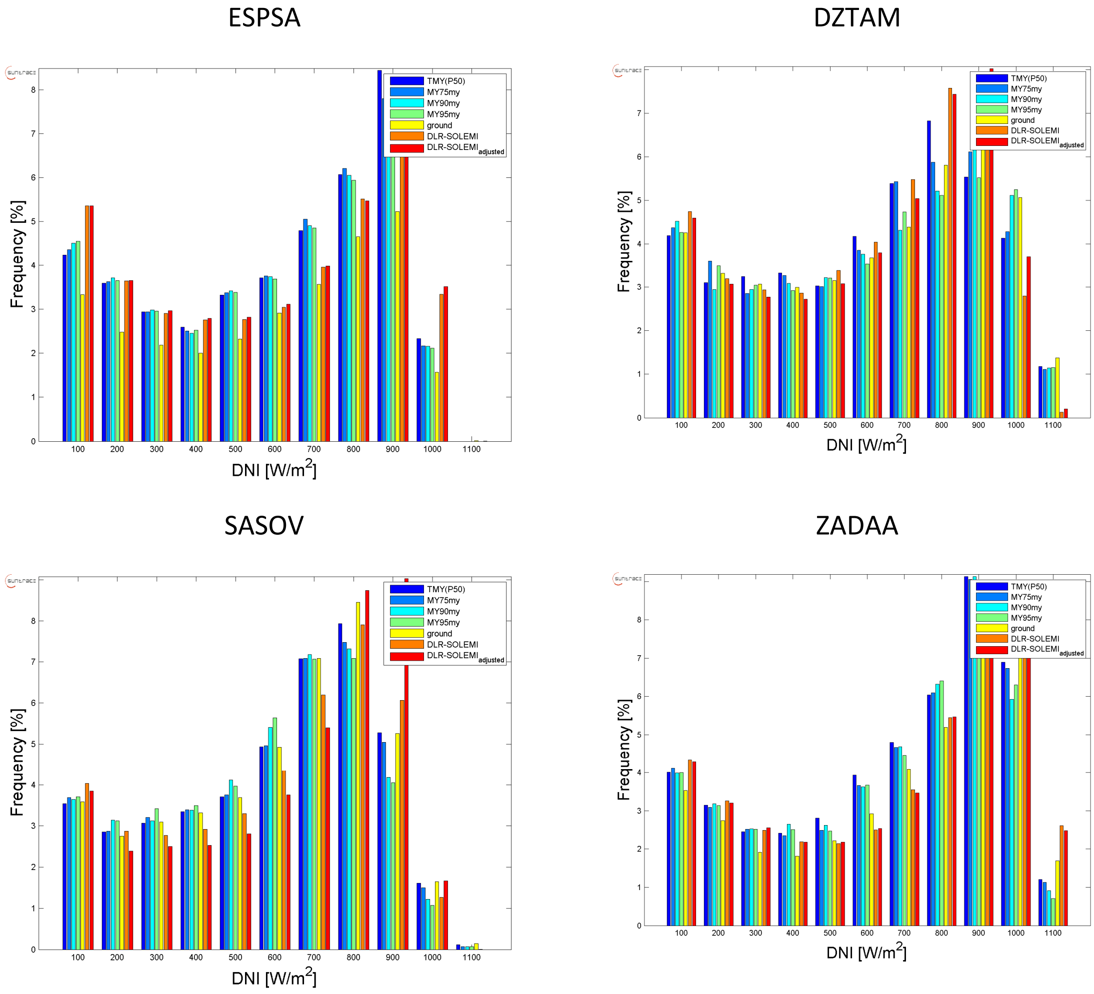

Figure 5-8: Frequency distribution of DNI obtained from adjusted DLR-SOLEMI, DLR-SOLEMI and on-site measurements datasets in comparison to TMY, MY75, MY90 and MY95 (multiple years).

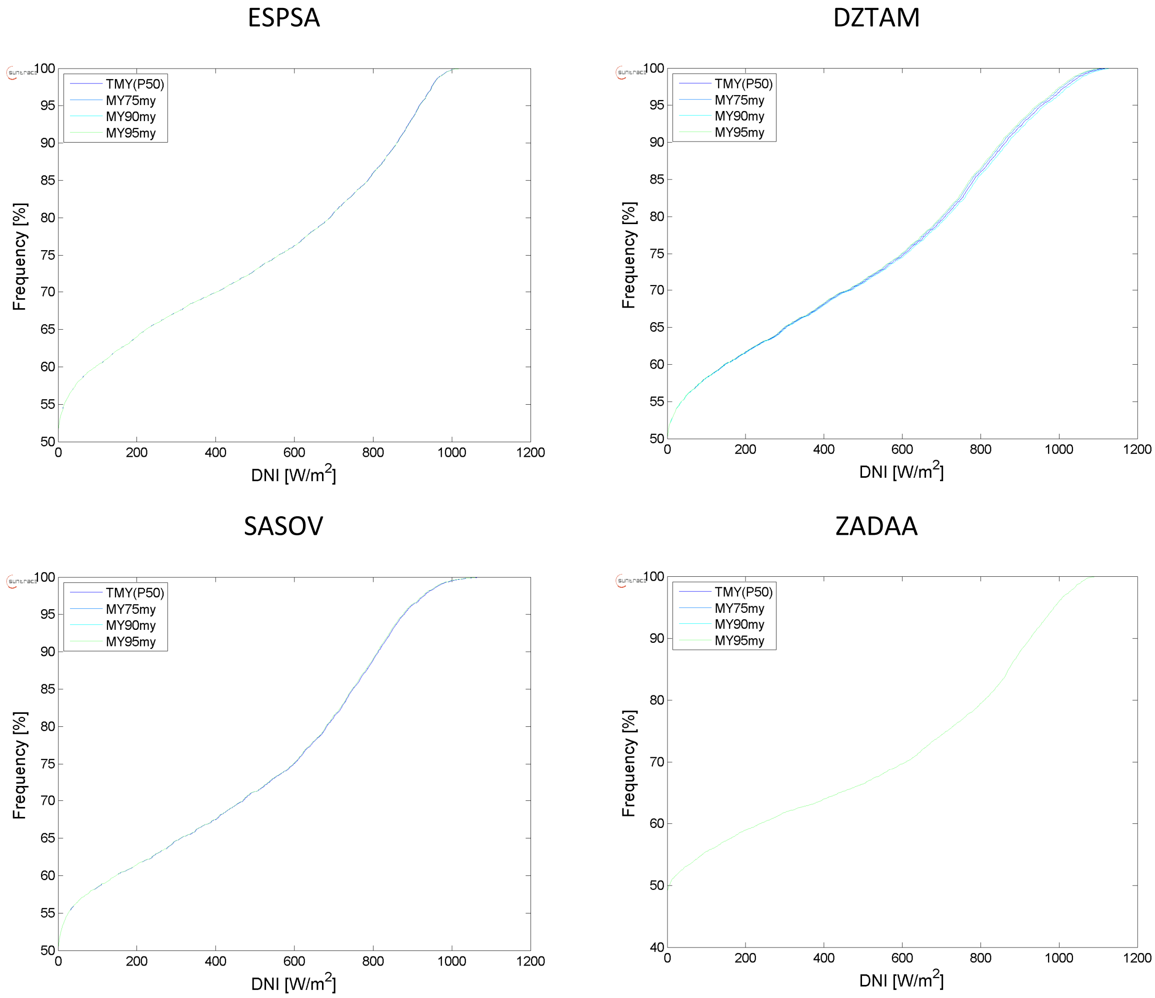

Figure 5-9: Duration curve of DNI obtained from TMY, MY75, MY90 and MY-P95 (multiple years).

5.8. Supplied CSP/STE-specific meteorological data sets

In the following the characteristics of the TMY and MY90 (with respect to multiple year uncertainty) in hourly time resolution are summarized for the four demo sites. Note that the given monthly minima and maxima are calculated by the hourly values of the TMY and MY90.

5.8.1. ESPSA

5.8.1.1. Direct Normal Irradiance

For the TMY (P50 value) of the demo site ESPSA the annual mean direct normal irradiance is 252 W/m^2 equal to an annual sum of 2207 kWh/m^2/a. The DNI exceeded for 2995 hours 250 W/m^2 with an average of 700 W/m^2 taking just the DNI values higher than 250 W/m^2 into account.

For the MY90 with respect to multiple year uncertainty the annual mean direct normal irradiance is 243 W/m^2 equal to an annual sum of 2132 kWh/m^2/a. The DNI exceeded for 2910 hours 250 W/m^2 with an average of 693 W/m^2 taking just the DNI values higher than 250 W/m^2 into account.

Figure 5-10 (TMY) and Figure 5-11 (MY90) show the monthly values, the hours of the day over the year as well as the relative frequency distribution of DNI for the TMY and MY90 at ESPSA. The monthly values at ESPSA for the TMY are shown in Table 5-9 and for the MY90 with respect to multiple year uncertainty in Table 5-10.

direct normal irradiance TMY

	average [W/m^2]	min [W/m^2]	max [W/m^2]	sum [kWh/m^2]
Jan	197	0	1000	147
Feb	225	0	997	151
Mar	234	0	1024	174
Apr	270	0	1022	194
May	261	0	999	194
Jun	336	0	974	242
Jul	346	0	964	258
Aug	312	0	925	232
Sep	250	0	962	180
Oct	218	0	1005	162
Nov	192	0	996	138
Dec	182	0	997	135
Year	252	0	1024	2207

Table 5-9: ESPSA: TMY - monthly values of DNI

direct normal irradiance MY90 (multiple year)

	average [W/m^2]	min [W/m^2]	max [W/m^2]	sum [kWh/m^2]
Jan	192	0	960	143
Feb	217	0	1025	146
Mar	225	0	1024	167
Apr	260	0	1007	187
May	254	0	992	189
Jun	323	0	981	232
Jul	333	0	964	248
Aug	302	0	921	225
Sep	241	0	962	174
Oct	210	0	1005	156
Nov	185	0	996	133
Dec	176	0	997	131
Year	243	0	1025	2132

Table 5-10: ESPSA: MY90my - monthly values of DNI

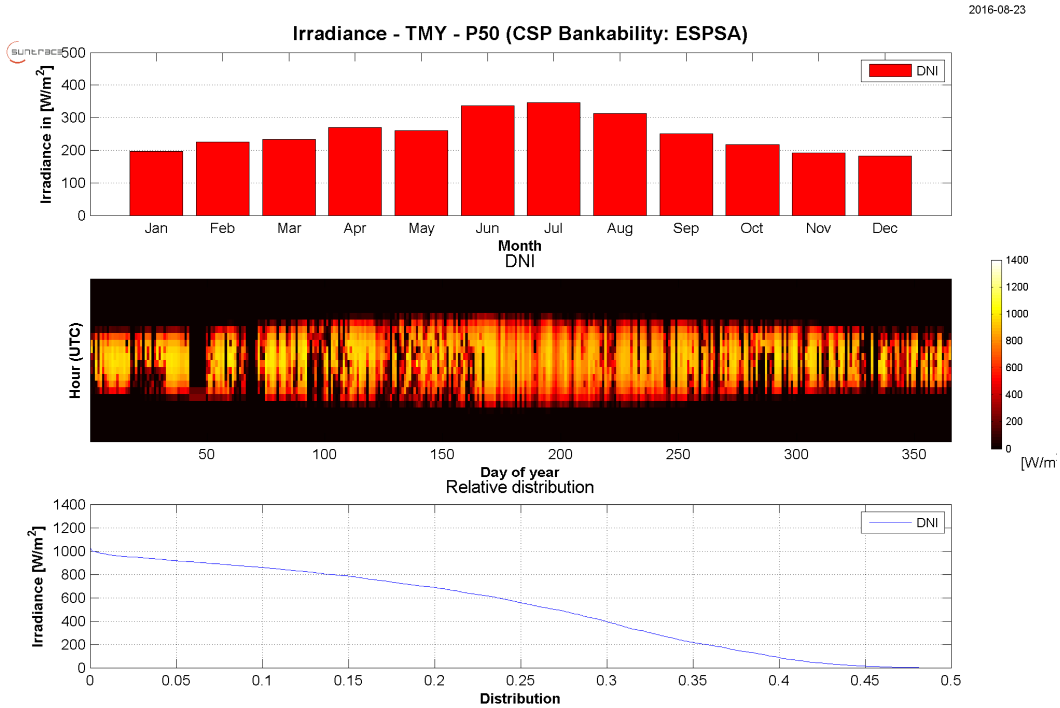

Figure 5-10: ESPSA: TMY - monthly values (top), hours of the day over the year (middle) and distribution (bottom) of DNI.

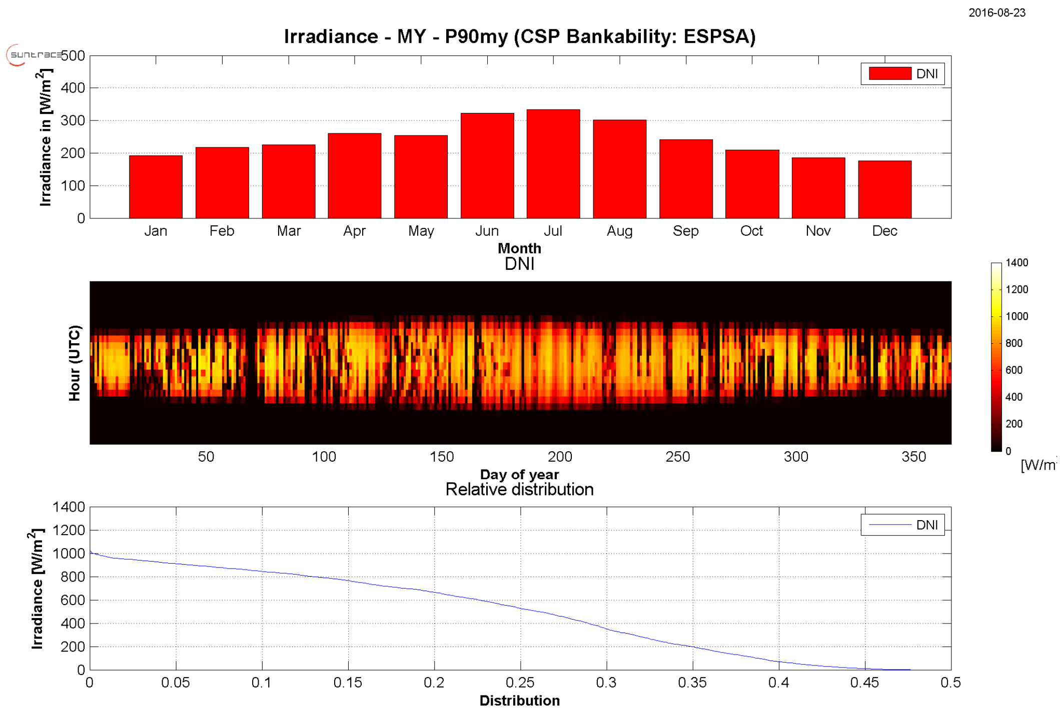

Figure 5-11: ESPSA: MY90 (multiple year) - monthly values (top), hours of the day over the year (middle) and distribution (bottom) of DNI.

5.8.1.2. Global and Diffuse Horizontal Irradiance

The monthly values of the TMY for GHI and DHI at ESPSA are listed in Table 5-11 to Table 5-14. Figure 5-12 to Figure 5-15 show the values in 60min time resolution over the year. For the TMY the annual mean GHI is 212 W/m^2 equal to an annual sum of 1860 kWh/m^2/a. For the MY90 (multiple year) the annual mean GHI is 209 W/m^2 equal to an annual sum of 1834 kWh/m^2/a.

global horizontal irradiance TMY

	average [W/m^2]	min [W/m^2]	max [W/m^2]	sum [kWh/m^2]
Jan	116	0	720	86
Feb	146	0	796	98
Mar	200	0	974	149
Apr	255	0	1034	184
May	285	0	1113	212
Jun	319	0	1066	230
Jul	327	0	997	243
Aug	288	0	1018	215
Sep	219	0	903	157
Oct	167	0	800	124
Nov	115	0	655	82
Dec	106	0	555	79
Year	212	0	1113	1860

Table 5-11: ESPSA: TMY - monthly values of GHI

global horizontal irradiance MY90 (mult. year)

	average [W/m^2]	min [W/m^2]	max [W/m^2]	sum [kWh/m^2]
Jan	114	0	699	85
Feb	151	0	948	101
Mar	196	0	974	146
Apr	252	0	1034	181
May	282	0	1106	210
Jun	313	0	1031	226
Jul	319	0	997	237
Aug	285	0	1018	212
Sep	214	0	903	154
Oct	164	0	773	122
Nov	113	0	655	81
Dec	106	0	555	79
Year	209	0	1106	1834

Table 5-12: ESPSA: MY90my - monthly values GHI

diffuse horizontal irradiance TMY

	average [W/m^2]	min [W/m^2]	max [W/m^2]	sum [kWh/m^2]
Jan	39	0	357	29
Feb	42	0	367	29
Mar	64	0	454	47
Apr	82	0	498	59
May	100	0	523	74
Jun	84	0	494	60
Jul	80	0	547	60
Aug	77	0	433	57
Sep	67	0	456	48
Oct	55	0	376	41
Nov	35	0	314	25
Dec	37	0	281	28
Year	64	0	547	557

Table 5-13: ESPSA: TMY - monthly values of DHI

diffuse horizontal irradiance MY90 (mult year)

	average [W/m^2]	min [W/m^2]	max [W/m^2]	sum [kWh/m^2]
Jan	39	0	357	29
Feb	47	0	363	32
Mar	66	0	454	49
Apr	86	0	498	62
May	103	0	540	77
Jun	83	0	510	60
Jul	81	0	547	60
Aug	81	0	433	60
Sep	68	0	456	49
Oct	56	0	376	42
Nov	35	0	314	25
Dec	38	0	276	28
Year	65	0	547	572

Table 5-14: ESPSA: MY90my - monthly values DHI

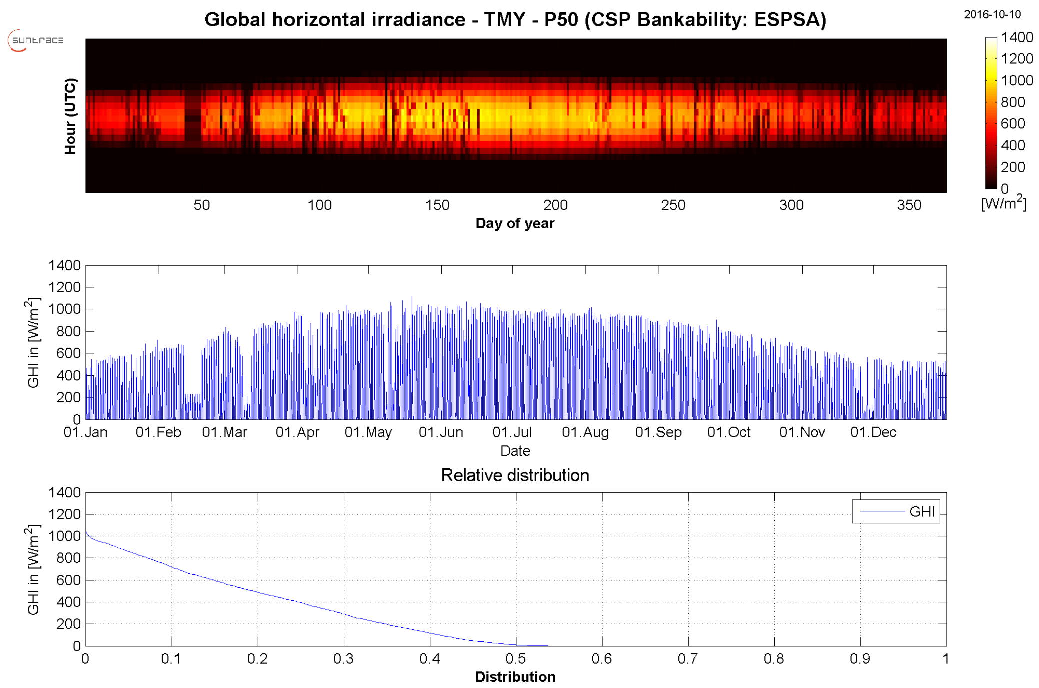

Figure 5-12: ESPSA: TMY - hours of the day over the year (top), hourly values (middle) and distribution (bottom) of GHI

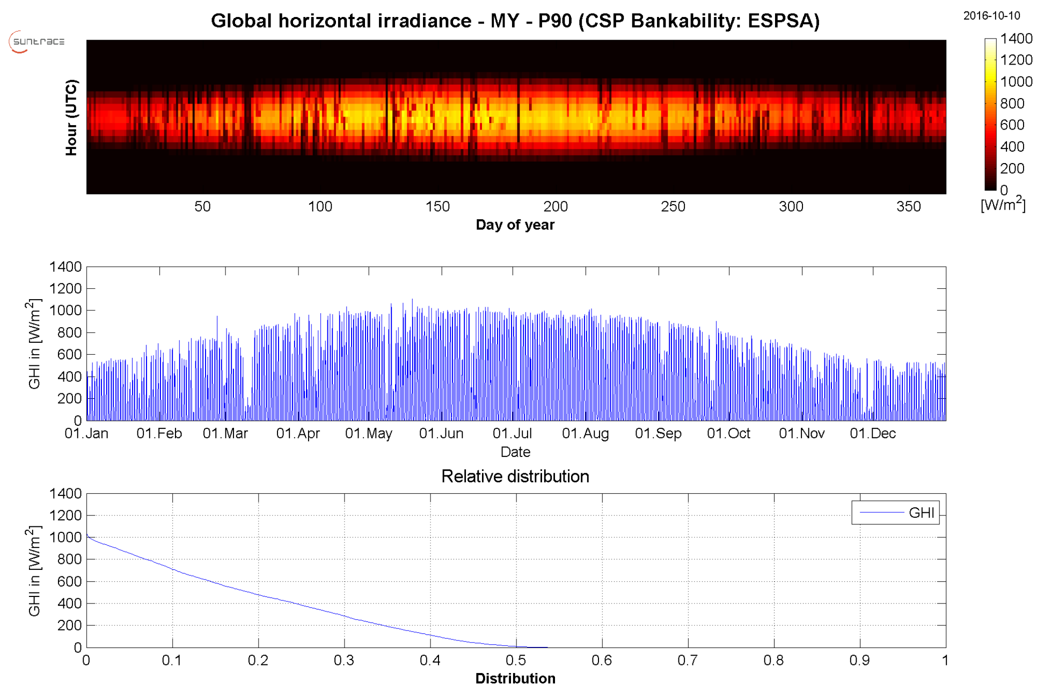

Figure 5-13: ESPSA: MY90my - hours of the day over the year (top), hourly values (middle) and distribution (bottom) of GHI

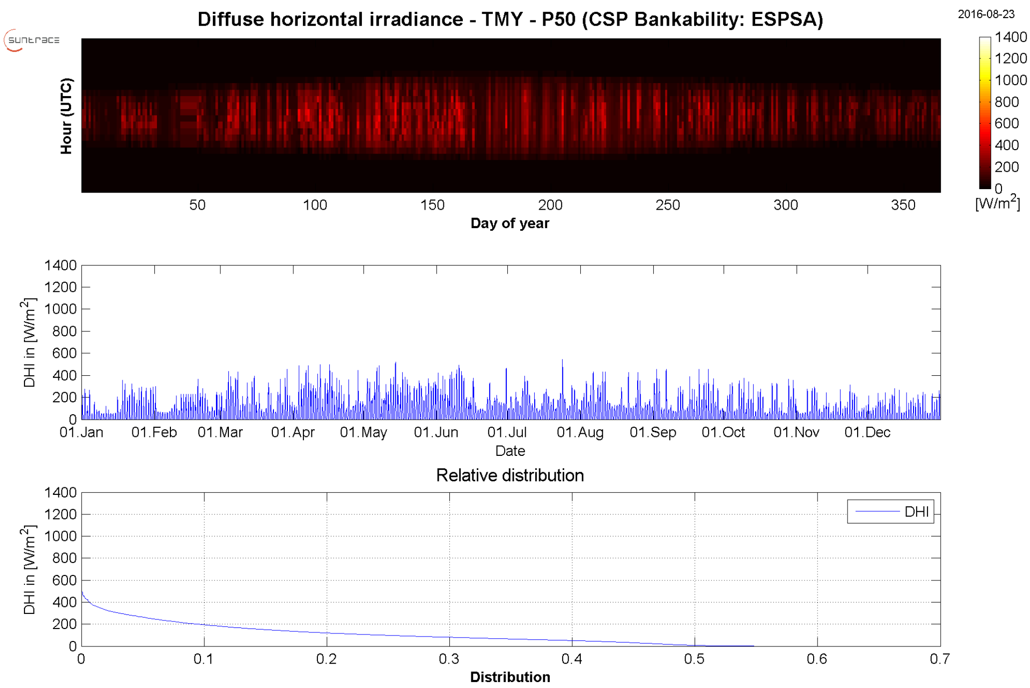

Figure 5-14: ESPSA: TMY - hours of the day over the year (top), hourly values (middle) and distribution (bottom) of DHI

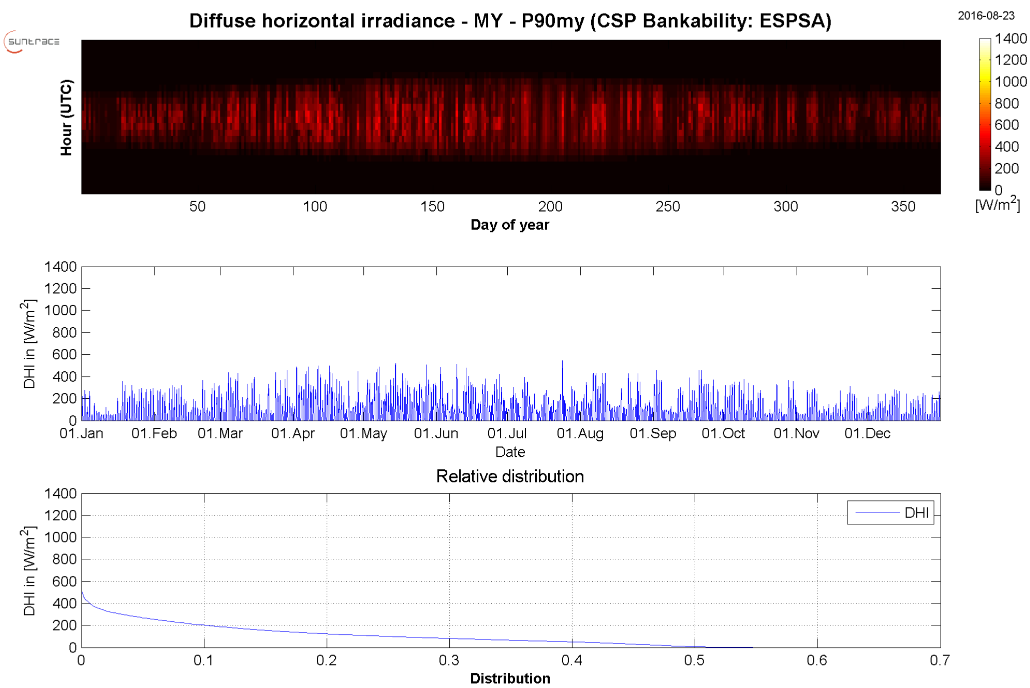

Figure 5-15: ESPSA: MY90my - hours of the day over the year (top), hourly values (middle) and distribution (bottom) of DHI

5.8.1.3. Auxiliary Meteorological Data (TMY)

The monthly values of the TMY for wind speed, wind direction, air temperature, wet bulb temperature, dew point temperature, relative humidity and barometric pressure at ESPSA are listed in Table 5-15 to Table 5-21. Figure 5-16 to Figure 5-23 show the values in 60min time resolution over the year.

<u>Wind</u>

For the TMY (P50) of ESPSA the mean horizontal wind speed is 3.4 m/s with a predominant wind direction of 41 ºN. The maximum hourly average wind speed is 18.1 m/s. This is an hourly average and can differ significantly from the wind gust, usually being defined as an average over three seconds. Wind gust values can be a multiple of the here displayed maximum hourly average wind speed. Therefore, the given values are not sufficient for plant construction.

wind speed

	average [m/s]	min [m/s]	max [m/s]
Jan	2.3	0.0	8.7
Feb	3.2	0.1	11.5
Mar	3.5	0.0	9.5
Apr	5.2	0.1	14.9
May	3.6	0.0	11.7
Jun	3.5	0.0	9.4
Jul	3.7	0.1	10.2
Aug	3.8	0.1	9.0
Sep	2.8	0.1	9.6
Oct	2.6	0.0	13.8
Nov	3.6	0.1	18.1
Dec	3.3	0.1	13.1
Year	3.4	0.0	18.1

Table 5-15: ESPSA: TMY - monthly values of wind speed

wind direction

	average [ºN]	min [ºN]	max [ºN]
Jan	28	0	359
Feb	312	0	360
Mar	47	0	360
Apr	270	2	359
May	322	0	358
Jun	77	0	360
Jul	88	1	358
Aug	78	1	360
Sep	69	1	359
Oct	353	0	360
Nov	338	0	360
Dec	342	1	357
Year	41	0	360

Table 5-16: ESPSA: TMY - monthly values of wind direction

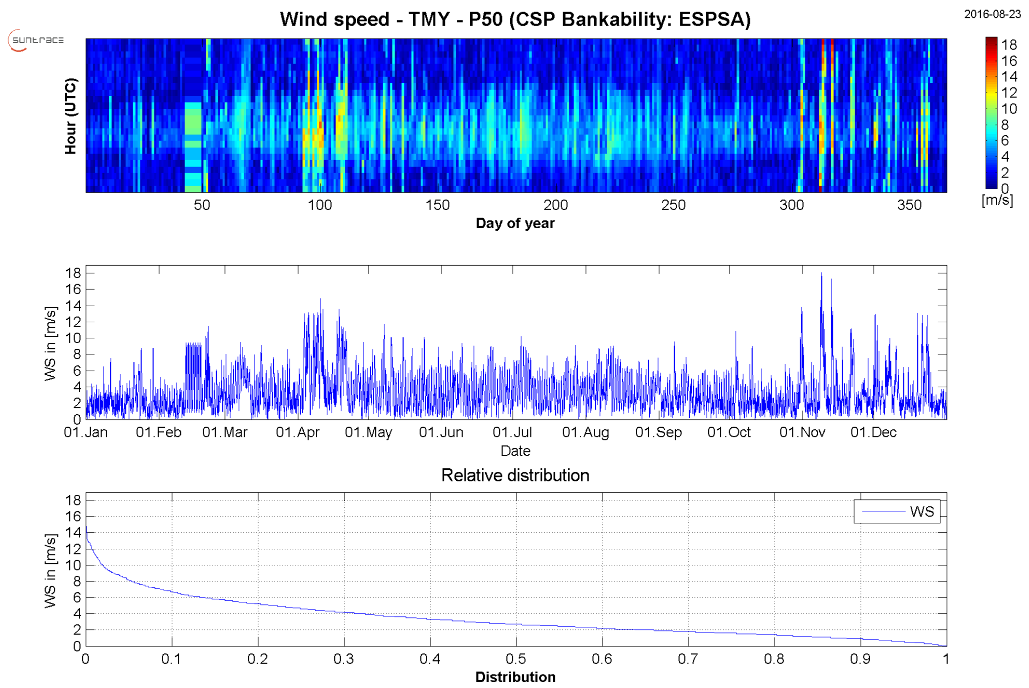

Figure 5-16: ESPSA: TMY - hours of the day over the year (top), hourly values (middle) and distribution (bottom) of wind speed

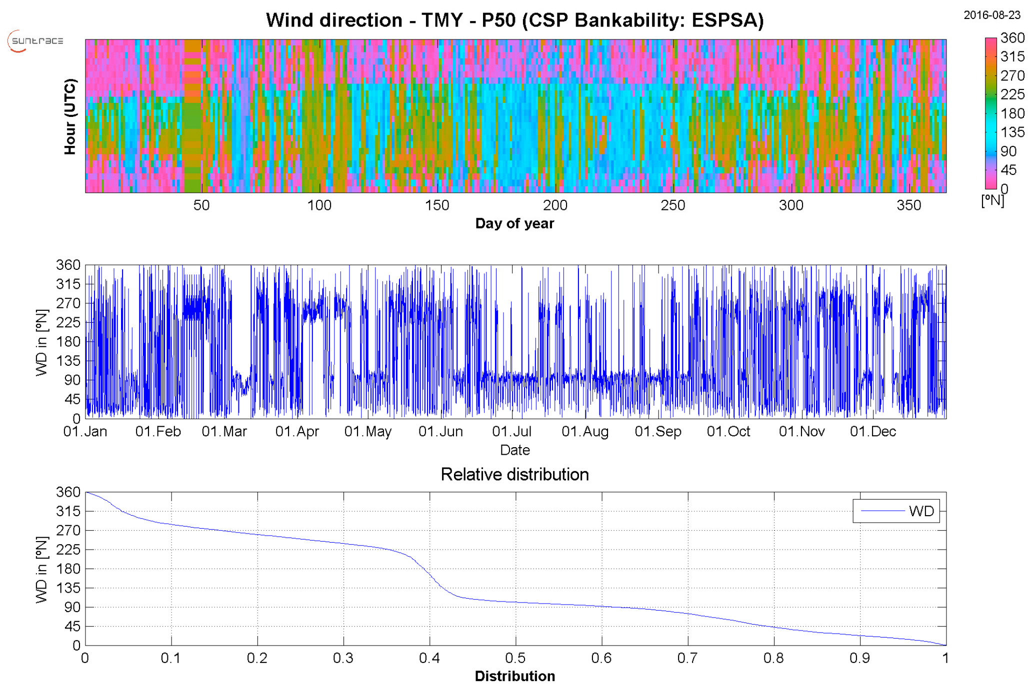

Figure 5-17: ESPSA: TMY - hours of the day over the year (top), hourly values (middle) and distribution (bottom) of wind direction

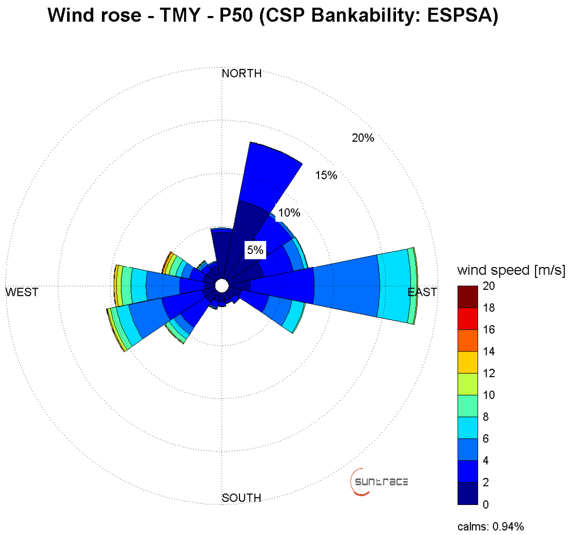

Figure 5-18: ESPSA: TMY – wind rose

Air-, Dew Point-, Wet Bulb- Temperatures and Relative Humidity

For the TMY of ESPSA the mean annual air temperature is 16.6ºC with a minimum of -3.0ºC and a maximum of 36.3ºC. The mean annual wet bulb temperature is 12.1ºC with a minimum of -3.5ºC and a maximum of 24.4ºC. The mean annual dew point temperature is 7.9ºC with a minimum of -11.0ºC and a maximum of 21.0ºC. The mean relative humidity is 60%.

air temperature

	average [ºC]	min [ºC]	max [ºC]
Jan	8.6	0.4	20.2
Feb	9.8	-0.5	24.5
Mar	11.5	-0.6	22.5
Apr	16.4	5.7	27.2
May	18.2	8.9	27.9
Jun	22.5	12.3	33.8
Jul	26.2	18.5	36.3
Aug	25.8	16.9	34.3
Sep	21.8	12.8	32.2
Oct	17.0	5.9	29.6
Nov	11.9	3.2	22.3
Dec	9.5	-3.0	27.2
Year	16.6	-3.0	36.3

Table 5-17: ESPSA: TMY - monthly values of air temperature

wet bulb temperature

	average [ºC]	min [ºC]	max [ºC]
Jan	6.4	-1.5	13.1
Feb	6.8	-1.3	15.5
Mar	8.5	-2.1	15.3
Apr	10.8	3.0	17.2
May	12.8	6.2	17.7
Jun	16.0	10.4	21.3
Jul	19.6	13.6	24.4
Aug	18.9	12.4	23.3
Sep	16.7	9.3	21.1
Oct	13.0	2.8	20.9
Nov	8.6	0.4	14.4
Dec	7.0	-3.5	18.1
Year	12.1	-3.5	24.4

Table 5-18: ESPSA: TMY - monthly values of wet bulb temperature

dew point temperature

	average	min	max
	[ºC]	[ºC]	[ºC]
Jan	3.8	-6.9	11.2
Feb	3.0	-5.3	11.7
Mar	5.3	-7.8	11.4
Apr	3.7	-8.6	12.2
May	7.5	-1.7	13.7
Jun	10.6	2.1	17.4
Jul	15.4	5.2	21.0
Aug	14.1	1.3	20.6
Sep	13.0	2.3	19.4
Oct	9.2	-8.8	17.9
Nov	4.7	-7.4	12.0
Dec	3.8	-11.0	12.9
Year	7.9	-11.0	21.0

Table 5-19: ESPSA: TMY - monthly values of dew point temperature

relative humidity

	average	min	max
	[%]	[%]	[%]
Jan	74	36	98
Feb	65	25	97
Mar	68	25	98
Apr	46	14	95
May	53	16	97
Jun	50	17	97
Jul	55	14	97
Aug	52	18	97
Sep	60	17	95
Oct	64	15	97
Nov	65	18	97
Dec	71	18	98
Year	60	14	98

Table 5-20: ESPSA: TMY - monthly values of relative humidity

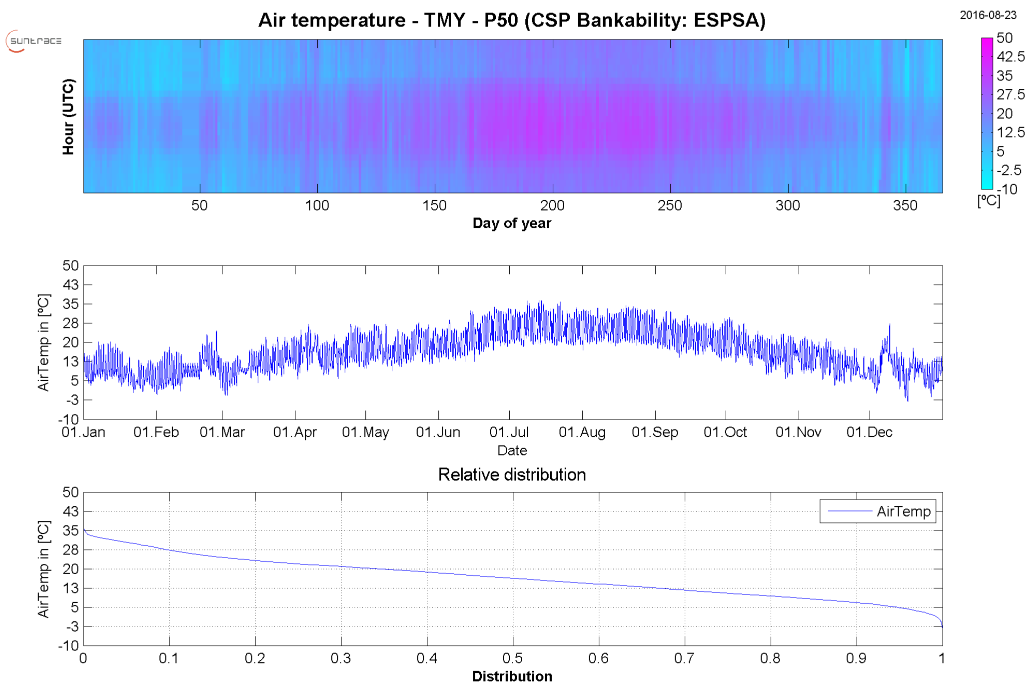

Figure 5-19: ESPSA: TMY - hours of the day over the year (top), hourly values (middle) and distribution (bottom) of air temperature

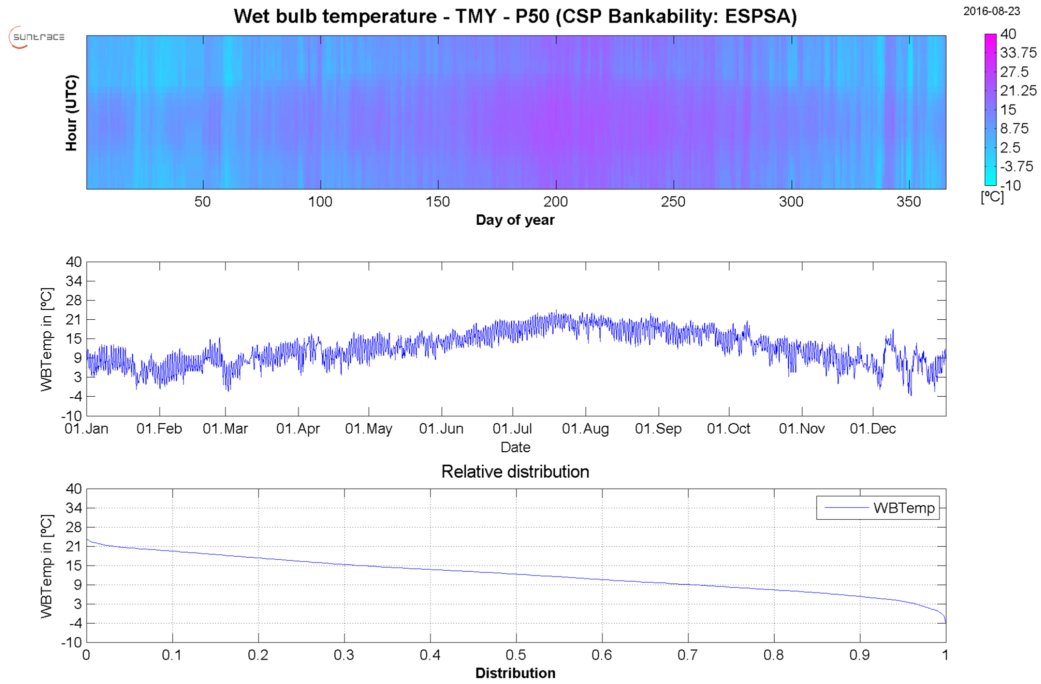

Figure 5-20: ESPSA: TMY - hours of the day over the year (top), hourly values (middle) and distribution (bottom) of wet bulb temperature

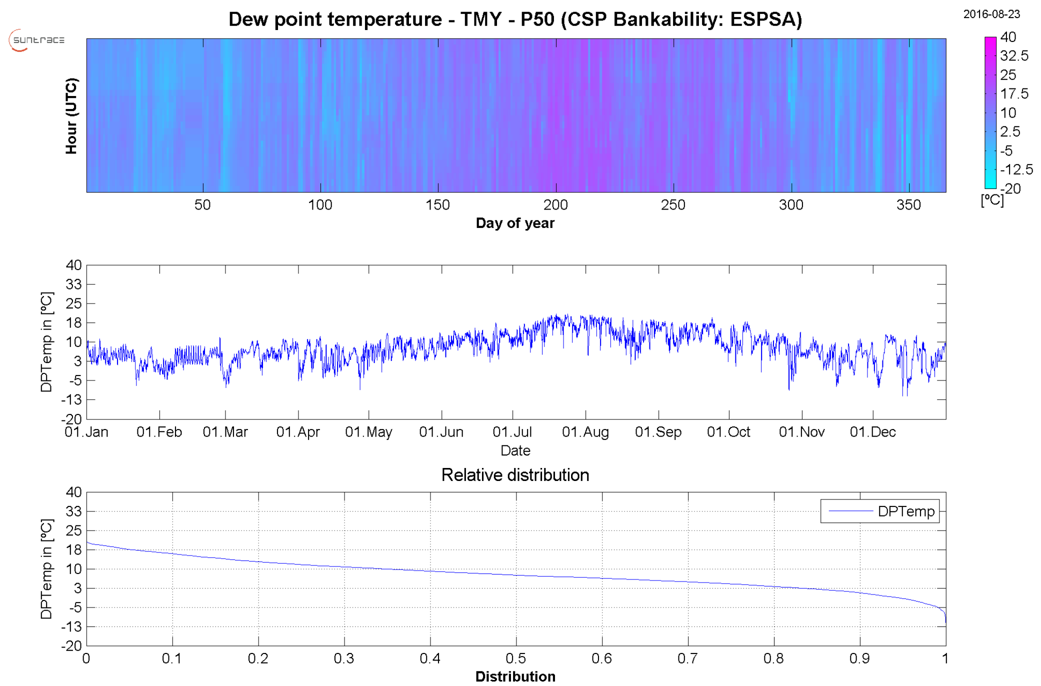

Figure 5-21: ESPSA: TMY - hours of the day over the year (top), hourly values (middle) and distribution (bottom) of dew point temperature

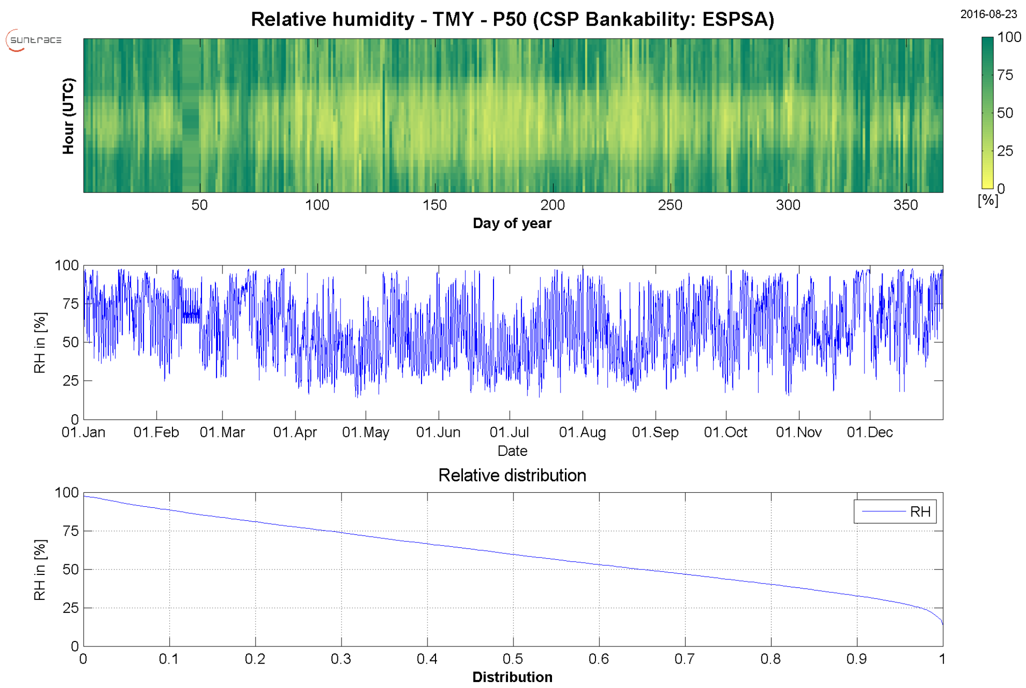

Figure 5-22: ESPSA: TMY - hours of the day over the year (top), hourly values (middle) and distribution (bottom) of relative humidity

Barometric pressure

For the TMY of ESPSA the mean barometric pressure is 959 hPa.

barometric pressure

	average [hPa]	min [hPa]	max [hPa]
Jan	962	942	972
Feb	962	946	977
Mar	961	943	971
Apr	956	943	972
May	957	949	965
Jun	960	953	965
Jul	961	953	966
Aug	960	953	965
Sep	960	951	969
Oct	957	943	969
Nov	956	938	972
Dec	957	939	971
Year	959	938	977

Table 5-21: ESPSA: TMY - monthly values of barometric pressure

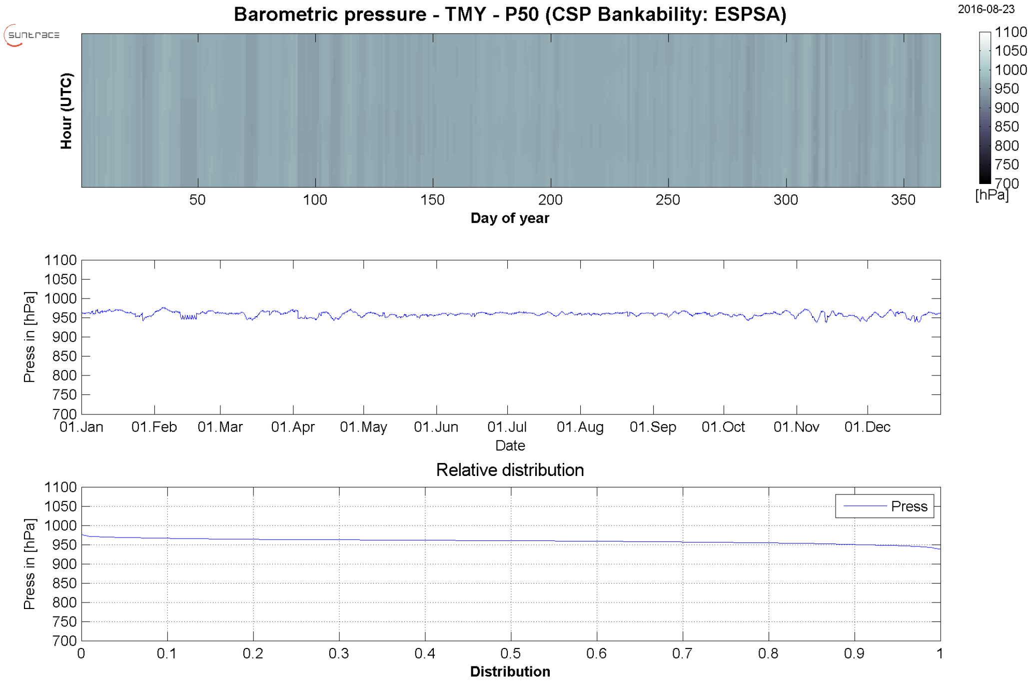

Figure 5-23: ESPSA: TMY - hours of the day over the year (top), hourly values (middle) and distribution (bottom) of barometric pressure

5.8.2. DZTAM

5.8.2.1. Direct Normal Irradiance

For the TMY (P50 value) of the demo site DZTAM the annual mean direct normal irradiance is 272 W/m^2 equal to an annual sum of 2385 kWh/m^2/a. The DNI exceeded for 3200 hours 250 W/m^2 with an average of 714 W/m^2 taking just the DNI values higher than 250 W/m^2 into account.

For the MY90 with respect to multiple year uncertainty the annual mean direct normal irradiance is 264 W/m^2 equal to an annual sum of 2313 kWh/m^2/a. The DNI exceeded for 3140 hours 250 W/m^2 with an average of 703 W/m^2 taking just the DNI values higher than 250 W/m^2 into account.

Figure 5-24 (TMY) and Figure 5-25 (MY90) show the monthly values, the hours of the day over the year as well as the relative frequency distribution of DNI for the TMY and MY90 at DZTAM. The monthly values at DZTAM for the TMY are shown in Table 5-22 and for the MY90 with respect to multiple year uncertainty in Table 5-23.

direct normal irradiance TMY

	average [W/m^2]	min [W/m^2]	max [W/m^2]	sum [kWh/m^2]
Jan	308	0	1094	229
Feb	304	0	1110	204
Mar	268	0	1133	199
Apr	256	0	995	184
May	218	0	957	162
Jun	214	0	928	154
Jul	284	0	999	211
Aug	266	0	970	198
Sep	263	0	1029	189
Oct	268	0	1005	200
Nov	318	0	1085	229
Dec	302	0	1068	225
Year	272	0	1133	2385

Table 5-22: DZTAM: TMY - monthly values of DNI

direct normal irradiance MY90 (multiple year)

	average [W/m^2]	min [W/m^2]	max [W/m^2]	sum [kWh/m^2]
Jan	298	0	1094	221
Feb	295	0	1110	198
Mar	259	0	1133	193
Apr	248	0	956	178
May	211	0	951	157
Jun	208	0	928	149
Jul	274	0	956	204
Aug	259	0	970	193
Sep	255	0	1029	183
Oct	260	0	1065	193
Nov	309	0	1057	222
Dec	296	0	1098	220
Year	264	0	1133	2313

Table 5-23: DZTAM: MY90my - monthly values of GHI

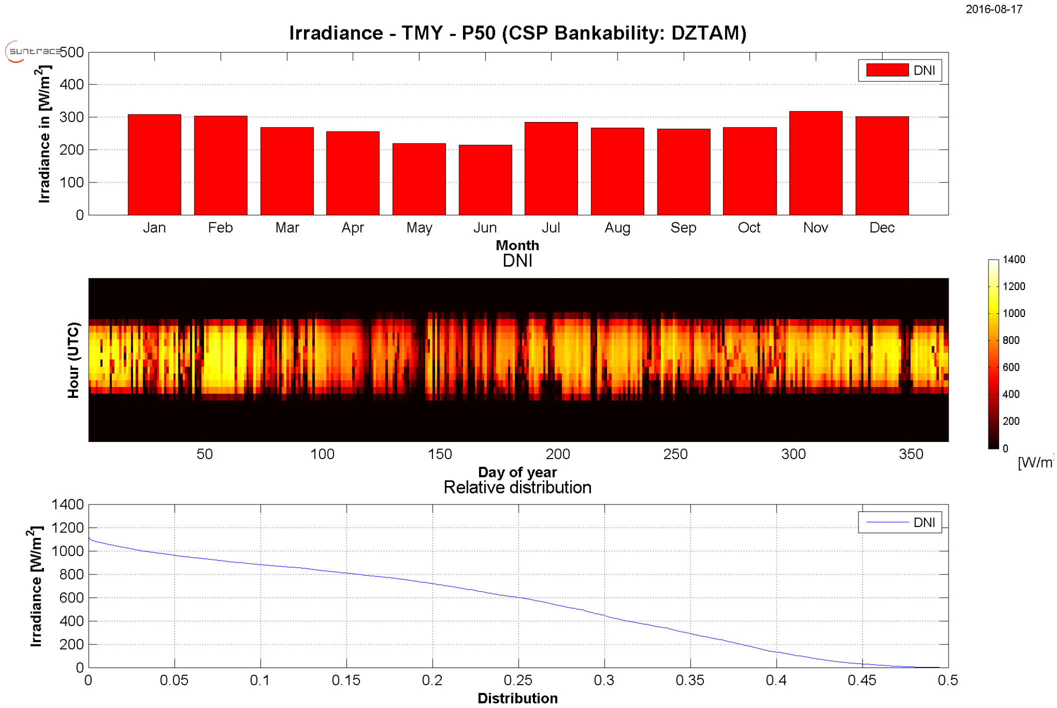

Figure 5-24: DZTAM: TMY - monthly values (top), hours of the day over the year (middle) and distribution (bottom) of DNI.

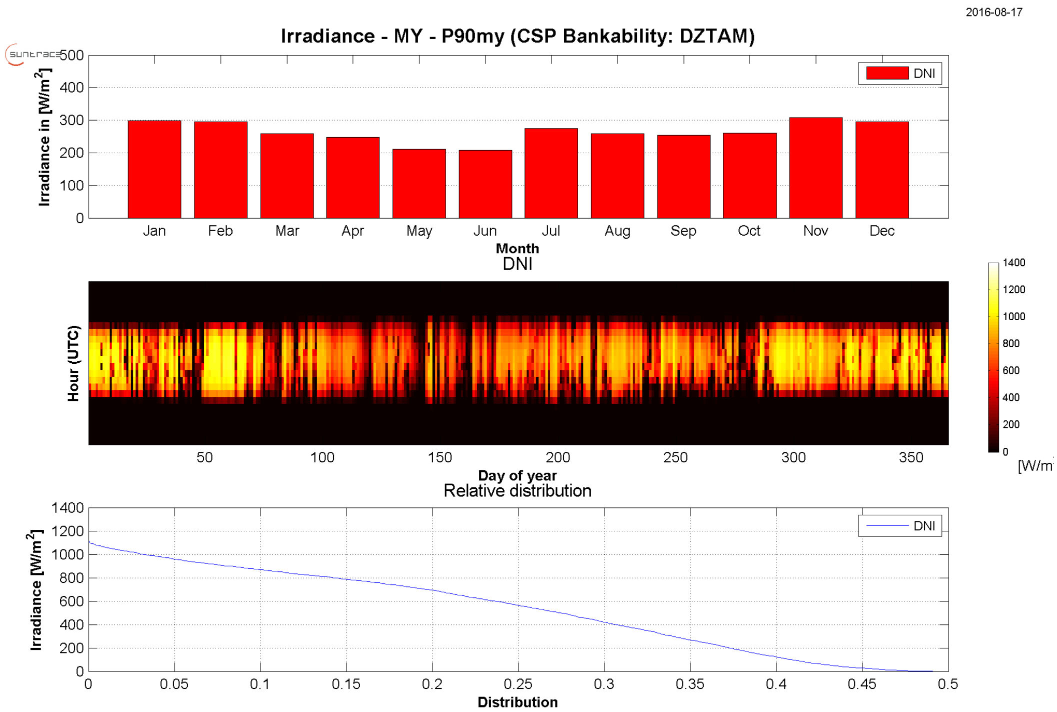

Figure 5-25: DZTAM: MY90 (multiple year) - monthly values (top), hours of the day over the year (middle) and distribution (bottom) of DNI.

5.8.2.2. Global and Diffuse Horizontal Irradiance

The monthly values of the TMY for GHI and DHI at DZTAM are listed in Table 5-24 to Table 5-27. Figure 5-26 to Figure 5-29 show the values in 60min time resolution over the year. For the TMY the annual mean GHI is 265 W/m^2 equal to an annual sum of 2325 kWh/m^2/a. For the MY90 (multiple year) the annual mean GHI is 261 W/m^2 equal to an annual sum of 2290 kWh/m^2/a.

global horizontal irradiance TMY

	average [W/m^2]	min [W/m^2]	max [W/m^2]	sum [kWh/m^2]
Jan	209	0	852	156
Feb	237	0	1004	159
Mar	271	0	1051	201
Apr	310	0	1083	223
May	300	0	1091	223
Jun	305	0	1070	219
Jul	307	0	1330	228
Aug	296	0	1072	220
Sep	282	0	1105	203
Oct	245	0	1008	182
Nov	225	0	864	162
Dec	198	0	818	147
Year	265	0	1330	2325

Table 5-24: DZTAM: TMY-monthly values of GHI

global horizontal irradiance MY90 (mult. year)

	average [W/m^2]	min [W/m^2]	max [W/m^2]	sum [kWh/m^2]
Jan	206	0	852	153
Feb	233	0	1004	157
Mar	268	0	1051	199
Apr	308	0	1083	222
May	296	0	1091	220
Jun	299	0	1070	215
Jul	308	0	1050	229
Aug	295	0	1072	220
Sep	276	0	1058	199
Oct	230	0	981	171
Nov	223	0	876	161
Dec	194	0	820	144
Year	261	0	1091	2290

Table 5-25: DZTAM: MY90my-monthly values GHI

diffuse horizontal irradiance TMY

	average [W/m^2]	min [W/m^2]	max [W/m^2]	sum [kWh/m^2]
Jan	49	0	500	36
Feb	59	0	534	39
Mar	91	0	581	68
Apr	121	0	627	87
May	134	0	740	100
Jun	137	0	668	99
Jul	95	0	687	70
Aug	96	0	595	72
Sep	90	0	552	65
Oct	74	0	508	55
Nov	48	0	473	35
Dec	44	0	415	33
Year	87	0	740	759

Table 5-26: DZTAM: TMY-monthly values of DHI

diffuse horizontal irradiance MY90 (mult year)

	average [W/m^2]	min [W/m^2]	max [W/m^2]	sum [kWh/m^2]
Jan	51	0	500	38
Feb	59	0	534	40
Mar	95	0	581	70
Apr	124	0	627	89
May	135	0	740	101
Jun	137	0	668	99
Jul	98	0	475	73
Aug	100	0	595	74
Sep	90	0	552	65
Oct	69	0	573	51
Nov	52	0	429	38
Dec	44	0	439	33
Year	88	0	740	771

Table 5-27: DZTAM: MY90my-monthly values DHI

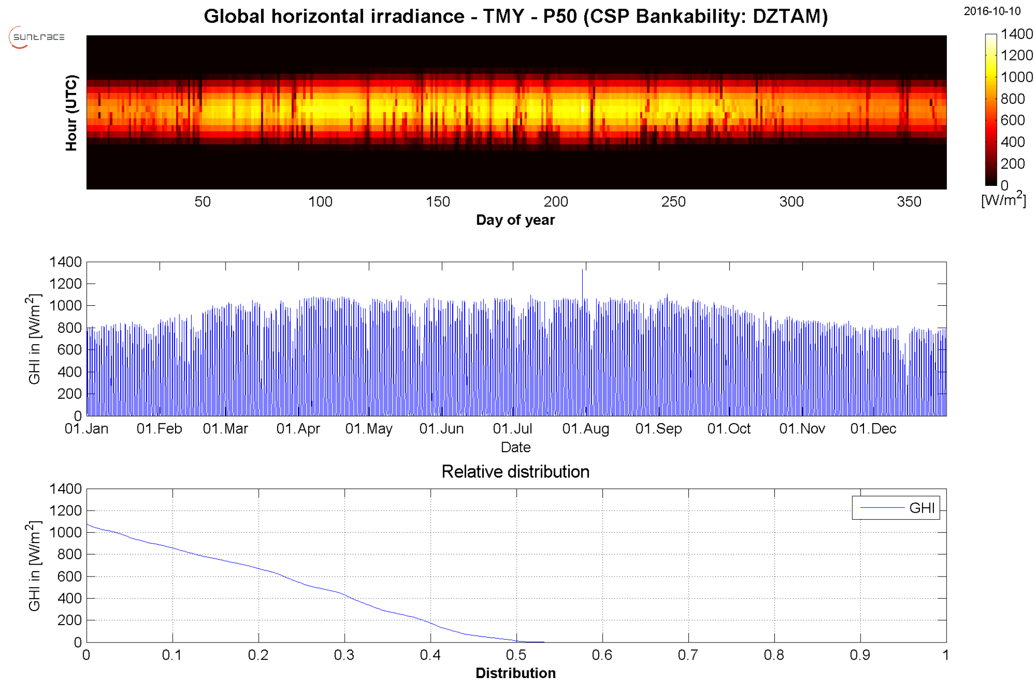

Figure 5-26: DZTAM: TMY - hours of the day over the year (top), hourly values (middle) and distribution (bottom) of GHI

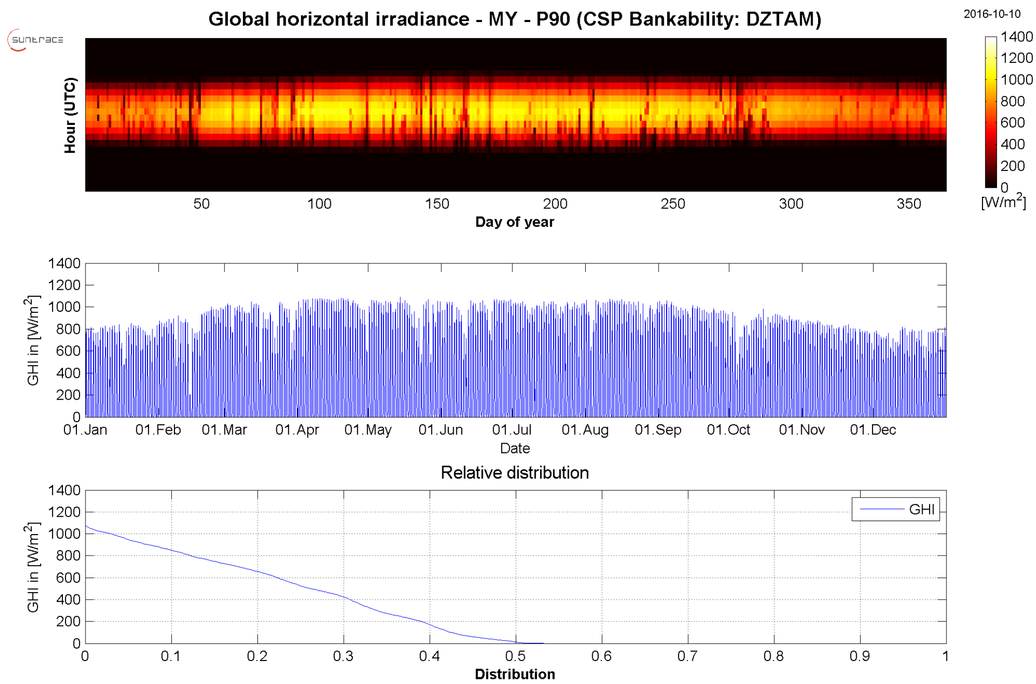

Figure 5-27: DZTAM: MY90my - hours of the day over the year (top), hourly values (middle) and distribution (bottom) of GHI

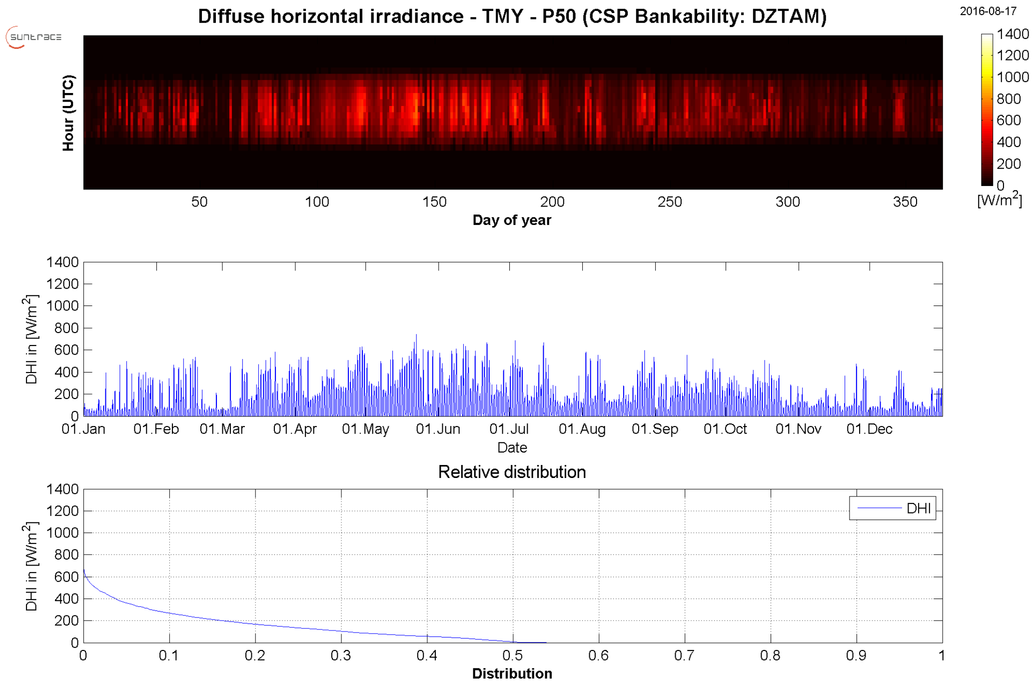

Figure 5-28: DZTAM: TMY - hours of the day over the year (top), hourly values (middle) and distribution (bottom) of DHI

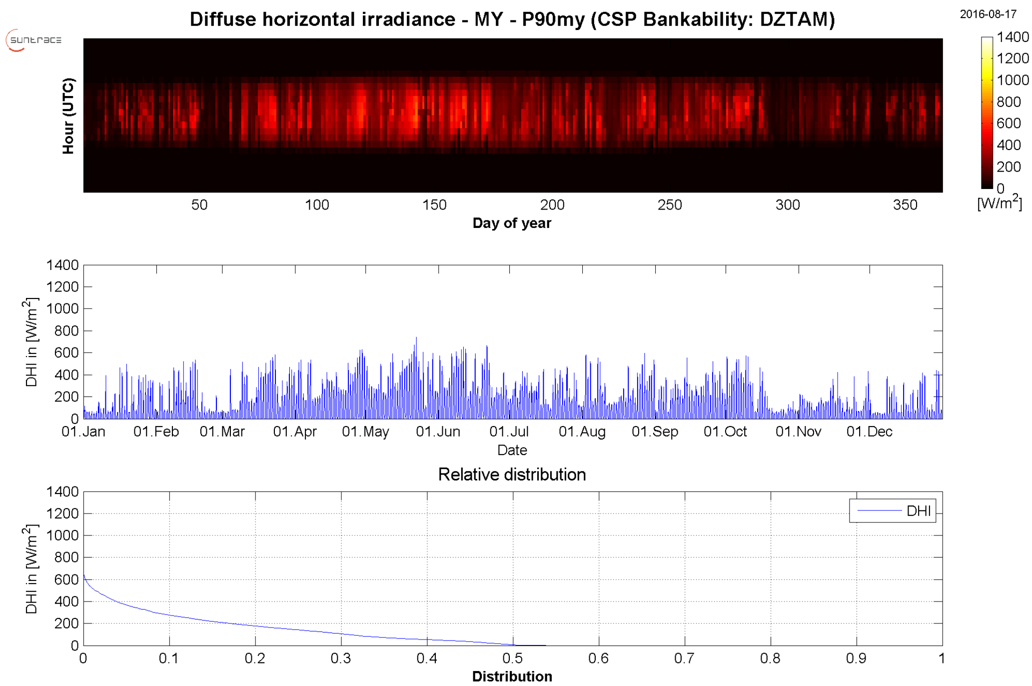

Figure 5-29: DZTAM: MY90my - hours of the day over the year (top), hourly values (middle) and distribution (bottom) of DHI

5.8.2.3. Auxiliary Meteorological Data (TMY)

The monthly values of the TMY for wind speed, wind direction, air temperature, wet bulb temperature, dew point temperature, relative humidity and barometric pressure at DZTAM are listed in Table 5-28 to Table 5-34. Figure 5-30 to Figure 5-37 show the values in 60min time resolution over the year.

Wind

For the TMY (P50) of DZTAM the mean horizontal wind speed is 4.5 m/s with a predominant wind direction of 90 ºN. The maximum hourly average wind speed is 12.9 m/s. This is an hourly average and can differ significantly from the wind gust, usually being defined as an average over three seconds. Wind gust values can be a multiple of the here displayed maximum hourly average wind speed. Therefore, the given values are not sufficient for plant construction.

wind speed

	average [m/s]	min [m/s]	max [m/s]
Jan	4.2	0.2	12.1
Feb	4.2	0.3	10.4
Mar	5.2	0.4	12.6
Apr	4.8	0.6	12.9
May	4.8	0.7	10.9
Jun	4.8	0.2	11.0
Jul	5.0	0.2	11.1
Aug	4.5	0.3	12.3
Sep	4.7	0.3	12.2
Oct	3.8	0.2	9.4
Nov	3.4	0.3	9.9
Dec	4.3	0.4	10.1
Year	4.5	0.2	12.9

Table 5-28: DZTAM: TMY - monthly values of wind speed

wind direction

	average [ºN]	min [ºN]	max [ºN]
Jan	78	3	360
Feb	338	0	359
Mar	2	0	360
Apr	115	1	360
May	256	0	360
Jun	100	0	360
Jul	88	2	359
Aug	109	1	359
Sep	100	0	358
Oct	125	0	360
Nov	94	1	360
Dec	81	0	360
Year	90	0	360

Table 5-29: DZTAM: TMY - monthly values of wind direction

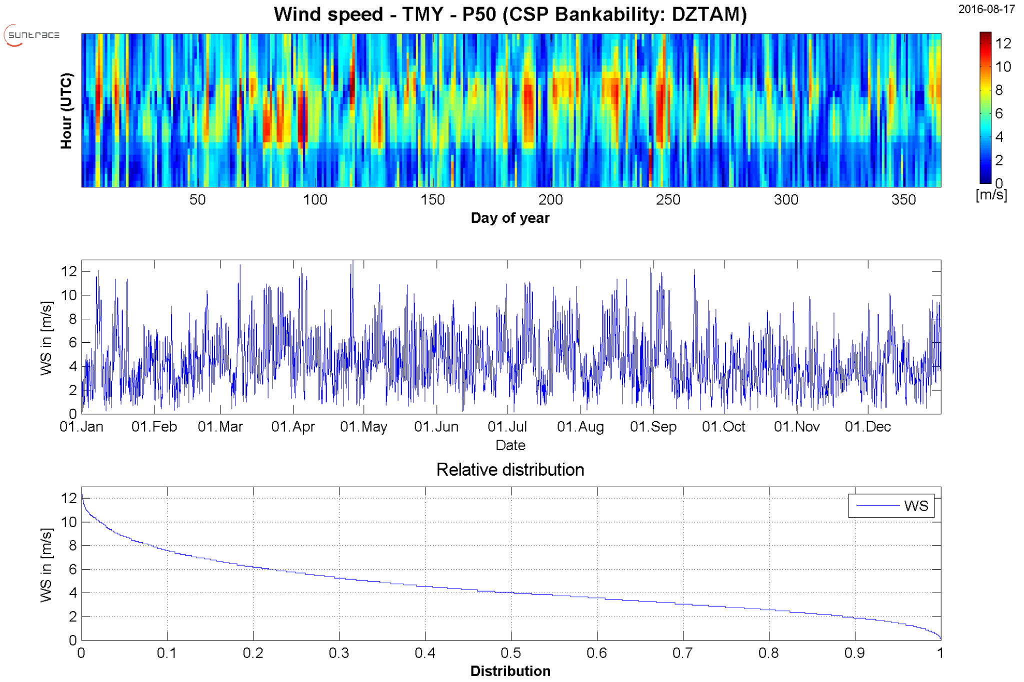

Figure 5-30: DZTAM: TMY - hours of the day over the year (top), hourly values (middle) and distribution (bottom) of wind speed

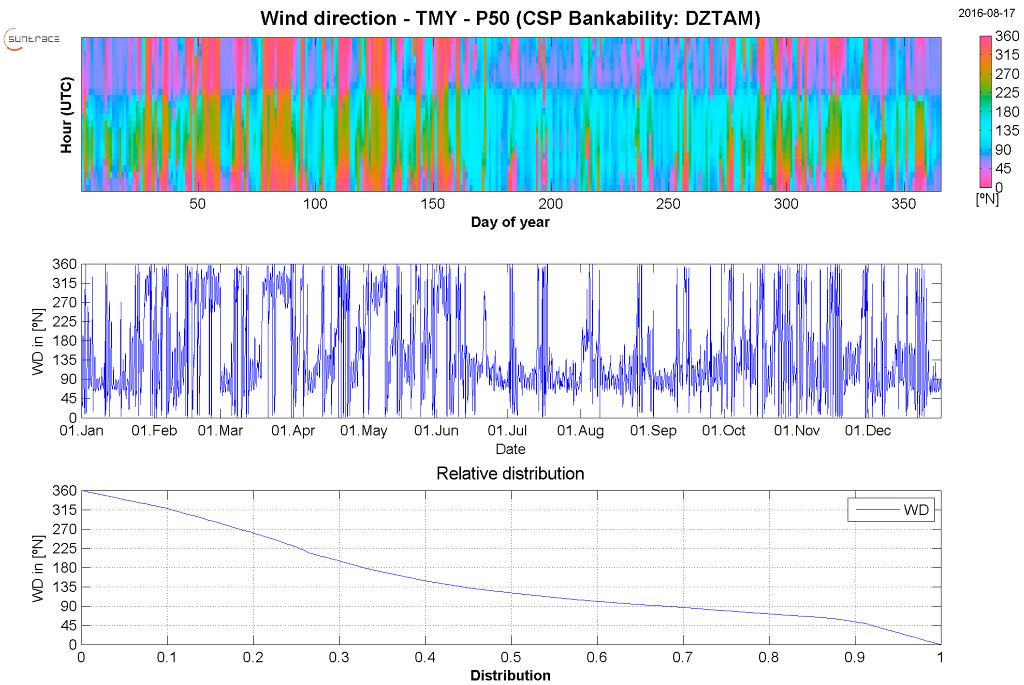

Figure 5-31: DZTAM: TMY - hours of the day over the year (top), hourly values (middle) and distribution (bottom) of wind direction

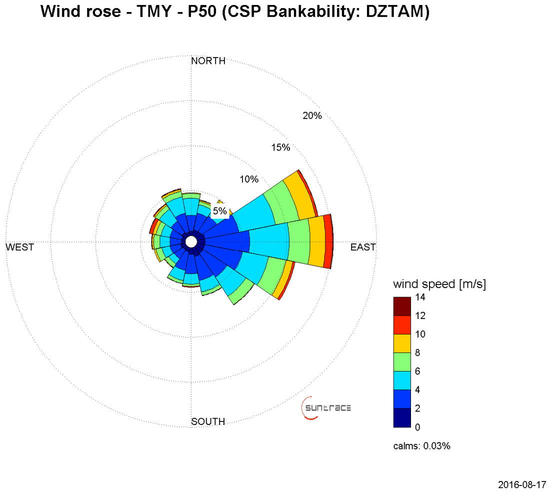

Figure 5-32: DZTAM: TMY – wind rose

Air-, Dew Point-, Wet Bulb- Temperatures and Relative Humidity

For the TMY of DZTAM the mean annual air temperature is 23.7ºC with a minimum of 3.9ºC and a maximum of 40.3ºC. The mean annual wet bulb temperature is 10.5ºC with a minimum of -1.2ºC and a maximum of 18.8ºC. The mean annual dew point temperature is -2.8ºC with a minimum of -18.3ºC and a maximum of 12.7ºC. The mean relative humidity is 19%.

air temperature

	average [ºC]	min [ºC]	max [ºC]
Jan	14.4	4.3	29.8
Feb	16.6	3.9	28.6
Mar	19.7	5.8	33.1
Apr	24.4	8.8	37.1
May	29.9	19.7	39.8
Jun	30.5	20.7	39.0
Jul	30.9	21.9	40.3
Aug	30.0	21.3	38.6
Sep	28.9	20.0	37.3
Oct	25.9	14.7	36.4
Nov	19.2	9.7	31.5
Dec	13.5	5.0	24.4
Year	23.7	3.9	40.3

Table 5-30: DZTAM: TMY - monthly values of air temperature

wet bulb temperature

	average [ºC]	min [ºC]	max [ºC]
Jan	5.6	-0.2	14.4
Feb	6.7	-1.2	13.3
Mar	8.1	0.2	15.7
Apr	10.1	2.3	15.4
May	13.5	7.7	17.4
Jun	13.5	8.7	17.4
Jul	14.4	9.1	18.8
Aug	14.6	9.5	18.4
Sep	13.3	9.3	17.2
Oct	12.1	6.5	17.2
Nov	8.1	2.9	13.6
Dec	5.0	0.0	10.0
Year	10.5	-1.2	18.8

Table 5-31: DZTAM: TMY - monthly values of wet bulb temperature

dew point temperature

	average	min	max
	[ºC]	[ºC]	[ºC]
Jan	-5.6	-13.3	5.9
Feb	-5.9	-18.2	7.4
Mar	-6.1	-18.3	5.3
Apr	-5.9	-13.9	3.5
May	-0.8	-11.1	7.5
Jun	-1.7	-6.9	8.4
Jul	1.1	-5.8	11.2
Aug	2.8	-5.1	12.7
Sep	-0.2	-6.0	10.9
Oct	-0.2	-6.9	10.3
Nov	-4.6	-13.4	1.5
Dec	-6.3	-13.1	6.4
Year	-2.8	-18.3	12.7

Table 5-32: DZTAM: TMY - monthly values of dew point temperature

relative humidity

	average	min	max
	[%]	[%]	[%]
Jan	27	8	64
Feb	24	4	66
Mar	19	4	73
Apr	14	5	63
May	15	5	37
Jun	13	7	31
Jul	16	7	35
Aug	19	8	48
Sep	16	7	40
Oct	19	9	53
Nov	21	9	42
Dec	27	9	67
Year	19	4	73

Table 5-33: DZTAM: TMY - monthly values of relative humidity

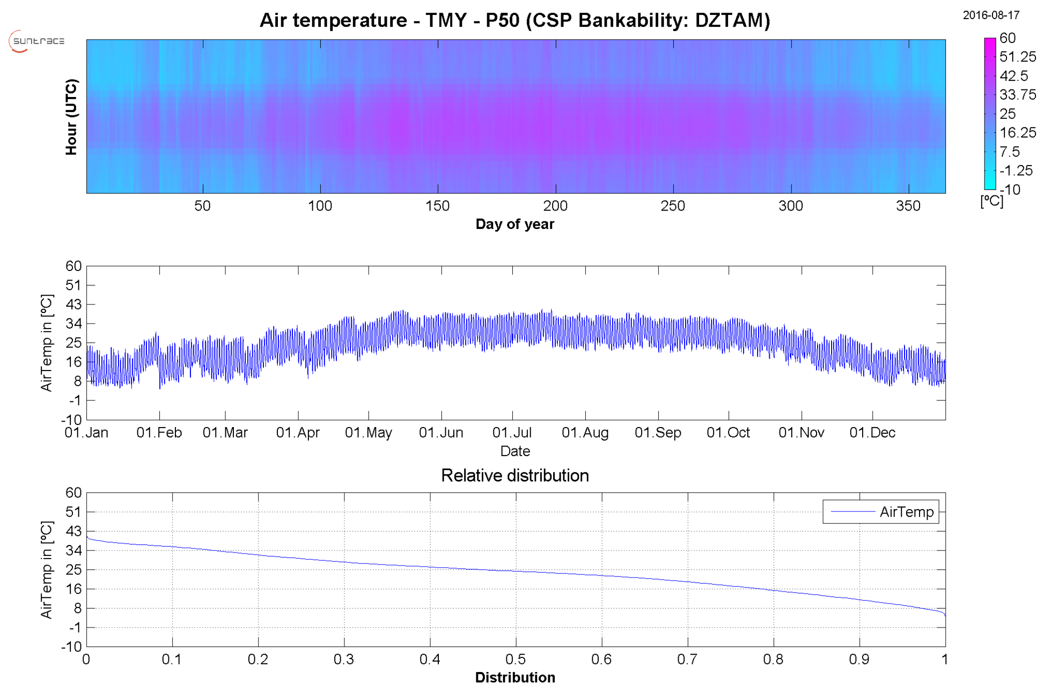

Figure 5-33: DZTAM: TMY - hours of the day over the year (top), hourly values (middle) and distribution (bottom) of air temperature

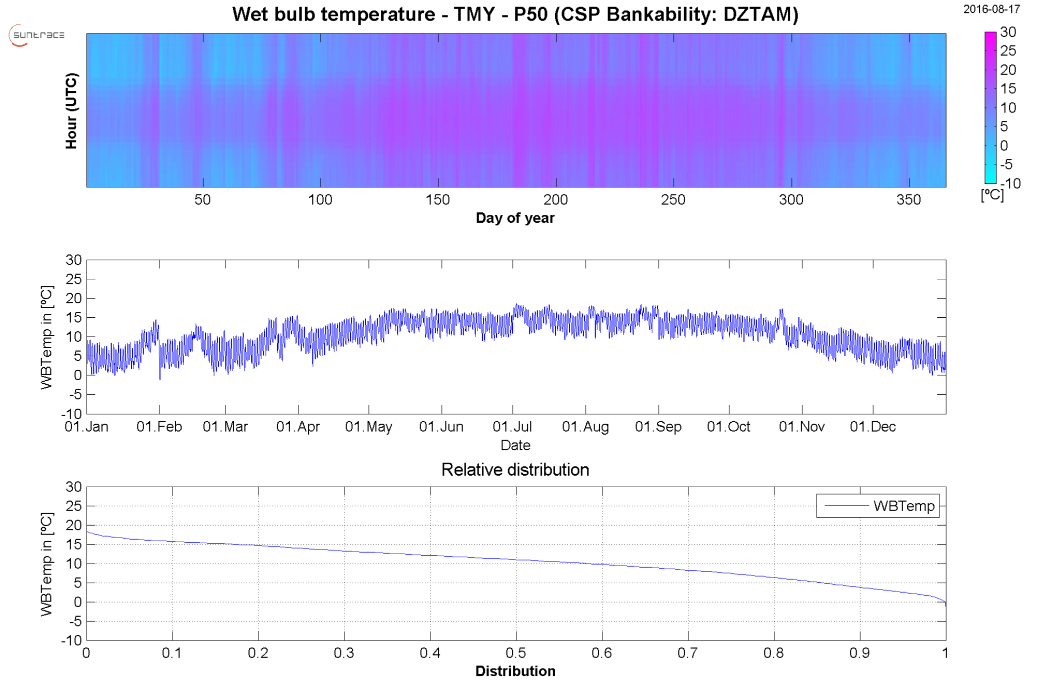

Figure 5-34: DZTAM: TMY - hours of the day over the year (top), hourly values (middle) and distribution (bottom) of wet bulb temperature

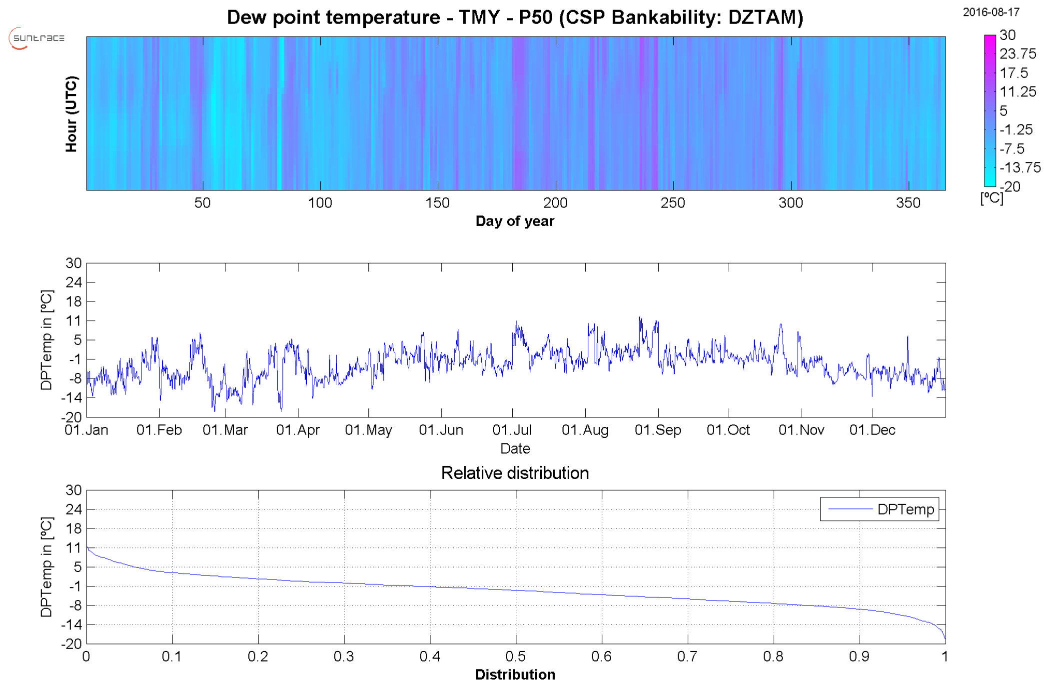

Figure 5-35: DZTAM: TMY - hours of the day over the year (top), hourly values (middle) and distribution (bottom) of dew point temperature

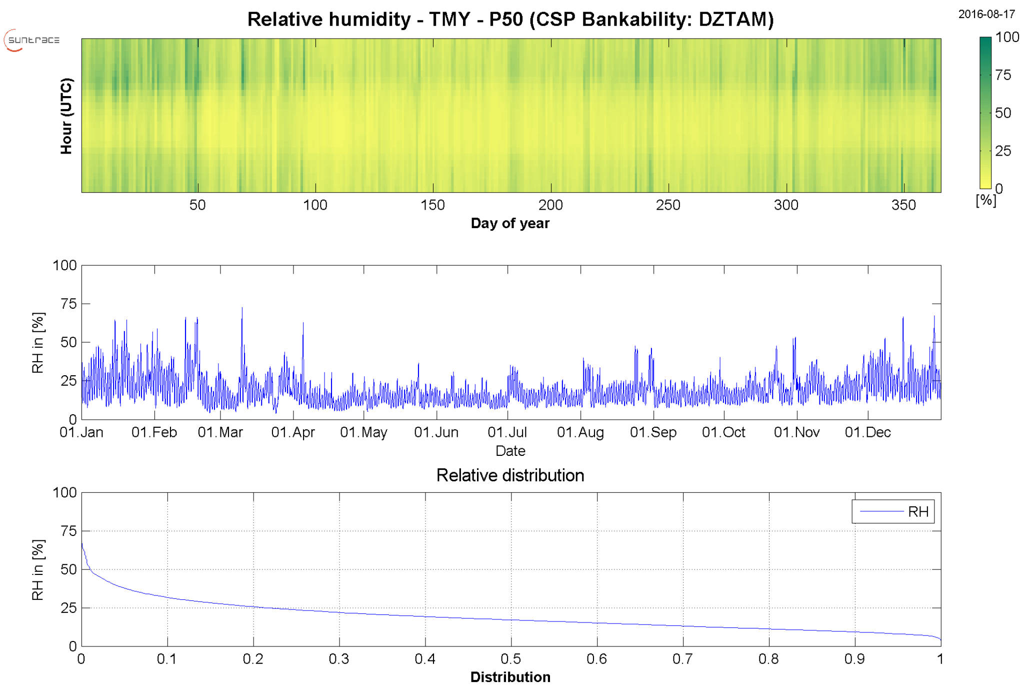

Figure 5-36: DZTAM: TMY - hours of the day over the year (top), hourly values (middle) and distribution (bottom) of relative humidity

<ins>Barometric pressure</ins>

For the TMY of DZTAM the mean barometric pressure is 885 hPa.

barometric pressure

	average [hPa]	min [hPa]	max [hPa]
Jan	887	882	893
Feb	884	881	890
Mar	885	879	891
Apr	884	878	890
May	884	880	887
Jun	885	880	889
Jul	885	882	889
Aug	885	880	888
Sep	886	882	890
Oct	885	880	890
Nov	886	882	890
Dec	889	883	894
Year	885	878	894

Table 5-34: DZTAM: TMY - monthly values of barometric pressure

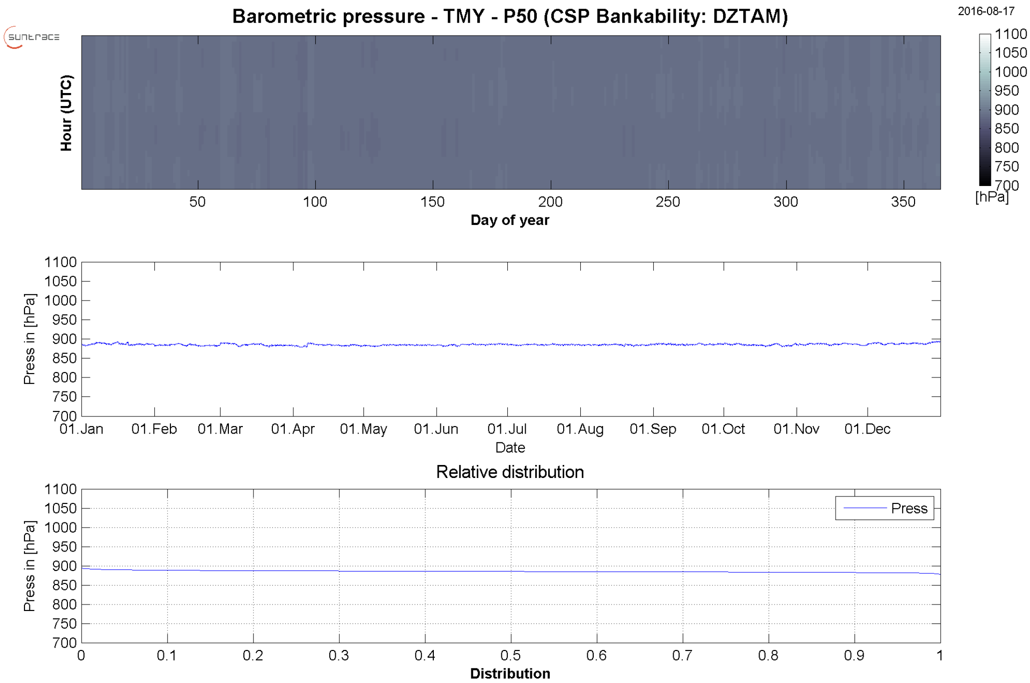

Figure 5-37: DZTAM: TMY - hours of the day over the year (top), hourly values (middle) and distribution (bottom) of barometric pressure

5.8.3. SASOV

5.8.3.1. Direct Normal Irradiance

For the TMY (P50 value) of the demo site SASOV the annual mean direct normal irradiance is 260 W/m^2 equal to an annual sum of 2275 kWh/m^2/a. The DNI exceeded for 3304 hours 250 W/m^2 with an average of 661 W/m^2 taking just the DNI values higher than 250 W/m^2 into account.

For the MY90 with respect to multiple year uncertainty the annual mean direct normal irradiance is 250 W/m^2 equal to an annual sum of 2191 kWh/m^2/a. The DNI exceeded for 3225 hours 250 W/m^2 with an average of 650 W/m^2 taking just the DNI values higher than 250 W/m^2 into account.

Figure 5-38 (TMY) and Figure 5-39 (MY90) show the monthly values, the hours of the day over the year as well as the relative frequency distribution of DNI for the TMY and MY90 at SASOV. The monthly values at SASOV for the TMY are shown in Table 5-35 and for the MY90 with respect to multiple year uncertainty in Table 5-36.

direct normal irradiance TMY

	average [W/m²]	min [W/m²]	max [W/m²]	sum [kWh/m²]
Jan	219	0	1051	163
Feb	218	0	1081	147
Mar	203	0	1077	151
Apr	218	0	964	157
May	258	0	857	192
Jun	316	0	911	227
Jul	315	0	924	234
Aug	294	0	907	219
Sep	306	0	916	221
Oct	298	0	1035	222
Nov	241	0	997	174
Dec	227	0	976	169
Year	260	0	1081	2275

Table 5-35: SASOV: TMY - monthly values of DNI

direct normal irradiance MY90 (multiple year)

	average [W/m²]	min [W/m²]	max [W/m²]	sum [kWh/m²]
Jan	212	0	1051	158
Feb	208	0	1081	140
Mar	195	0	1019	145
Apr	210	0	964	151
May	248	0	857	185
Jun	302	0	911	218
Jul	305	0	924	227
Aug	280	0	974	208
Sep	296	0	916	213
Oct	292	0	1035	217
Nov	232	0	997	167
Dec	219	0	976	163
Year	250	0	1081	2191

Table 5-36: SASOV: MY90my - monthly values of DNI

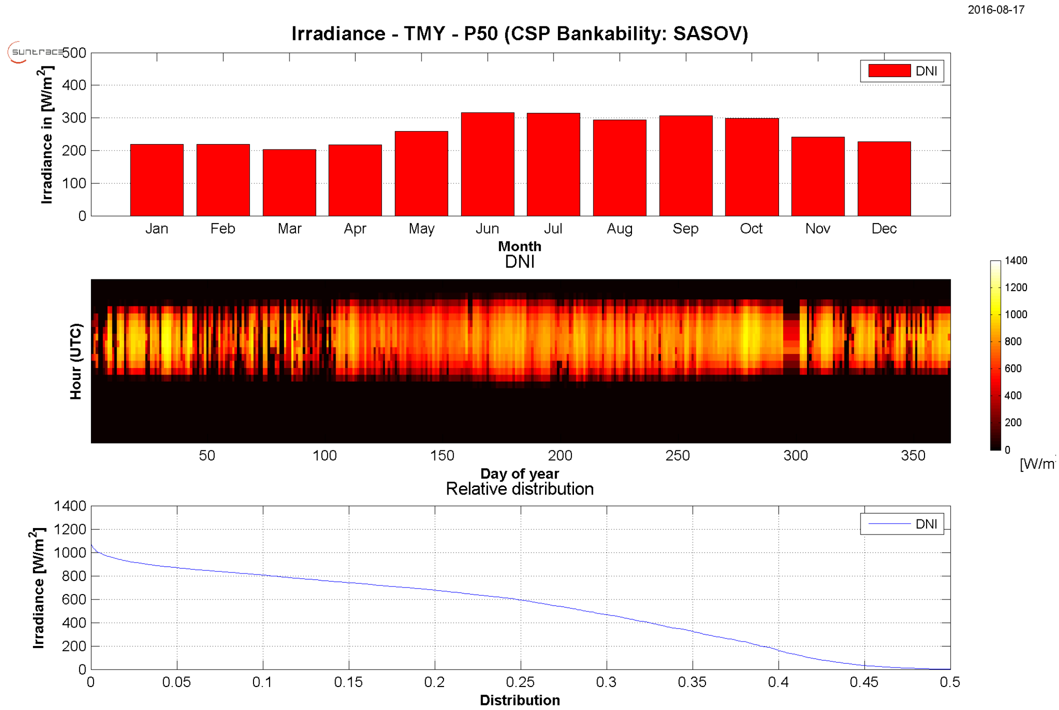

Figure 5-38: SASOV: TMY - monthly values (top), hours of the day over the year (middle) and distribution (bottom) of DNI.

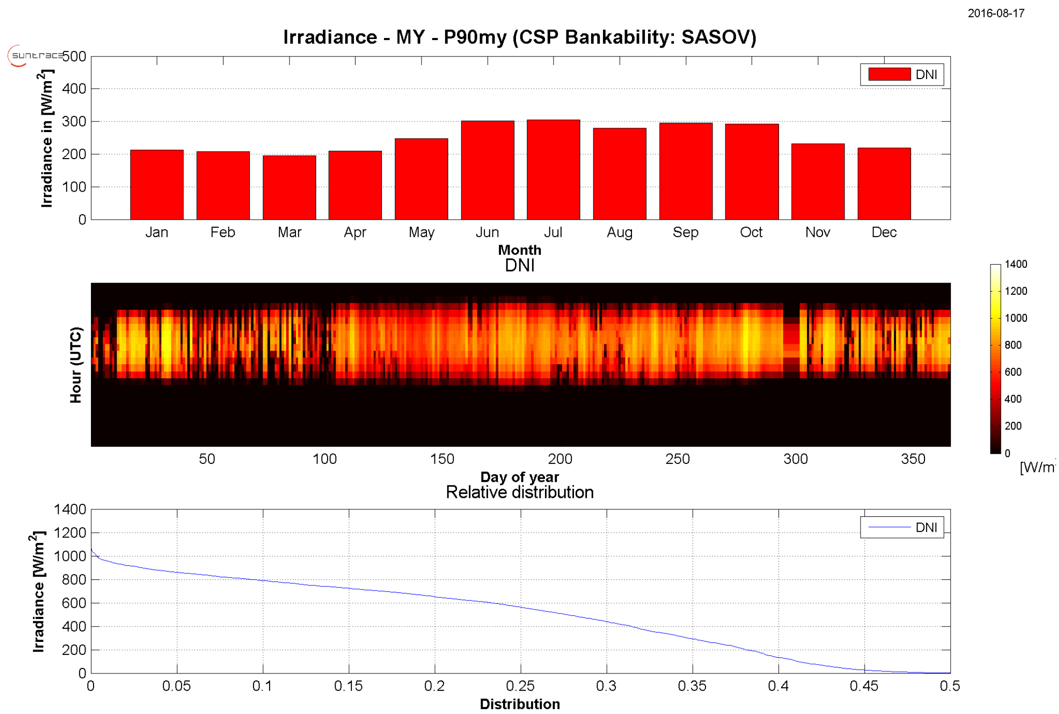

Figure 5-39: SASOV: MY90 (multiple year) - monthly values (top), hours of the day over the year (middle) and distribution (bottom) of DNI.

5.8.3.2. Global and Diffuse Horizontal Irradiance

The monthly values of the TMY for GHI and DHI at SASOV are listed in Table 5-11 to Table 5-14. Figure 5-12 to Figure 5-15 show the values in 60min time resolution over the year. For the TMY the annual mean GHI is 255 W/m^2 equal to an annual sum of 2236 kWh/m^2/a. For the MY90 (multiple year) the annual mean GHI is 251 W/m^2 equal to an annual sum of 2200 kWh/m^2/a.

global horizontal irradiance TMY

	average [W/m^2]	min [W/m^2]	max [W/m^2]	sum [kWh/m^2]
Jan	170	0	840	127
Feb	213	0	910	143
Mar	233	0	1358	174
Apr	271	0	1061	195
May	310	0	1045	231
Jun	335	0	1076	241
Jul	327	0	1058	243
Aug	310	0	1040	230
Sep	285	0	998	205
Oct	246	0	970	183
Nov	188	0	821	136
Dec	171	0	751	127
Year	255	0	1358	2236

Table 5-37: SASOV: TMY - monthly values of GHI

global horizontal irradiance MY90 (mult. year)

	average [W/m^2]	min [W/m^2]	max [W/m^2]	sum [kWh/m^2]
Jan	168	0	840	125
Feb	212	0	910	142
Mar	229	0	1371	171
Apr	265	0	1061	191
May	302	0	1045	225
Jun	333	0	1076	239
Jul	324	0	1057	241
Aug	303	0	1079	226
Sep	283	0	995	204
Oct	243	0	970	181
Nov	185	0	812	133
Dec	166	0	751	123
Year	251	0	1371	2200

Table 5-38: SASOV: MY90my - monthly values GHI

diffuse horizontal irradiance TMY

	average [W/m^2]	min [W/m^2]	max [W/m^2]	sum [kWh/m^2]
Jan	54	0	484	40
Feb	84	0	543	56
Mar	95	0	598	71
Apr	109	0	593	78
May	110	0	527	82
Jun	96	0	425	69
Jul	88	0	396	66
Aug	90	0	480	67
Sep	72	0	377	51
Oct	60	0	376	44
Nov	56	0	461	41
Dec	54	0	392	40
Year	81	0	598	706

Table 5-39: SASOV: MY90my - monthly values of DHI

diffuse horizontal irradiance MY90 (mult year)

	average [W/m^2]	min [W/m^2]	max [W/m^2]	sum [kWh/m^2]
Jan	55	0	484	41
Feb	88	0	543	59
Mar	96	0	598	71
Apr	109	0	593	78
May	110	0	527	82
Jun	102	0	425	73
Jul	92	0	396	68
Aug	93	0	470	69
Sep	76	0	378	55
Oct	60	0	376	44
Nov	58	0	461	42
Dec	54	0	392	40
Year	83	0	598	724

Table 5-40: SASOV: MY90my - monthly values of DHI

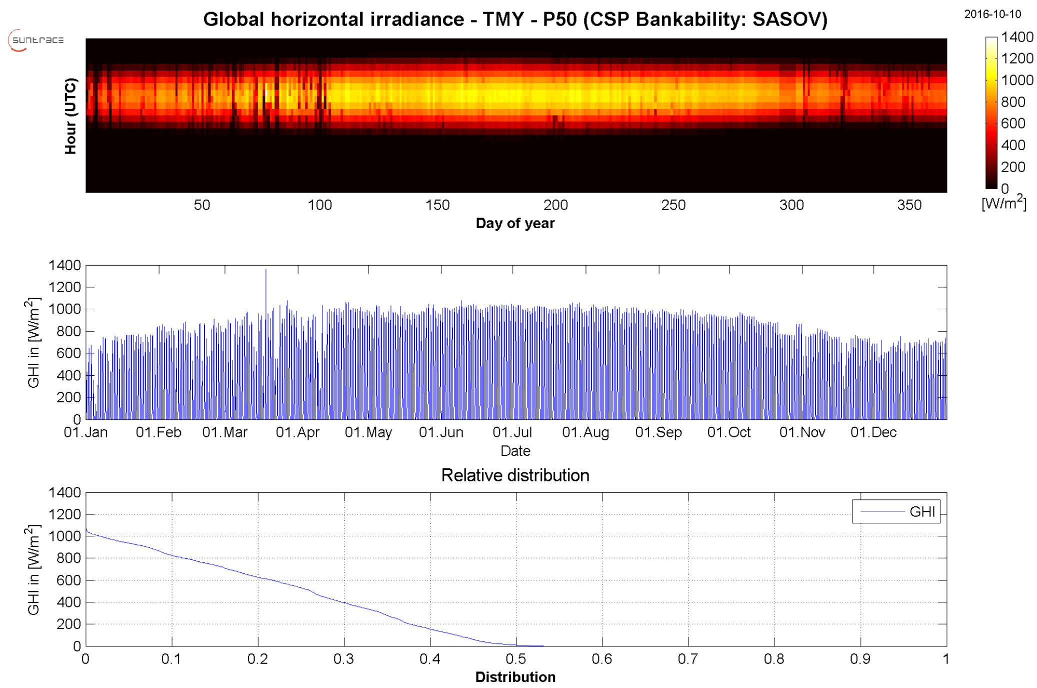

Figure 5-40: SASOV: TMY - hours of the day over the year (top), hourly values (middle) and distribution (bottom) of GHI

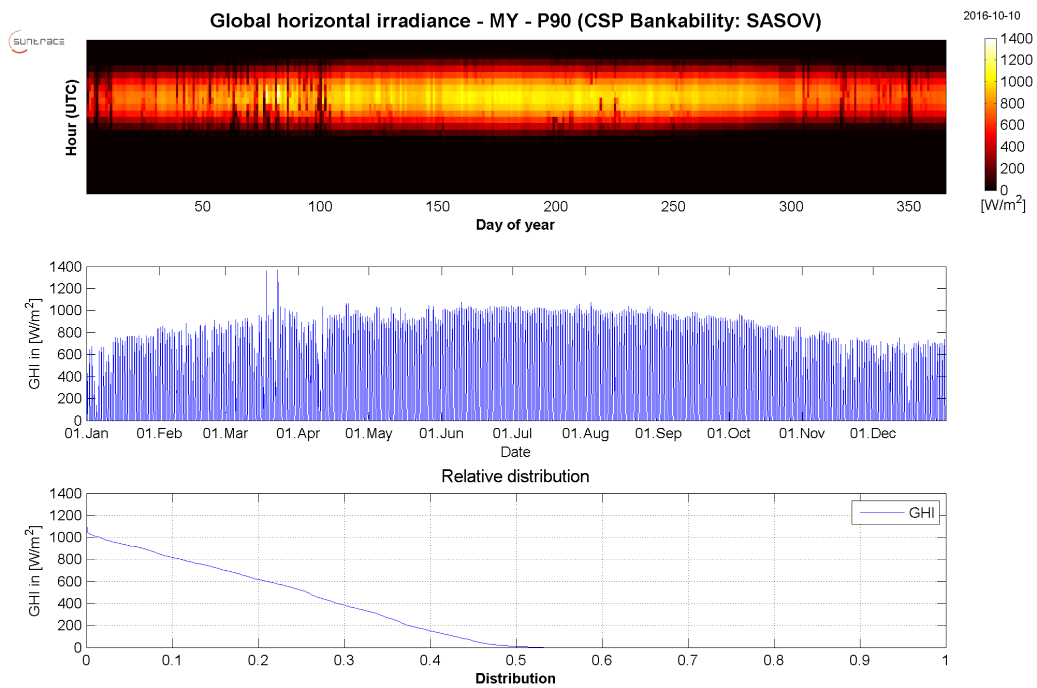

Figure 5-41: SASOV: MY90my - hours of the day over the year (top), hourly values (middle) and distribution (bottom) of GHI

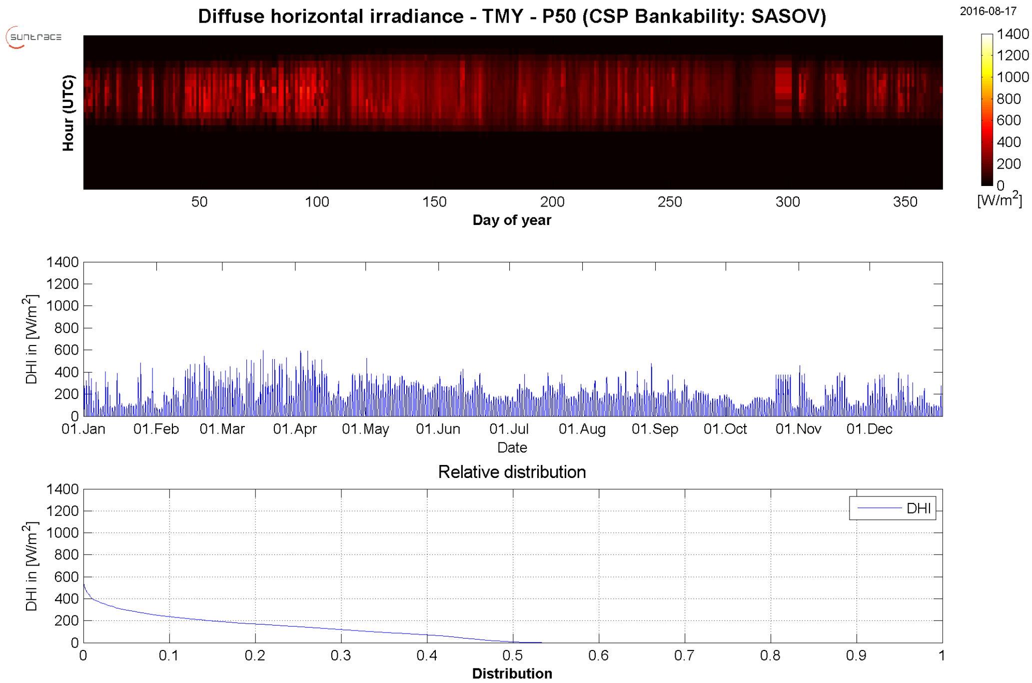

Figure 5-42: SASOV: TMY - hours of the day over the year (top), hourly values (middle) and distribution (bottom) of DHI

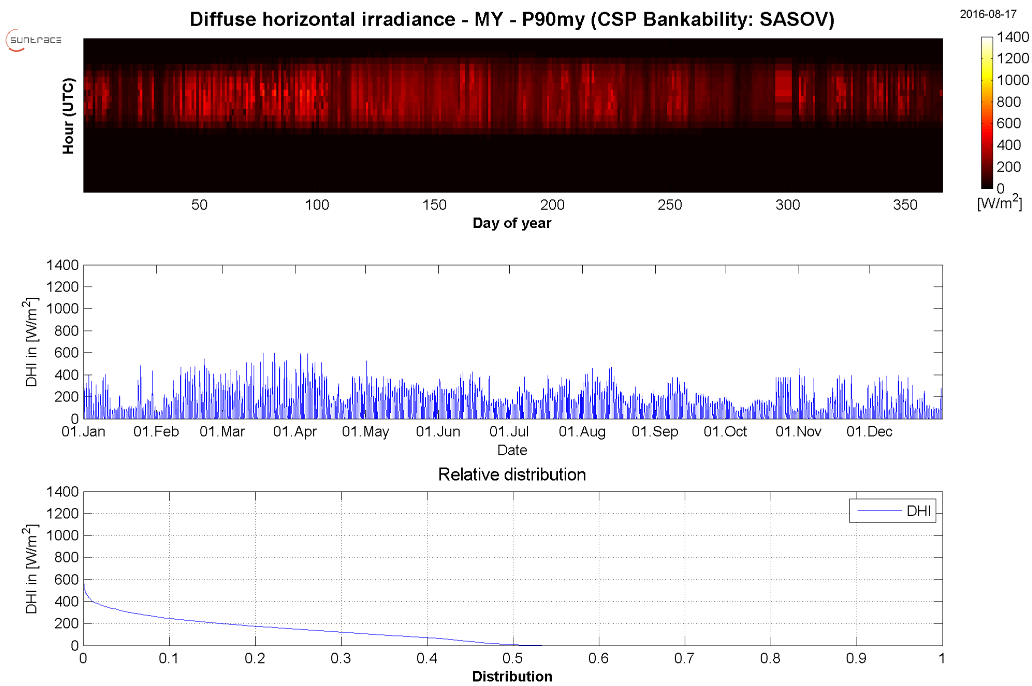

Figure 5-43: SASOV: MY90my - hours of the day over the year (top), hourly values (middle) and distribution (bottom) of DHI

5.8.3.3. Auxiliary Meteorological Data (TMY)

The monthly values of the TMY for wind speed, wind direction, air temperature, wet bulb temperature, dew point temperature, relative humidity and barometric pressure at SASOV are listed in Table 5-15 to Table 5-21. Figure 5-16 to Figure 5-23 show the values in 60min time resolution over the year.

Wind

For the TMY (P50) of SASOV the mean horizontal wind speed is 4.0 m/s with a predominant wind direction of 96 ºN. The maximum hourly average wind speed is 11.4 m/s. This is an hourly average and can differ significantly from the wind gust, usually being defined as an average over three seconds. Wind gust values can be a multiple of the here displayed maximum hourly average wind speed. Therefore, the given values are not sufficient for plant construction.

wind speed

	average [m/s]	min [m/s]	max [m/s]
Jan	4.1	0.3	11.4
Feb	4.4	0.5	9.8
Mar	3.9	0.4	9.8
Apr	4.7	0.6	10.3
May	4.5	0.3	9.4
Jun	4.1	0.4	9.7
Jul	3.7	0.2	9.8
Aug	4.1	0.3	9.3
Sep	3.5	0.5	7.7
Oct	3.3	0.2	7.8
Nov	3.5	0.3	9.7
Dec	4.7	0.7	11.1
Year	4.0	0.2	11.4

Table 5-41: SASOV: TMY - monthly values of wind speed

wind direction

	average [ºN]	min [ºN]	max [ºN]
Jan	93	0	360
Feb	116	0	360
Mar	151	0	360
Apr	175	0	360
May	152	0	359
Jun	12	1	360
Jul	34	0	360
Aug	28	0	359
Sep	61	1	360
Oct	148	0	360
Nov	91	0	359
Dec	158	5	350
Year	96	0	360

Table 5-42: SASOV: TMY - monthly values of wind direction

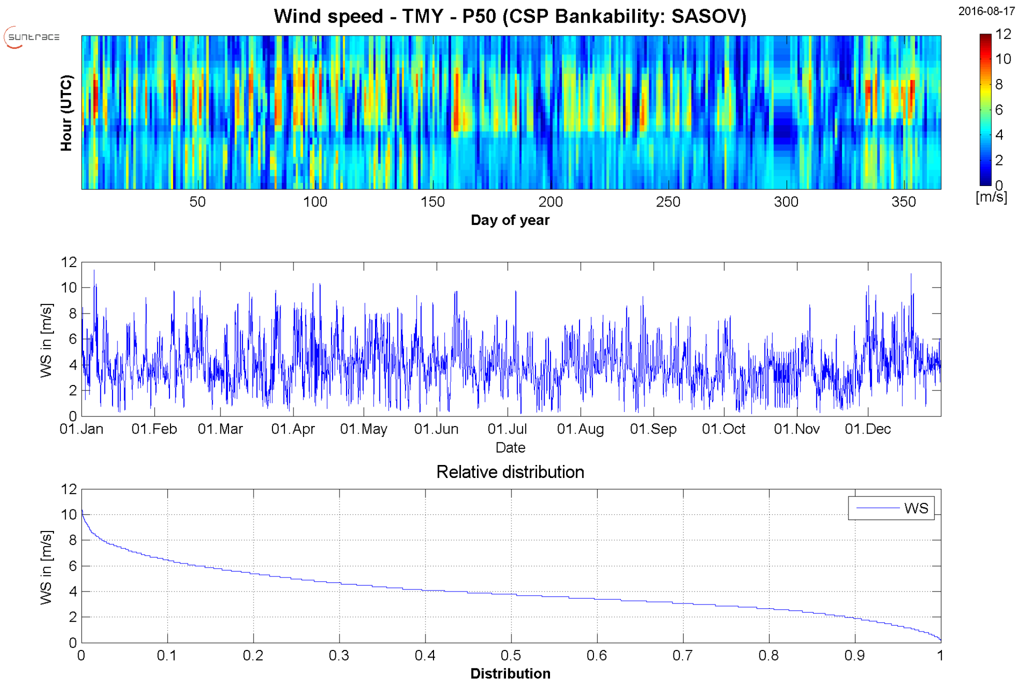

Figure 5-44: SASOV: TMY - hours of the day over the year (top), hourly values (middle) and distribution (bottom) of wind speed

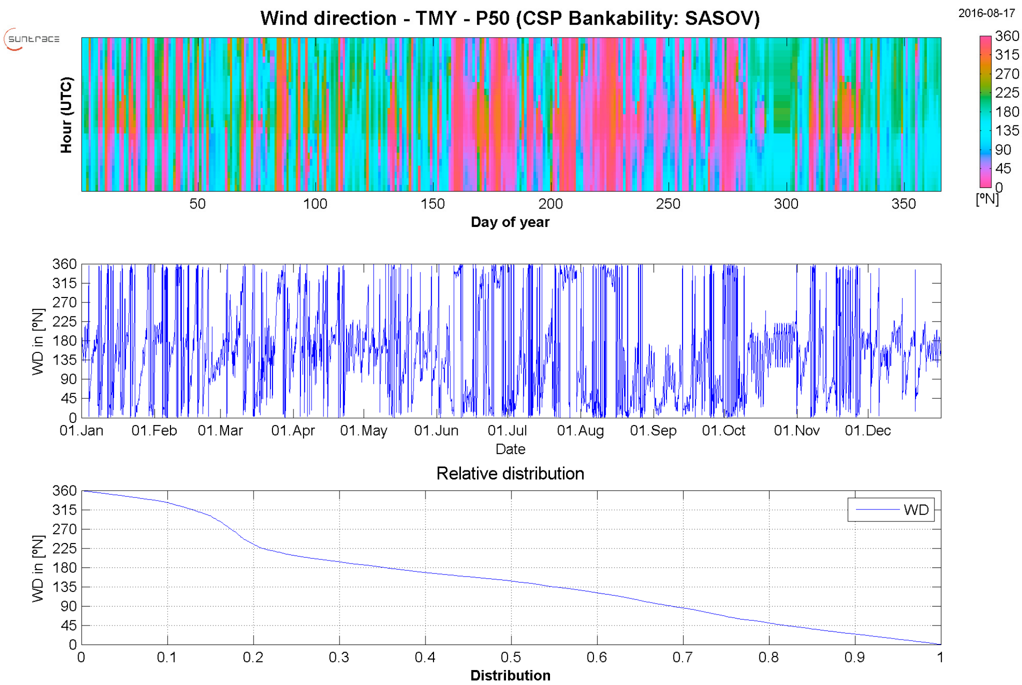

Figure 5-45: SASOV: TMY - hours of the day over the year (top), hourly values (middle) and distribution (bottom) of wind direction

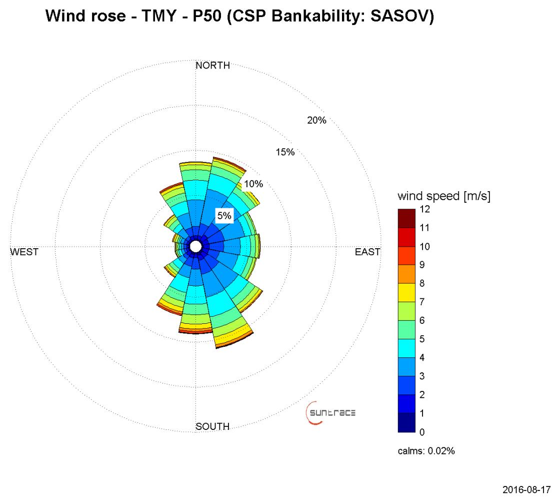

Figure 5-46: SASOV: TMY – wind rose

Air-, Dew Point-, Wet Bulb- Temperatures and Relative Humidity

For the TMY of SASOV the mean annual air temperature is 26.0ºC with a minimum of 2.5ºC and a maximum of 44.3ºC. The mean annual wet bulb temperature is 14.2ºC with a minimum of -1.2ºC and a maximum of 23.0ºC. The mean annual dew point temperature is 5.1ºC with a minimum of -13.7ºC and a maximum of 19.87ºC. The mean relative humidity is 33%.

air temperature

	average [ºC]	min [ºC]	max [ºC]
Jan	13.1	3.5	23.9
Feb	15.3	2.5	26.9
Mar	21.2	12.6	30.9
Apr	25.7	14.6	38.8
May	32.9	20.9	42.4
Jun	34.3	24.3	42.0
Jul	36.1	25.4	44.3
Aug	34.9	25.8	42.8
Sep	32.1	20.9	40.9
Oct	27.1	16.2	38.5
Nov	19.5	9.3	31.5
Dec	19.0	7.2	28.2
Year	26.0	2.5	44.3

Table 5-43: SASOV: TMY - monthly values of air temperature

wet bulb temperature

	average [ºC]	min [ºC]	max [ºC]
Jan	8.7	1.2	18.3
Feb	8.4	-1.2	14.5
Mar	13.7	6.1	18.9
Apr	14.8	7.9	19.6
May	16.6	10.4	21.2
Jun	16.4	11.1	20.6
Jul	17.4	11.5	23.0
Aug	17.5	11.6	21.5
Sep	16.1	10.4	20.3
Oct	13.4	5.7	19.1
Nov	12.9	6.2	20.3
Dec	13.9	4.5	21.2
Year	14.2	-1.2	23.0

Table 5-44: SASOV: TMY - monthly values of wet bulb temperature

dew point temperature

	average	min	max
	[ºC]	[ºC]	[ºC]
Jan	4.0	-8.1	17.7
Feb	1.2	-9.7	12.1
Mar	8.1	-2.6	18.2
Apr	6.7	-2.8	18.4
May	4.9	-4.3	15.3
Jun	3.1	-2.4	12.6
Jul	4.2	-3.4	18.3
Aug	5.9	-3.2	12.3
Sep	4.4	-1.7	12.3
Oct	0.4	-13.7	15.3
Nov	7.9	-2.3	19.1
Dec	10.3	-1.6	19.8
Year	5.1	-13.7	19.8

Table 5-45: SASOV: TMY - monthly values of dew point temperature

relative humidity

	average	min	max
	[%]	[%]	[%]
Jan	58	18	100
Feb	41	11	84
Mar	48	15	100
Apr	34	10	97
May	19	8	57
Jun	15	8	35
Jul	14	8	44
Aug	17	8	30
Sep	18	9	44
Oct	21	4	66
Nov	50	22	100
Dec	60	27	100
Year	33	4	100

Table 5-46: SASOV: TMY - monthly values of relative humidity

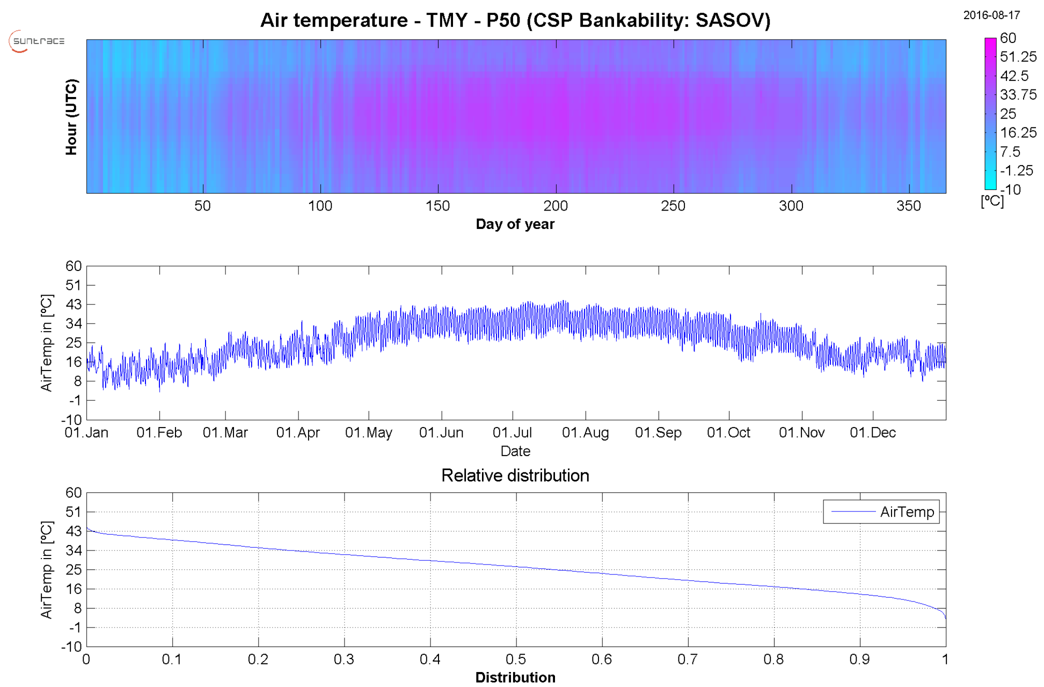

Figure 5-47: SASOV: TMY - hours of the day over the year (top), hourly values (middle) and distribution (bottom) of air temperature

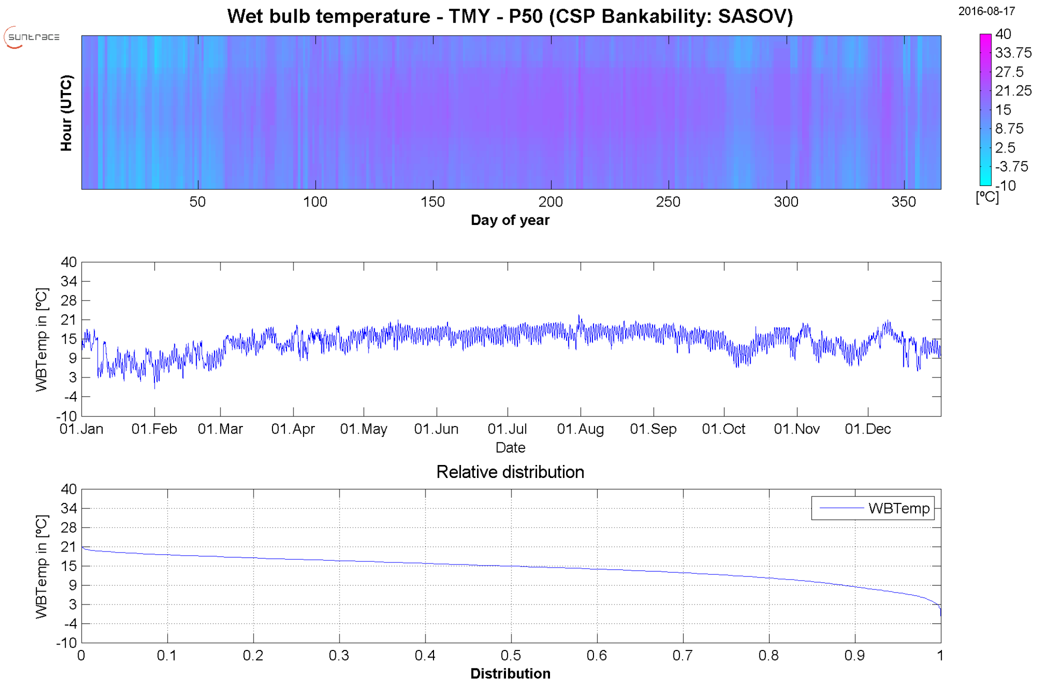

Figure 5-48: SASOV: TMY - hours of the day over the year (top), hourly values (middle) and distribution (bottom) of wet bulb temperature

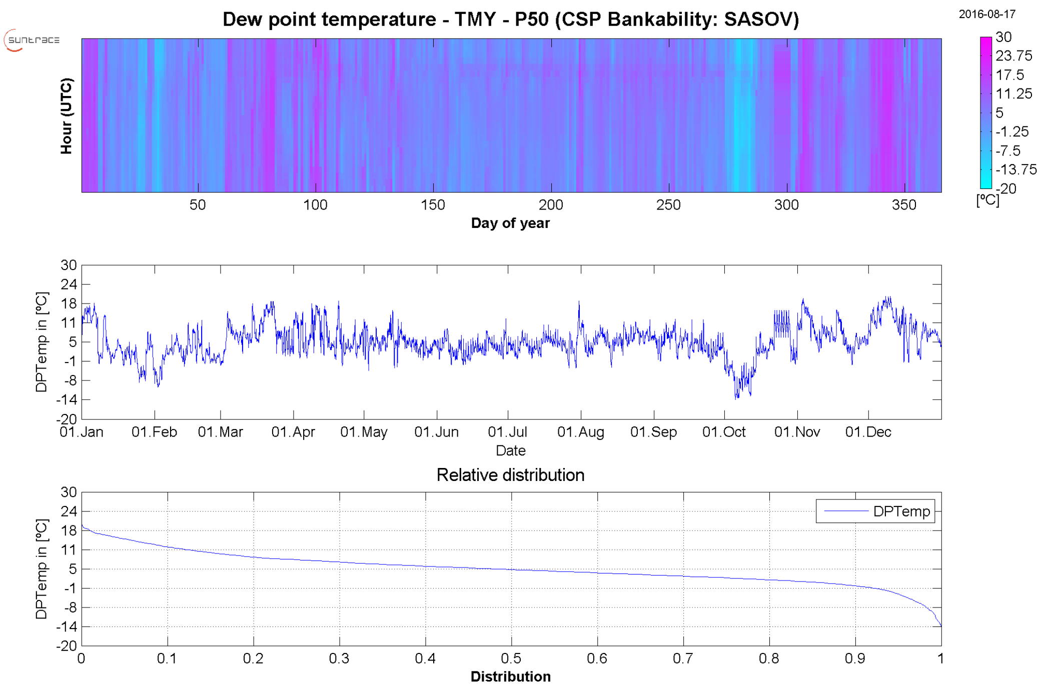

Figure 5-49: SASOV: TMY - hours of the day over the year (top), hourly values (middle) and distribution (bottom) of dew point temperature

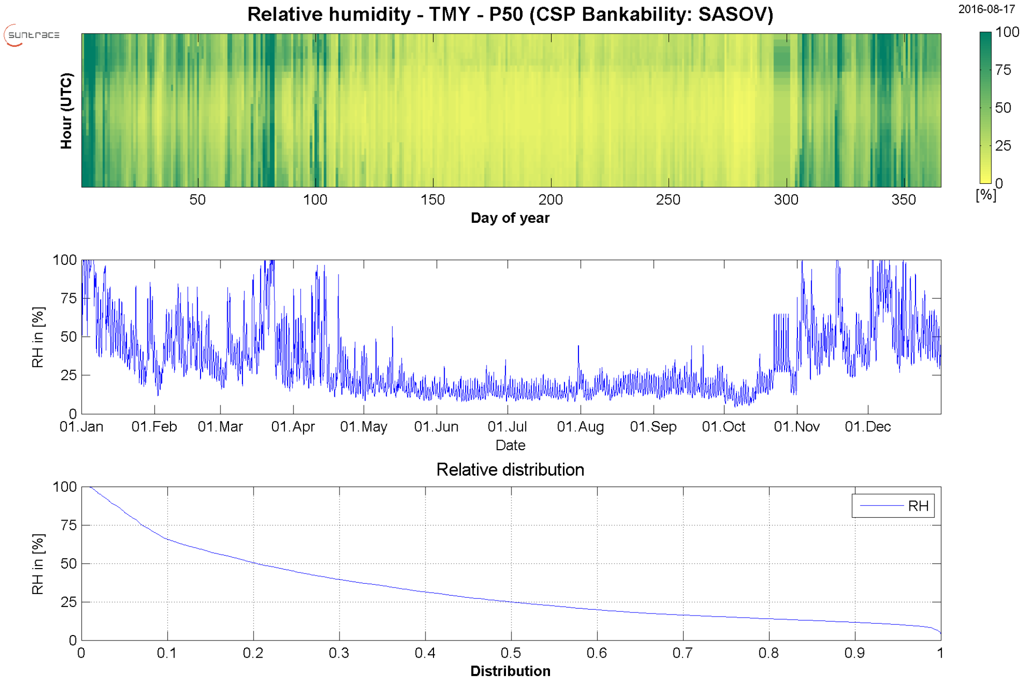

Figure 5-50: SASOV: TMY - hours of the day over the year (top), hourly values (middle) and distribution (bottom) of relative humidity

Barometric pressure

For the TMY of SASOV the mean barometric pressure is 928 hPa.

barometric pressure

	average [hPa]	min [hPa]	max [hPa]
Jan	934	927	941
Feb	931	925	940
Mar	929	920	937
Apr	927	920	933
May	924	920	929
Jun	922	918	928
Jul	921	917	925
Aug	922	918	926
Sep	927	923	931
Oct	929	925	932
Nov	933	927	938
Dec	933	926	941
Year	928	917	941

Table 5-47: SASOV: TMY - monthly values of barometric pressure

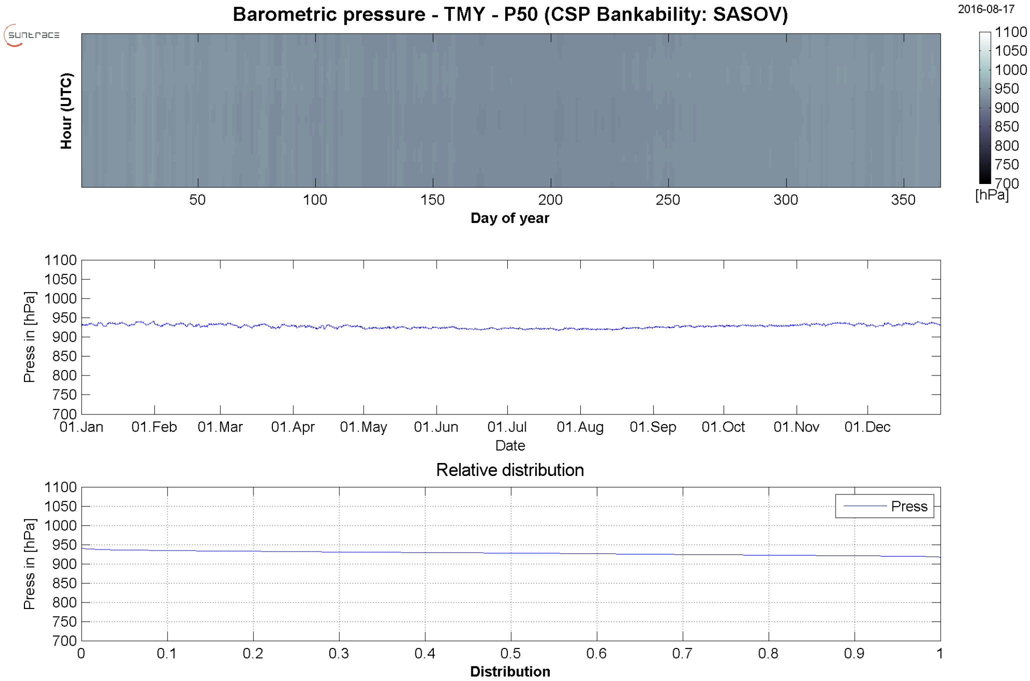

Figure 5-51: SASOV: TMY - hours of the day over the year (top), hourly values (middle) and distribution (bottom) of barometric pressure

5.8.4. ZADAA

5.8.4.1. Direct Normal Irradiance

For the TMY (P50 value) of the demo site ZADAA the annual mean direct normal irradiance is 310 W/m^2 equal to an annual sum of 2712 kWh/m^2/a. The DNI exceeded for 3441 hours 250 W/m^2 with an average of 760 W/m^2 taking just the DNI values higher than 250 W/m^2 into account.

For the MY90 with respect to multiple year uncertainty the annual mean direct normal irradiance is 299 W/m^2 equal to an annual sum of 2619 kWh/m^2/a. The DNI exceeded for 3371 hours 250 W/m^2 with an average of 748 W/m^2 taking just the DNI values higher than 250 W/m^2 into account.

Figure 5-10 (TMY) and Figure 5-11 (MY90) show the monthly values, the hours of the day over the year as well as the cumulative frequency distribution of DNI for the TMY and MY90 at ZADAA. The monthly values at ZADAA for the TMY are shown in Table 5-9 and for the MY90 with respect to multiple year uncertainty in Table 5-10.

direct normal irradiance TMY

	average [W/m^2]	min [W/m^2]	max [W/m^2]	sum [kWh/m^2]
Jan	354	0	1100	263
Feb	328	0	1075	220
Mar	296	0	1017	220
Apr	273	0	1057	197
May	260	0	927	194
Jun	261	0	921	188
Jul	272	0	987	202
Aug	278	0	1004	206
Sep	303	0	1035	218
Oct	334	0	1059	248
Nov	358	0	1079	257
Dec	401	0	1086	298
Year	310	0	1100	2712

Table 5-48: ZADAA: TMY - monthly values of DNI

direct normal irradiance MY90 (multiple year)

	average [W/m^2]	min [W/m^2]	max [W/m^2]	sum [kWh/m^2]
Jan	347	0	1100	258
Feb	315	0	1075	212
Mar	285	0	1017	212
Apr	263	0	1057	189
May	252	0	927	188
Jun	251	0	921	181
Jul	264	0	987	197
Aug	267	0	1004	199
Sep	292	0	1035	210
Oct	321	0	1059	239
Nov	345	0	1079	248
Dec	386	0	1086	287
Year	299	0	1100	2619

Table 5-49: ZADAA: MY90my - monthly values of DNI

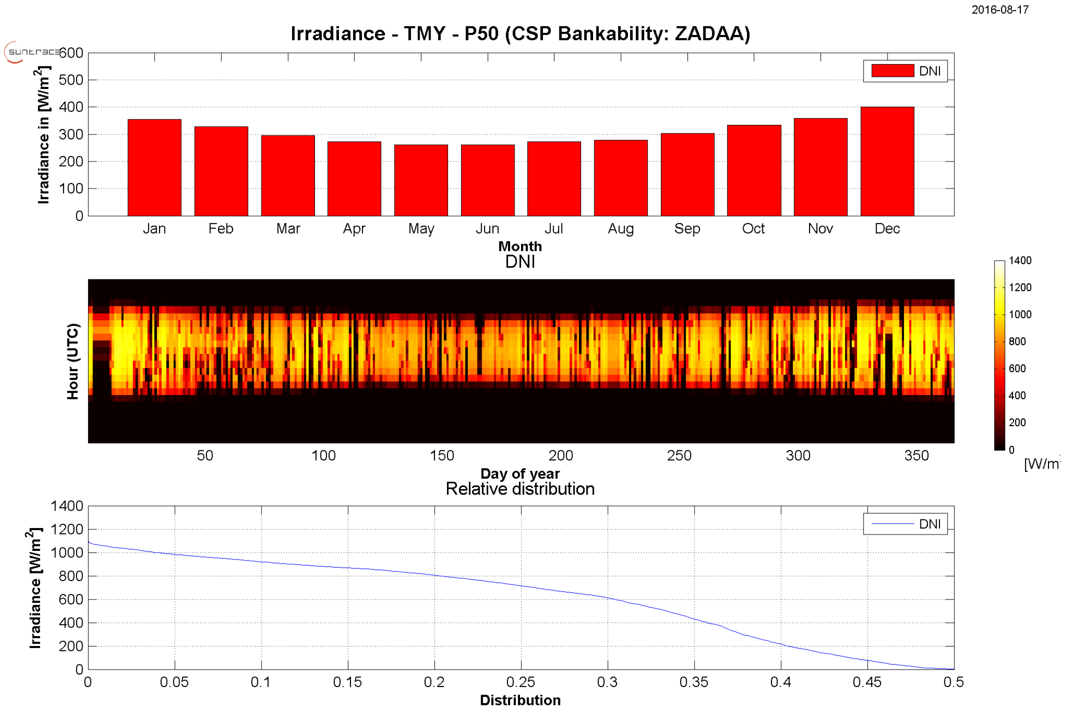

Figure 5-52: ZADAA: TMY - monthly values (top), hours of the day over the year (middle) and distribution (bottom) of DNI.

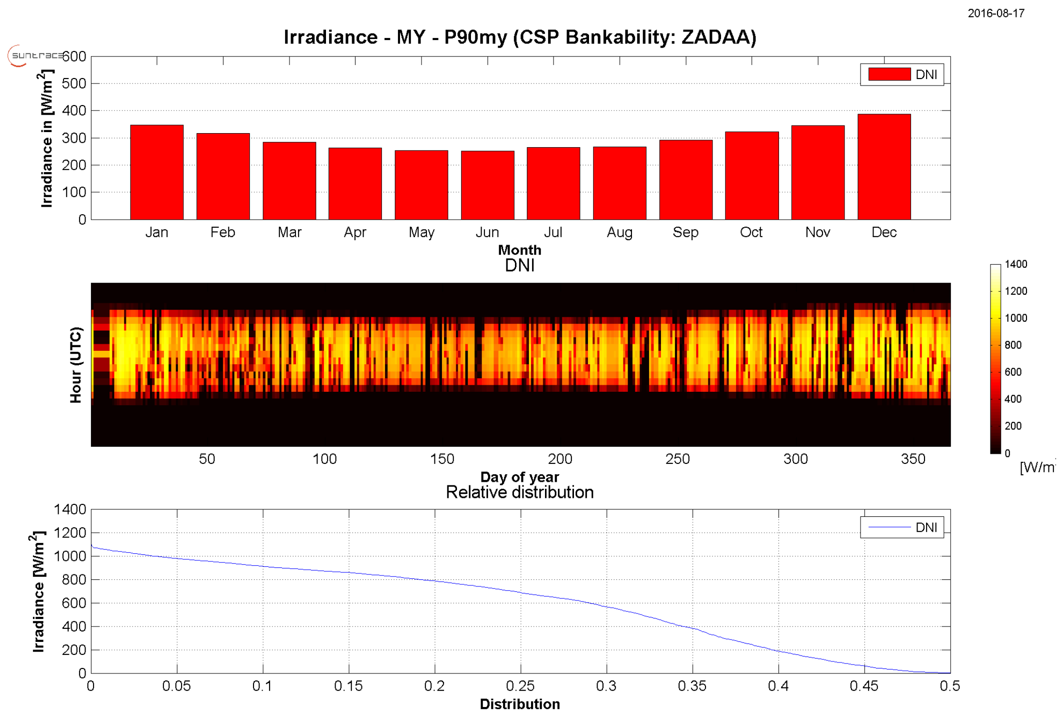

Figure 5-53: ZADAA: MY90 (multiple year) - monthly values (top), hours of the day over the year (middle) and distribution (bottom) of DNI.

5.8.4.2. Global and Diffuse Horizontal Irradiance

The monthly values of the TMY for GHI and DHI at ZADAA are listed in Table 5-11 to Table 5-14. Figure 5-12 to Figure 5-15 show the values in 60min time resolution over the year. For the TMY the annual mean GHI is 233 W/m^2 equal to an annual sum of 2040 kWh/m^2/a. For the MY90 (multiple year) the annual mean GHI is 229 W/m^2 equal to an annual sum of 2008 kWh/m^2/a.

global horizontal irradiance TMY

	average [W/m^2]	min [W/m^2]	max [W/m^2]	sum [kWh/m^2]
Jan	313	0	1151	233
Feb	286	0	1092	192
Mar	243	0	991	180
Apr	196	0	887	141
May	152	0	673	113
Jun	135	0	596	97
Jul	152	0	673	113
Aug	178	0	823	133
Sep	233	0	961	168
Oct	270	0	1017	201
Nov	312	0	1536	224
Dec	328	0	1128	244
Year	233	0	1536	2040

Table 5-50: ZADAA: TMY - monthly values of GHI

global horizontal irradiance MY90 (mult. year)

	average [W/m^2]	min [W/m^2]	max [W/m^2]	sum [kWh/m^2]
Jan	314	0	1141	233
Feb	277	0	1092	186
Mar	238	0	991	177
Apr	193	0	885	139
May	149	0	673	111
Jun	132	0	596	95
Jul	152	0	673	113
Aug	175	0	823	130
Sep	229	0	961	165
Oct	265	0	1017	197
Nov	305	0	1536	220
Dec	326	0	1128	242
Year	229	0	1536	2008

Table 5-51: ZADAA: MY90my - monthly values GHI

diffuse horizontal irradiance TMY

	average [W/m^2]	min [W/m^2]	max [W/m^2]	sum [kWh/m^2]
Jan	68	0	484	51
Feb	66	0	445	45
Mar	59	0	553	44
Apr	47	0	451	34
May	29	0	358	22
Jun	24	0	356	17
Jul	30	0	352	23
Aug	37	0	370	28
Sep	50	0	433	36
Oct	49	0	457	37
Nov	69	0	575	49
Dec	52	0	462	39
Year	48	0	575	423

Table 5-52: ZADAA: TMY - monthly values of DHI

diffuse horizontal irradiance MY90 (mult year)

	average [W/m^2]	min [W/m^2]	max [W/m^2]	sum [kWh/m^2]
Jan	71	0	484	53
Feb	66	0	445	45
Mar	61	0	553	45
Apr	49	0	499	36
May	29	0	358	22
Jun	25	0	356	18
Jul	33	0	352	24
Aug	38	0	370	28
Sep	54	0	433	39
Oct	51	0	457	38
Nov	70	0	575	51
Dec	58	0	462	43
Year	50	0	575	442

Table 5-53: ZADAA: MY90my - monthly values of DHI

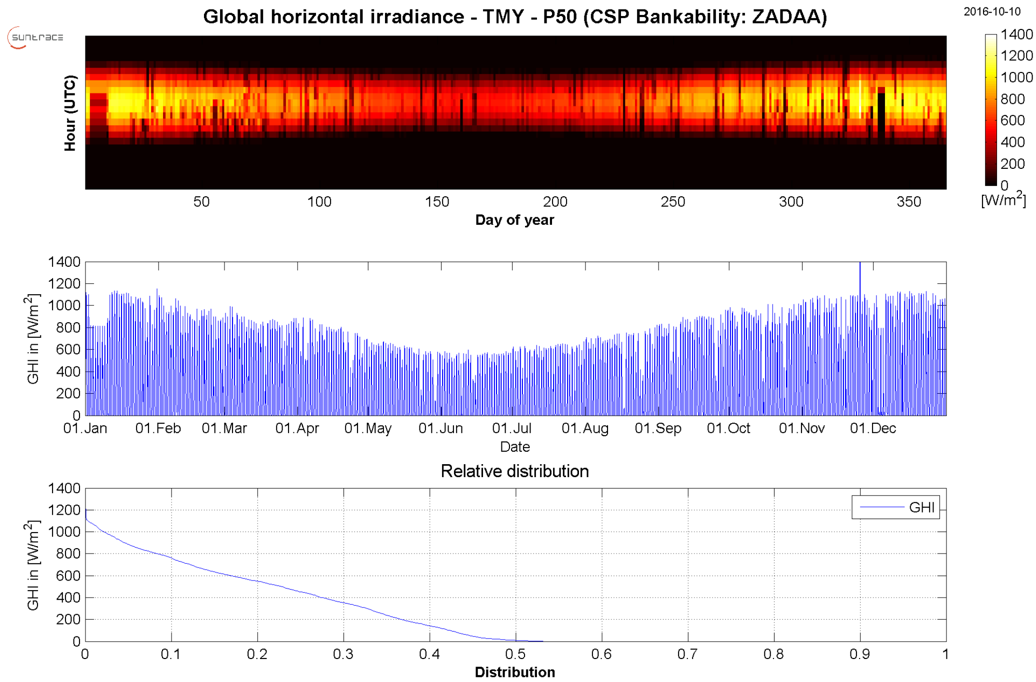

Figure 5-54: ZADAA: TMY - hours of the day over the year (top), hourly values (middle) and distribution (bottom) of GHI

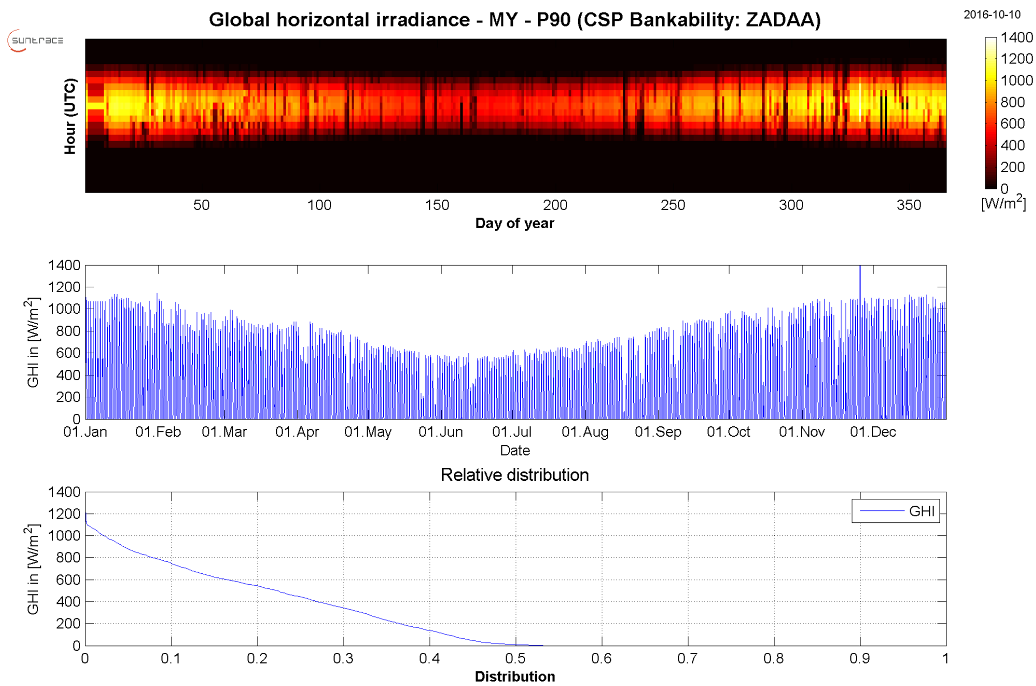

Figure 5-55: ZADAA: MY90my - hours of the day over the year (top), hourly values (middle) and distribution (bottom) of GHI

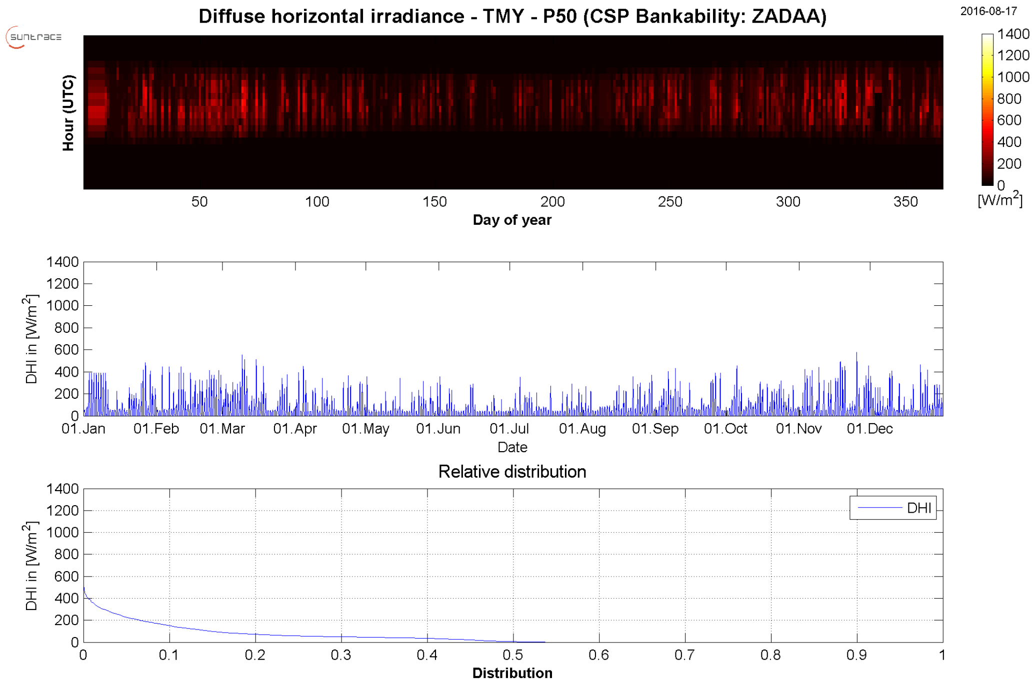

Figure 5-56: ZADAA: TMY - hours of the day over the year (top), hourly values (middle) and distribution (bottom) of DHI

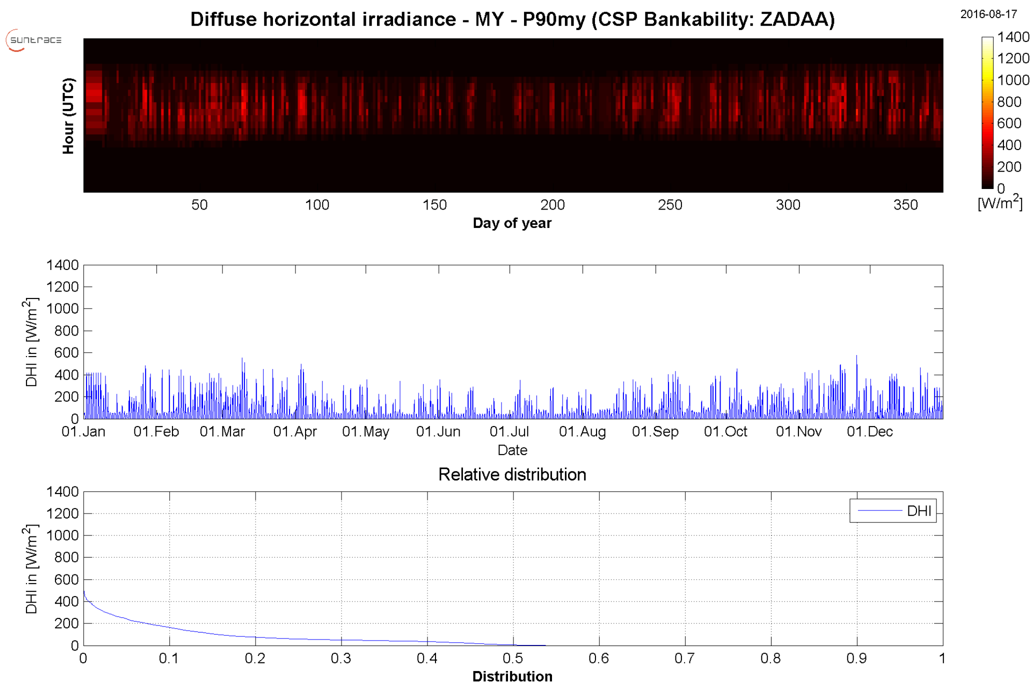

Figure 5-57: ZADAA: MY90my - hours of the day over the year (top), hourly values (middle) and distribution (bottom) of DHI

5.8.4.3. Auxiliary Meteorological Data (TMY)

The monthly values of the TMY for wind speed, wind direction, air temperature, wet bulb temperature, dew point temperature, relative humidity and barometric pressure at ZADAA are listed in Table 5-15 to Table 5-21. Figure 5-16 to Figure 5-23 show the values in 60min time resolution over the year.

Wind

For the TMY (P50) of ZADAA the mean horizontal wind speed is 6.8 m/s with a predominant wind direction of 8 ºN. The maximum hourly average wind speed is 19.5 m/s. This is an hourly average and can differ significantly from the wind gust, usually being defined as an average over three seconds. Wind gust values can be a multiple of the here displayed maximum hourly average wind speed. Therefore, the given values are not sufficient for plant construction.

wind speed

	average [m/s]	min [m/s]	max [m/s]
Jan	6.2	1.6	11.0
Feb	6.7	0.8	11.3
Mar	6.2	0.2	16.1
Apr	6.8	0.6	15.5
May	7.0	0.5	14.1
Jun	6.7	0.3	11.9
Jul	9.2	1.7	19.5
Aug	7.1	1.6	14.6
Sep	7.4	0.5	16.3
Oct	6.7	0.7	13.4
Nov	6.2	0.4	11.4
Dec	5.7	0.8	12.5
Year	6.8	0.2	19.5

Table 5-54: ZADAA: TMY - monthly values of wind speed

wind direction

	average [ºN]	min [ºN]	max [ºN]
Jan	17	0	360
Feb	85	0	359
Mar	308	0	360
Apr	210	0	360
May	56	0	360
Jun	336	1	360
Jul	320	0	360
Aug	349	0	360
Sep	193	0	360
Oct	89	1	360
Nov	347	0	360
Dec	36	0	360
Year	8	0	360

Table 5-55: ZADAA: TMY - monthly values of wind direction

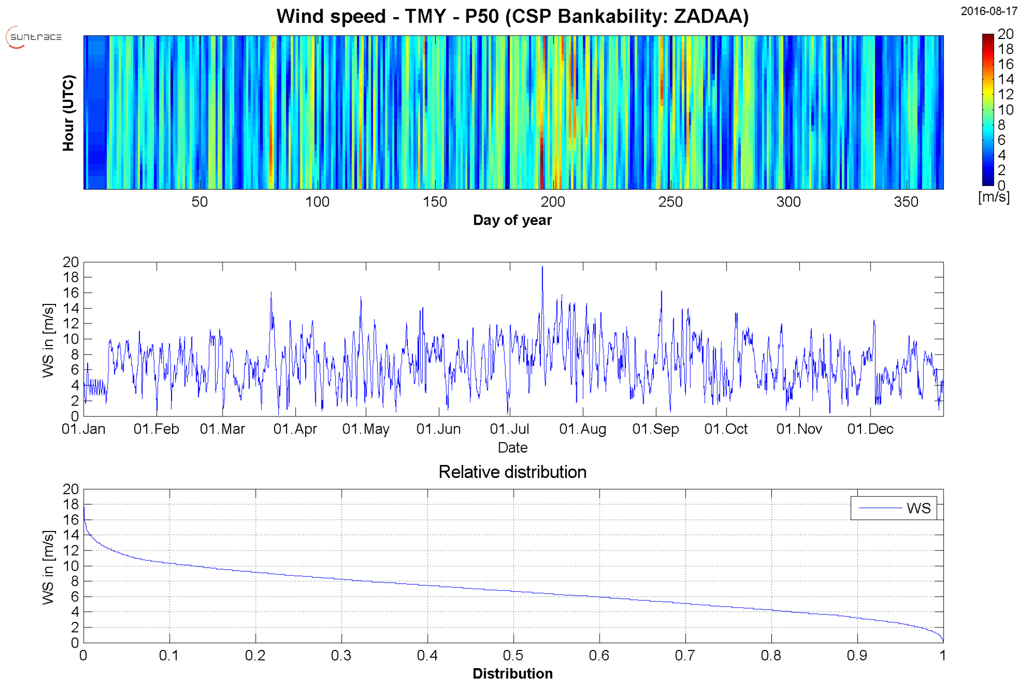

Figure 5-58: ZADAA: TMY - hours of the day over the year (top), hourly values (middle) and distribution (bottom) of wind speed

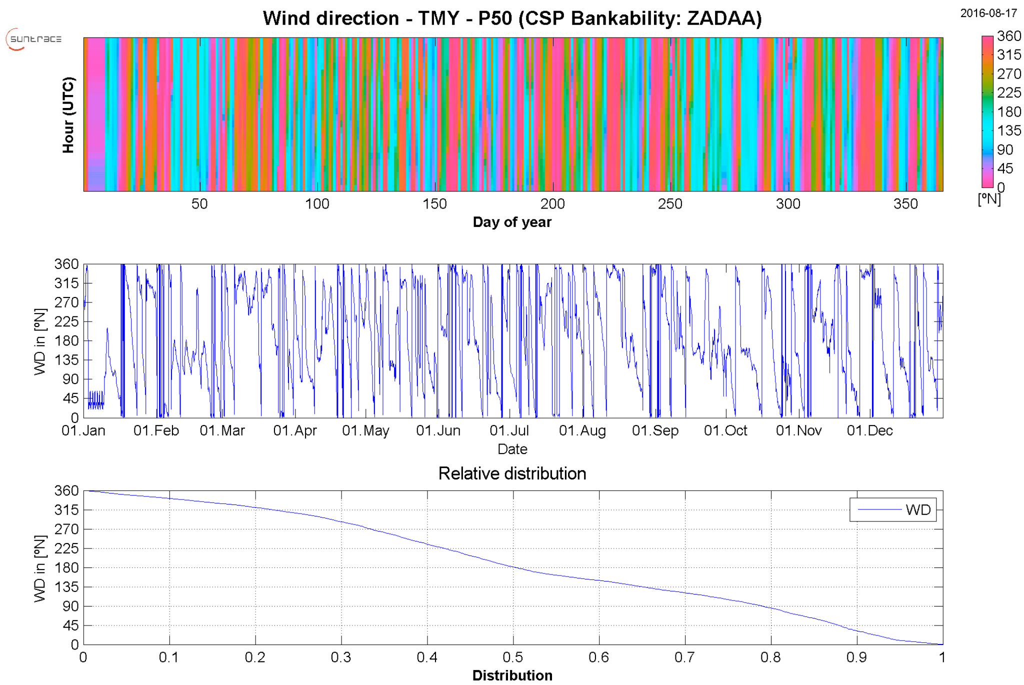

Figure 5-59: ZADAA: TMY - hours of the day over the year (top), hourly values (middle) and distribution (bottom) of wind direction

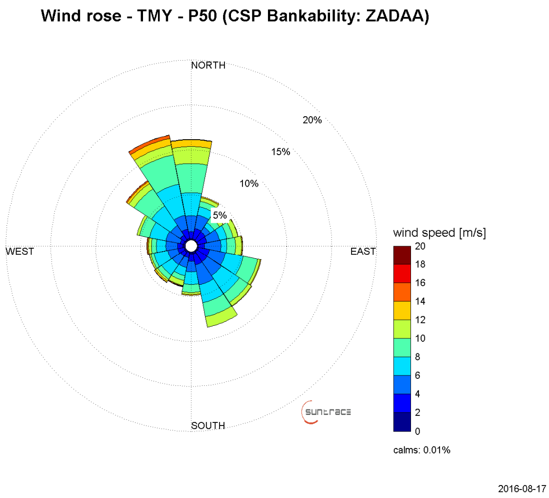

Figure 5-60: ZADAA: TMY – wind rose

Air-, Dew Point-, Wet Bulb- Temperatures and Relative Humidity

For the TMY of ZADAA the mean annual air temperature is 17.5ºC with a minimum of 0.1ºC and a maximum of 36.8ºC. The mean annual wet bulb temperature is 10.4ºC with a minimum of -2.8ºC and a maximum of 20.7ºC. The mean annual dew point temperature is 4.3ºC with a minimum of -15.5ºC and a maximum of 19.4ºC. The mean relative humidity is 49%.

air temperature

	average [ºC]	min [ºC]	max [ºC]
Jan	23.5	9.2	36.8
Feb	24.7	8.9	35.6
Mar	22.1	4.3	33.3
Apr	19.3	4.3	32.4
May	14.2	0.3	27.9
Jun	8.5	0.1	21.3
Jul	8.7	0.1	21.6
Aug	11.3	0.2	24.8
Sep	15.9	2.4	29.6
Oct	19.8	4.7	32.5
Nov	20.1	8.5	32.6
Dec	22.2	10.9	35.8
Year	17.5	0.1	36.8

Table 5-56: ZADAA: TMY - monthly values of air temperature

wet bulb temperature

	average [ºC]	min [ºC]	max [ºC]
Jan	14.5	5.1	19.9
Feb	14.2	7.4	18.8
Mar	14.5	2.5	20.3
Apr	10.7	1.5	16.2
May	7.1	-0.2	14.7
Jun	4.9	-1.3	11.2
Jul	4.5	-2.8	12.0
Aug	6.6	-2.5	14.5
Sep	8.9	0.6	14.6
Oct	11.7	1.8	18.8
Nov	13.4	6.2	19.7
Dec	14.5	7.6	20.7
Year	10.4	-2.8	20.7

Table 5-57: ZADAA: TMY - monthly values of wet bulb temperature

dew point temperature

	average	min	max
	[ºC]	[ºC]	[ºC]
Jan	7.7	-12.0	19.0
Feb	6.6	-8.1	15.4
Mar	8.7	-10.7	19.4
Apr	3.0	-13.7	15.1
May	-1.1	-10.7	12.5
Jun	1.0	-9.3	9.3
Jul	-0.2	-10.6	9.1
Aug	1.3	-15.5	11.7
Sep	2.4	-12.2	13.0
Oct	5.0	-10.1	16.6
Nov	8.3	-7.6	18.1
Dec	9.3	-13.0	19.2
Year	4.3	-15.5	19.4

Table 5-58: ZADAA: TMY - monthly values of dew point temperature

relative humidity

	average	min	max
	[%]	[%]	[%]
Jan	44	5	100
Feb	37	6	92
Mar	50	8	100
Apr	40	7	100
May	42	9	100
Jun	63	14	100
Jul	59	15	100
Aug	57	8	100
Sep	47	8	100
Oct	43	7	91
Nov	54	10	100
Dec	51	6	100
Year	49	5	100

Table 5-59: ZADAA: TMY - monthly values of relative humidity

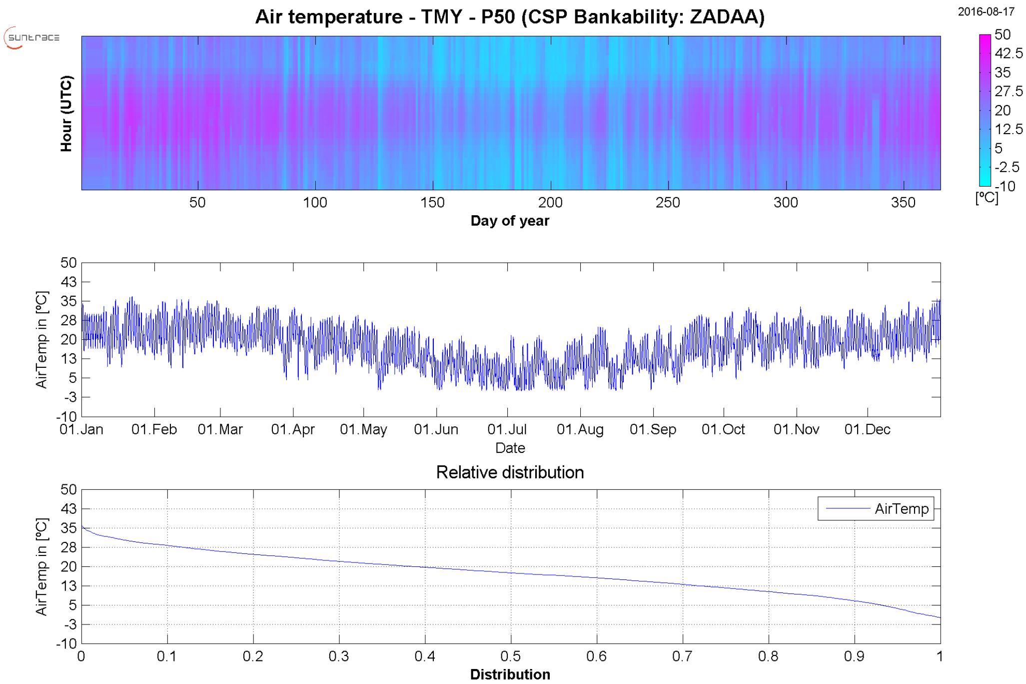

Figure 5-61: ZADAA: TMY - hours of the day over the year (top), hourly values (middle) and distribution (bottom) of air temperature

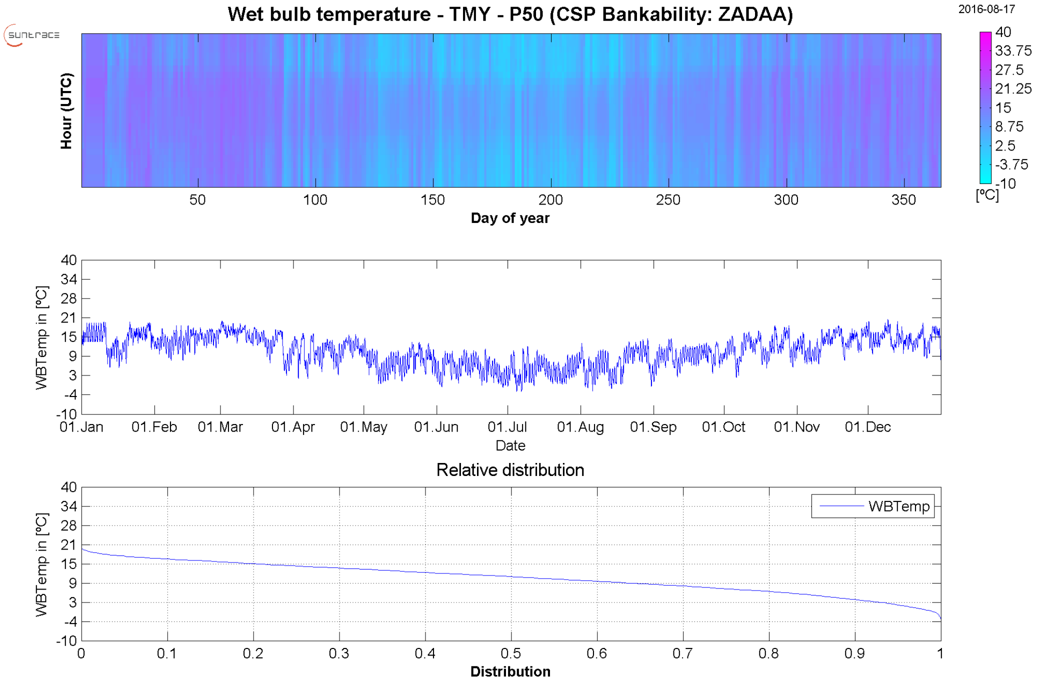

Figure 5-62: ZADAA: TMY - hours of the day over the year (top), hourly values (middle) and distribution (bottom) of wet bulb temperature

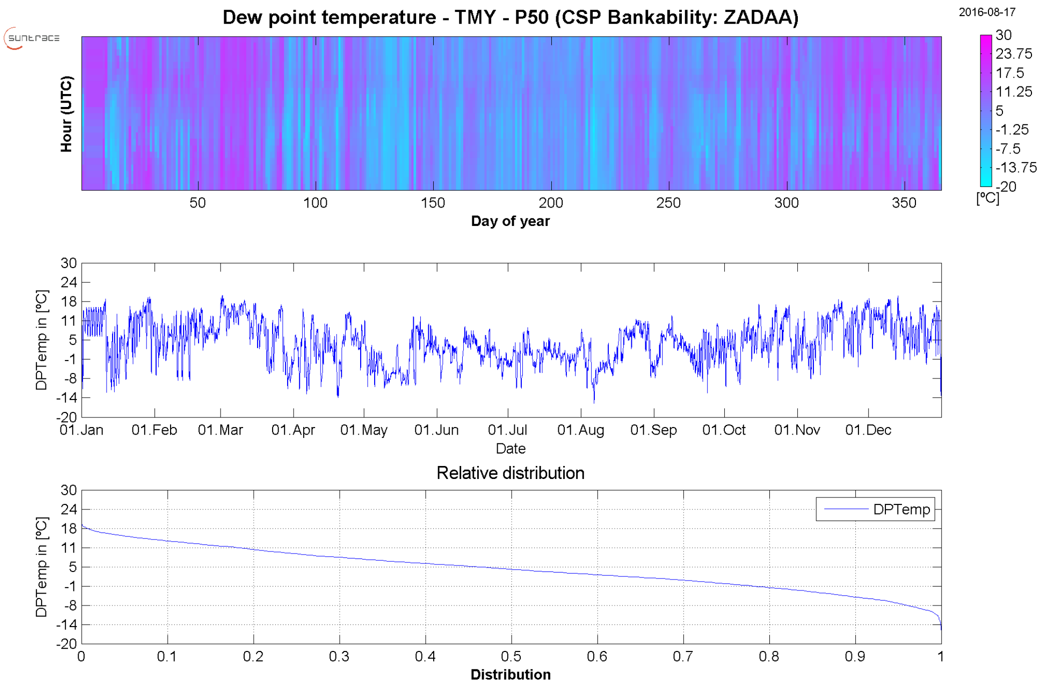

Figure 5-63: ZADAA: TMY - hours of the day over the year (top), hourly values (middle) and distribution (bottom) of dew point temperature

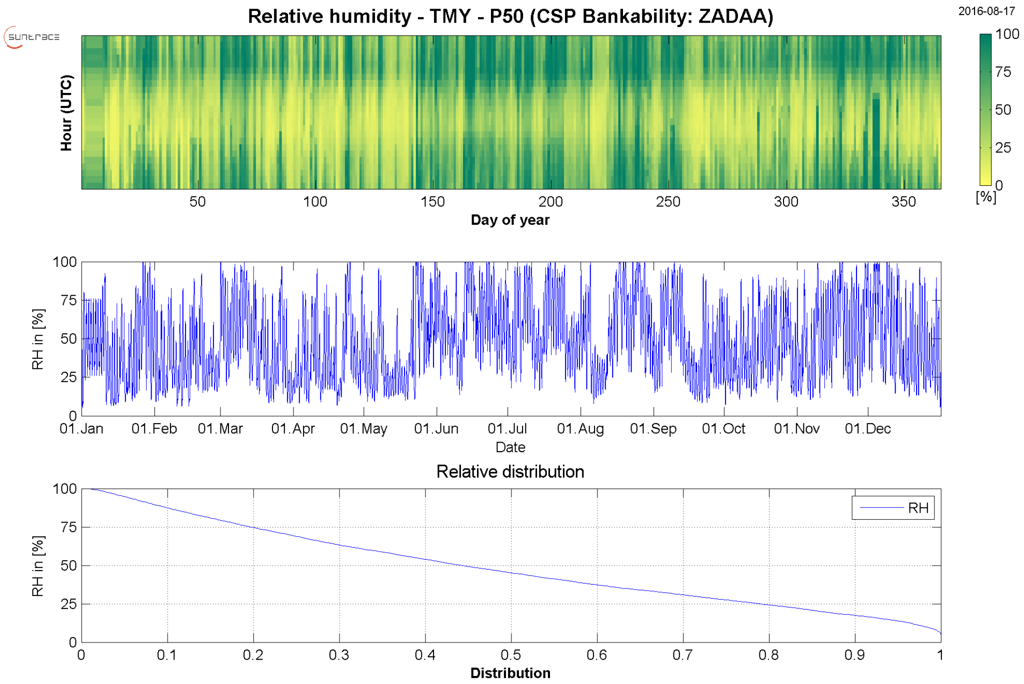

Figure 5-64: ZADAA: TMY - hours of the day over the year (top), hourly values (middle) and distribution (bottom) of relative humidity

Barometric pressure

For the TMY of ZADAA the mean barometric pressure is 874 hPa.

barometric pressure

	average [hPa]	min [hPa]	max [hPa]
Jan	868	861	875
Feb	872	863	879
Mar	874	867	879
Apr	872	864	877
May	875	866	882
Jun	879	868	888
Jul	878	865	887
Aug	876	867	884
Sep	875	862	885
Oct	873	864	880
Nov	872	865	877
Dec	869	862	876
Year	874	861	888

Table 5-60: ZADAA: TMY - monthly values of barometric pressure

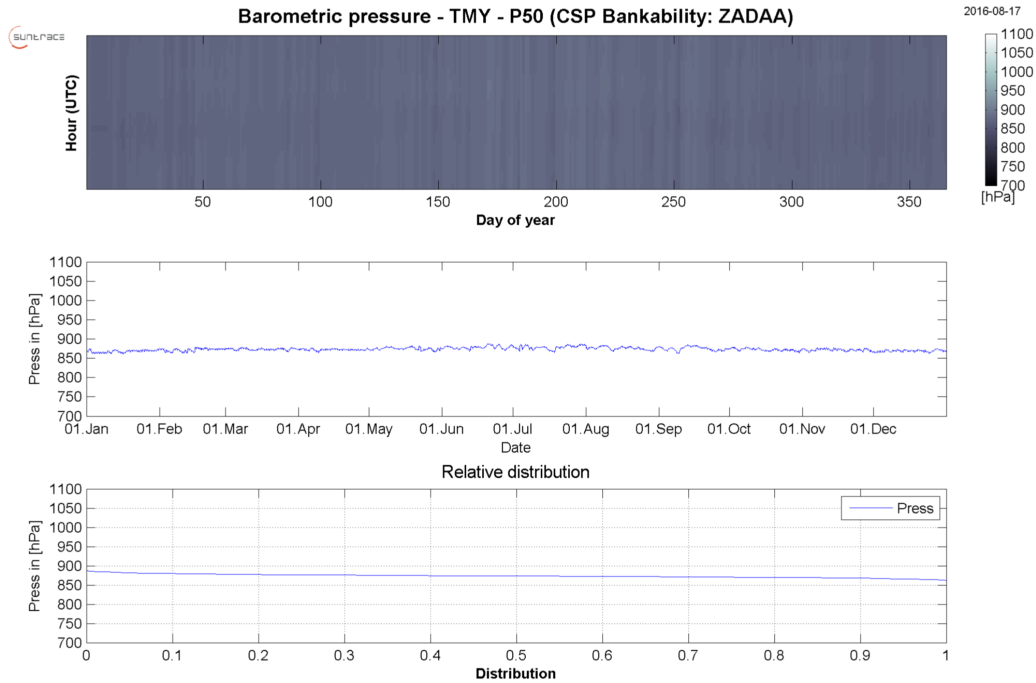

Figure 5-65: ZADAA: TMY - hours of the day over the year (top), hourly values (middle) and distribution (bottom) of barometric pressure

5.9. List of delivered data files

In the course of this solar resource assessment a total of 112 data files have been generated. These are regarded as an annex to this report and listed in Table 61 to Table 64. For each site all data sets are packed in one container file and uploaded on the project team site.

ESPSA			
Filename	**description of contents**	**time res.**	**temporal coverage**
guiSmo_ESPSA_TMY_P50_10min_2207kWh_DNI_mltyear_20160823.txt	- TMY in MET_IEC Data format 1.0 - site: ESPSA - P50 case DNI - measurements as described in 3.8 - time stamp in UTC	10min	from 2015-01-01 to 2005-12-31
guiSmo_ESPSA_TMY_P50_15min_2207kWh_DNI_mltyear_20160823.txt		15min	
guiSmo_ESPSA_TMY_P50_30min_2207kWh_DNI_mltyear_20160823.txt		30min	
guiSmo_ESPSA_TMY_P50_60min_2207kWh_DNI_mltyear_20160823.txt		60min	
guiSmo_ESPSA_MY_P75_10min_2171kWh_DNI_mltyear_20160823.txt	- MY in MET_IEC Data format 1.0 - site: ESPSA - P75 case DNI - multiple year uncertainty - measurements as described in 3.9 - time stamp in UTC	10min	from 2015-01-01 to 2005-12-31
guiSmo_ESPSA_MY_P75_15min_2171kWh_DNI_mltyear_20160823.txt		15min	
guiSmo_ESPSA_MY_P75_30min_2171kWh_DNI_mltyear_20160823.txt		30min	
guiSmo_ESPSA_MY_P75_60min_2171kWh_DNI_mltyear_20160823.txt		60min	
guiSmo_ESPSA_MY_P75_10min_2128kWh_DNI_sglyear_20160823.txt	- MY in MET_IEC Data format 1.0 - site: ESPSA - P75 case DNI - single year uncertainty - measurements as described in 3.9 - time stamp in UTC	10min	from 2015-01-01 to 2005-12-31
guiSmo_ESPSA_MY_P75_15min_2128kWh_DNI_sglyear_20160823.txt		15min	
guiSmo_ESPSA_MY_P75_30min_2128kWh_DNI_sglyear_20160823.txt		30min	
guiSmo_ESPSA_MY_P75_60min_2128kWh_DNI_sglyear_20160823.txt		60min	
guiSmo_ESPSA_MY_P90_10min_2132kWh_DNI_mltyear_20160823.txt	- MY in MET_IEC Data format 1.0 - site: ESPSA - P90 case DNI - multiple year uncertainty - measurements as described in 3.9 - time stamp in UTC	10min	from 2015-01-01 to 2005-12-31
guiSmo_ESPSA_MY_P90_15min_2132kWh_DNI_mltyear_20160823.txt		15min	
guiSmo_ESPSA_MY_P90_30min_2132kWh_DNI_mltyear_20160823.txt		30min	
guiSmo_ESPSA_MY_P90_60min_2132kWh_DNI_mltyear_20160823.txt		60min	
guiSmo_ESPSA_MY_P90_10min_2057kWh_DNI_sglyear_20160823.txt	- MY in MET_IEC Data format 1.0 - site: ESPSA - P90 case DNI - single year uncertainty - measurements as described in 3.9 - time stamp in UTC	10min	from 2015-01-01 to 2005-12-31
guiSmo_ESPSA_MY_P90_15min_2057kWh_DNI_sglyear_20160823.txt		15min	
guiSmo_ESPSA_MY_P90_30min_2057kWh_DNI_sglyear_20160823.txt		30min	
guiSmo_ESPSA_MY_P90_60min_2057kWh_DNI_sglyear_20160823.txt		60min	
guiSmo_ESPSA_MY_P95_10min_2110kWh_DNI_mltyear_20160823.txt	- MY in MET_IEC Data format 1.0 - site: ESPSA - P95 case DNI - multiple year uncertainty - measurements as described in 3.9 - time stamp in UTC	10min	from 2015-01-01 to 2005-12-31
guiSmo_ESPSA_MY_P95_15min_2110kWh_DNI_mltyear_20160823.txt		15min	
guiSmo_ESPSA_MY_P95_30min_2110kWh_DNI_mltyear_20160823.txt		30min	
guiSmo_ESPSA_MY_P95_60min_2110kWh_DNI_mltyear_20160823.txt		60min	
guiSmo_ESPSA_MY_P95_10min_2012kWh_DNI_sglyear_20160823.txt	- MY in MET_IEC Data format 1.0 - site: ESPSA - P95 case DNI - single year uncertainty - measurements as described in 3.9 - time stamp in UTC	10min	from 2015-01-01 to 2005-12-31
guiSmo_ESPSA_MY_P95_15min_2012kWh_DNI_sglyear_20160823.txt		15min	
guiSmo_ESPSA_MY_P95_30min_2012kWh_DNI_sglyear_20160823.txt		30min	
guiSmo_ESPSA_MY_P95_60min_2012kWh_DNI_sglyear_20160823.txt		60min	

Table 61: Listing and description of delivered data files, ESPSA

DZTAM			
Filename	**description of contents**	**time res.**	**temporal coverage**
guiSmo_DZTAM_TMY_P50_10min_2385kWh_DNI_mltyear_20160817.txt	- TMY in MET_IEC Data format 1.0 - site: DZTAM - P50 case DNI - measurements as described in 3.8 - time stamp in UTC	10min	from 2015-01-01 to 2005-12-31
guiSmo_DZTAM_TMY_P50_15min_2385kWh_DNI_mltyear_20160817.txt		15min	
guiSmo_DZTAM_TMY_P50_30min_2385kWh_DNI_mltyear_20160817.txt		30min	
guiSmo_DZTAM_TMY_P50_60min_2385kWh_DNI_mltyear_20160817.txt		60min	
guiSmo_DZTAM_MY_P75_10min_2348kWh_DNI_mltyear_20160817.txt	- MY in MET_IEC Data format 1.0 - site: DZTAM - P75 case DNI - multiple year uncertainty - measurements as described in 3.9 - time stamp in UTC	10min	from 2015-01-01 to 2005-12-31
guiSmo_DZTAM_MY_P75_15min_2348kWh_DNI_mltyear_20160817.txt		15min	
guiSmo_DZTAM_MY_P75_30min_2348kWh_DNI_mltyear_20160817.txt		30min	
guiSmo_DZTAM_MY_P75_60min_2348kWh_DNI_mltyear_20160817.txt		60min	
guiSmo_DZTAM_MY_P75_10min_2307kWh_DNI_sglyear_20160817.txt	- MY in MET_IEC Data format 1.0 - site: DZTAM - P75 case DNI - single year uncertainty - measurements as described in 3.9 - time stamp in UTC	10min	from 2015-01-01 to 2005-12-31
guiSmo_DZTAM_MY_P75_15min_2307kWh_DNI_sglyear_20160817.txt		15min	
guiSmo_DZTAM_MY_P75_30min_2307kWh_DNI_sglyear_20160817.txt		30min	
guiSmo_DZTAM_MY_P75_60min_2307kWh_DNI_sglyear_20160817.txt		60min	
guiSmo_DZTAM_MY_P90_10min_2313kWh_DNI_mltyear_20160817.txt	- MY in MET_IEC Data format 1.0 - site: DZTAM - P90 case DNI - multiple year uncertainty - measurements as described in 3.9 - time stamp in UTC	10min	from 2015-01-01 to 2005-12-31
guiSmo_DZTAM_MY_P90_15min_2313kWh_DNI_mltyear_20160817.txt		15min	
guiSmo_DZTAM_MY_P90_30min_2313kWh_DNI_mltyear_20160817.txt		30min	
guiSmo_DZTAM_MY_P90_60min_2313kWh_DNI_mltyear_20160817.txt		60min	
guiSmo_DZTAM_MY_P90_10min_2230kWh_DNI_sglyear_20160817.txt	- MY in MET_IEC Data format 1.0 - site: DZTAM - P90 case DNI - single year uncertainty - measurements as described in 3.9 - time stamp in UTC	10min	from 2015-01-01 to 2005-12-31
guiSmo_DZTAM_MY_P90_15min_2230kWh_DNI_sglyear_20160817.txt		15min	
guiSmo_DZTAM_MY_P90_30min_2230kWh_DNI_sglyear_20160817.txt		30min	
guiSmo_DZTAM_MY_P90_60min_2230kWh_DNI_sglyear_20160817.txt		60min	
guiSmo_DZTAM_MY_P95_10min_2294kWh_DNI_mltyear_20160817.txt	- MY in MET_IEC Data format 1.0 - site: DZTAM - P95 case DNI - multiple year uncertainty - measurements as described in 3.9 - time stamp in UTC	10min	from 2015-01-01 to 2005-12-31
guiSmo_DZTAM_MY_P95_15min_2294kWh_DNI_mltyear_20160817.txt		15min	
guiSmo_DZTAM_MY_P95_30min_2294kWh_DNI_mltyear_20160817.txt		30min	
guiSmo_DZTAM_MY_P95_60min_2294kWh_DNI_mltyear_20160817.txt		60min	
guiSmo_DZTAM_MY_P95_10min_2187kWh_DNI_sglyear_20160817.txt	- MY in MET_IEC Data format 1.0 - site: DZTAM - P95 case DNI - single year uncertainty - measurements as described in 3.9 - time stamp in UTC	10min	from 2015-01-01 to 2005-12-31
guiSmo_DZTAM_MY_P95_15min_2187kWh_DNI_sglyear_20160817.txt		15min	
guiSmo_DZTAM_MY_P95_30min_2187kWh_DNI_sglyear_20160817.txt		30min	
guiSmo_DZTAM_MY_P95_60min_2187kWh_DNI_sglyear_20160817.txt		60min	

Table 65: Listing and description of delivered data files, DZTAM

SASOV			
Filename	**description of contents**	**time res.**	**temporal coverage**
guiSmo_SASOV_TMY_P50_10min_2275kWh_DNI_mltyear_20160817.txt	- TMY in MET_IEC Data format 1.0 - site: SASOV - P50 case DNI - measurements as described in 3.8 - time stamp in UTC	10min	from 2015-01-01 to 2005-12-31
guiSmo_SASOV_TMY_P50_15min_2275kWh_DNI_mltyear_20160817.txt		15min	
guiSmo_SASOV_TMY_P50_30min_2275kWh_DNI_mltyear_20160817.txt		30min	
guiSmo_SASOV_TMY_P50_60min_2275kWh_DNI_mltyear_20160817.txt		60min	
guiSmo_SASOV_MY_P75_10min_2234kWh_DNI_mltyear_20160817.txt	- MY in MET_IEC Data format 1.0 - site: SASOV - P75 case DNI - multiple year uncertainty - measurements as described in 3.9 - time stamp in UTC	10min	from 2015-01-01 to 2005-12-31
guiSmo_SASOV_MY_P75_15min_2234kWh_DNI_mltyear_20160817.txt		15min	
guiSmo_SASOV_MY_P75_30min_2234kWh_DNI_mltyear_20160817.txt		30min	
guiSmo_SASOV_MY_P75_60min_2234kWh_DNI_mltyear_20160817.txt		60min	
guiSmo_SASOV_MY_P75_10min_2193kWh_DNI_sglyear_20160817.txt	- MY in MET_IEC Data format 1.0 - site: ESPSA - P75 case DNI - single year uncertainty - measurements as described in 3.9 - time stamp in UTC	10min	from 2015-01-01 to 2005-12-31
guiSmo_ESPSA_MY_P75_15min_2193kWh_DNI_sglyear_20160817.txt		15min	
guiSmo_ESPSA_MY_P75_30min_2193kWh_DNI_sglyear_20160817.txt		30min	
guiSmo_ESPSA_MY_P75_60min_2193kWh_DNI_sglyear_20160817.txt		60min	
guiSmo_ESPSA_MY_P90_10min_2191kWh_DNI_mltyear_20160817.txt	- MY in MET_IEC Data format 1.0 - site: ESPSA - P90 case DNI - multiple year uncertainty - measurements as described in 3.9 - time stamp in UTC	10min	from 2015-01-01 to 2005-12-31
guiSmo_ESPSA_MY_P90_15min_2191kWh_DNI_mltyear_20160817.txt		15min	
guiSmo_SASOV_MY_P90_30min_2191kWh_DNI_mltyear_20160817.txt		30min	
guiSmo_SASOV_MY_P90_60min_2191kWh_DNI_mltyear_20160817.txt		60min	
guiSmo_SASOV_MY_P90_10min_2121kWh_DNI_sglyear_20160817.txt	- MY in MET_IEC Data format 1.0 - site: SASOV - P90 case DNI - single year uncertainty - measurements as described in 3.9 - time stamp in UTC	10min	from 2015-01-01 to 2005-12-31
guiSmo_SASOV_MY_P90_15min_2121kWh_DNI_sglyear_20160817.txt		15min	
guiSmo_SASOV_MY_P90_30min_2121kWh_DNI_sglyear_20160817.txt		30min	
guiSmo_SASOV_MY_P90_60min_2121kWh_DNI_sglyear_20160817.txt		60min	
guiSmo_SASOV_MY_P95_10min_2168kWh_DNI_mltyear_20160817.txt	- MY in MET_IEC Data format 1.0 - site: SASOV - P95 case DNI - multiple year uncertainty - measurements as described in 3.9 - time stamp in UTC	10min	from 2015-01-01 to 2005-12-31
guiSmo_SASOV_MY_P95_15min_2168kWh_DNI_mltyear_20160817.txt		15min	
guiSmo_SASOV_MY_P95_30min_2168kWh_DNI_mltyear_20160817.txt		30min	
guiSmo_SASOV_MY_P95_60min_2168kWh_DNI_mltyear_20160817.txt		60min	
guiSmo_SASOV_MY_P95_10min_2077kWh_DNI_sglyear_20160817.txt	- MY in MET_IEC Data format 1.0 - site: SASOV - P95 case DNI - single year uncertainty - measurements as described in 3.9 - time stamp in UTC	10min	from 2015-01-01 to 2005-12-31
guiSmo_SASOV_MY_P95_15min_2077kWh_DNI_sglyear_20160817.txt		15min	
guiSmo_SASOV_MY_P95_30min_2077kWh_DNI_sglyear_20160817.txt		30min	
guiSmo_SASOV_MY_P95_60min_2077kWh_DNI_sglyear_20160817.txt		60min	

Table 66: Listing and description of delivered data files, SASOV

ZADAA			
Filename	**description of contents**	**time res.**	**temporal coverage**
guiSmo_ZADAA_TMY_P50_10min_2712kWh_DNI_mltyear_20160817.txt	- TMY in MET_IEC Data format 1.0 - site: ZADAA - P50 case DNI - measurements as described in 3.8 - time stamp in UTC	10min	from 2015-01-01 to 2005-12-31
guiSmo_ZADAA_TMY_P50_15min_2712kWh_DNI_mltyear_20160817.txt		15min	
guiSmo_ZADAA_TMY_P50_30min_2712kWh_DNI_mltyear_20160817.txt		30min	
guiSmo_ZADAA_TMY_P50_60min_2712kWh_DNI_mltyear_20160817.txt		60min	
guiSmo_ZADAA_MY_P75_10min_2658kWh_DNI_mltyear_20160817.txt	- MY in MET_IEC Data format 1.0 - site: ZADAA - P75 case DNI - multiple year uncertainty - measurements as described in 3.9 - time stamp in UTC	10min	from 2015-01-01 to 2005-12-31
guiSmo_ZADAA_MY_P75_15min_2658kWh_DNI_mltyear_20160817.txt		15min	
guiSmo_ZADAA_MY_P75_30min_2658kWh_DNI_mltyear_20160817.txt		30min	
guiSmo_ZADAA_MY_P75_60min_2658kWh_DNI_mltyear_20160817.txt		60min	
guiSmo_ZADAA_MY_P75_10min_2644kWh_DNI_sglyear_20160817.txt	- MY in MET_IEC Data format 1.0 - site: ZADAA - P75 case DNI - single year uncertainty - measurements as described in 3.9 - time stamp in UTC	10min	from 2015-01-01 to 2005-12-31
guiSmo_ZADAA_MY_P75_15min_2644kWh_DNI_sglyear_20160817.txt		15min	
guiSmo_ZADAA_MY_P75_30min_2644kWh_DNI_sglyear_20160817.txt		30min	
guiSmo_ZADAA_MY_P75_60min_2644kWh_DNI_sglyear_20160817.txt		60min	
guiSmo_ZADAA_MY_P90_10min_2619kWh_DNI_mltyear_20160817.txt	- MY in MET_IEC Data format 1.0 - site: ZADAA - P90 case DNI - multiple year uncertainty - measurements as described in 3.9 - time stamp in UTC	10min	from 2015-01-01 to 2005-12-31
guiSmo_ZADAA_MY_P90_15min_2619kWh_DNI_mltyear_20160817.txt		15min	
guiSmo_ZADAA_MY_P90_30min_2619kWh_DNI_mltyear_20160817.txt		30min	
guiSmo_ZADAA_MY_P90_60min_2619kWh_DNI_mltyear_20160817.txt		60min	
guiSmo_ZADAA_MY_P90_10min_2572kWh_DNI_sglyear_20160817.txt	- MY in MET_IEC Data format 1.0 - site: ZADAA - P90 case DNI - single year uncertainty - measurements as described in 3.9 - time stamp in UTC	10min	from 2015-01-01 to 2005-12-31
guiSmo_ZADAA_MY_P90_15min_2572kWh_DNI_sglyear_20160817.txt		15min	
guiSmo_ZADAA_MY_P90_30min_2572kWh_DNI_sglyear_20160817.txt		30min	
guiSmo_ZADAA_MY_P90_60min_2572kWh_DNI_sglyear_20160817.txt		60min	
guiSmo_ZADAA_MY_P95_10min_2587kWh_DNI_mltyear_20160817.txt	- MY in MET_IEC Data format 1.0 - site: ZADAA - P95 case DNI - multiple year uncertainty - measurements as described in 3.9 - time stamp in UTC	10min	from 2015-01-01 to 2005-12-31
guiSmo_ZADAA_MY_P95_15min_2587kWh_DNI_mltyear_20160817.txt		15min	
guiSmo_ZADAA_MY_P95_30min_2587kWh_DNI_mltyear_20160817.txt		30min	
guiSmo_ZADAA_MY_P95_60min_2587kWh_DNI_mltyear_20160817.txt		60min	
guiSmo_ZADAA_MY_P95_10min_2535kWh_DNI_sglyear_20160817.txt	- MY in MET_IEC Data format 1.0 - site: ZADAA - P95 case DNI - single year uncertainty - measurements as described in 3.9 - time stamp in UTC	10min	from 2015-01-01 to 2005-12-31
guiSmo_ZADAA_MY_P95_15min_2535kWh_DNI_sglyear_20160817.txt		15min	
guiSmo_ZADAA_MY_P95_30min_2535kWh_DNI_sglyear_20160817.txt		30min	
guiSmo_ZADAA_MY_P95_60min_2535kWh_DNI_sglyear_20160817.txt		60min	

Table 64: Listing and description of delivered data files, ZADAA

6. Conclusions

In the context of this study as a part of the 'guideline for standardized yields analysis of solar thermal power plants' (guiSmo) and the BMWi founded project CSP Bankability, the long-term averages of DNI with the associated uncertainties are provided for four considered demo sites. Typical Meteorological Year (TMY) data sets - representing the long-term average of DNI - and Meteorological Year (MYs) data sets - representing P75, P90 and P95 cases - in different time resolutions (10min, 15min, 30min, 60min) are created using on-site measurement data as well as site-specific satellite data obtained from DLR-SOLEMI. These data sets serve as input for the yield simulations performed for elaborating the guideline for standardized yields analysis of solar thermal power plants.

The quality of obtained satellite-derived data is found to be very high. The ground-based measurements are taken with good instrumentations, which are well maintained. The length of the measurement period is for all four sites more than 4 years (more than 15 years for DZTAM), which is very good situation for the qualification of a CSP project. This allows a really good adjustment of satellite-derived solar radiation time-series.

For the demo site 1, ESPSA, the long-term average for DNI amounts to 252 W/m^2, which is equivalent to 2212 kWh/m^2 per year or 6.06 kWh/m^2 per day. For the demo site 2, DZTAM, the long-term average for DNI amounts to 273 W/m^2, which is equivalent to 2393 kWh/m^2 per year or 6.55 kWh/m^2 per day. For the demo site 3, SASOV, the long-term average for DNI amounts to 260 W/m^2, which is equivalent to 2275 kWh/m^2 per year or 6.23 kWh/m^2 per day. For the demo site 4, ZADAA, the long-term average for DNI amounts to 310 W/m^2, which is equivalent to 2716 kWh/m^2 per year or 7.43 kWh/m^2 per day.

For ESPSA the total uncertainty of the long-term value of DNI is found to be 2.7% for multiple years and 5.6% for single year. For DZTAM the total uncertainty of the long-term value of DNI is found to be 2.5% for multiple years and 5.2% for single year. For SASOV the total uncertainty of the long-term value of DNI is found to be 3.0% for multiple years and 5.5% for single year. For ZADAA the total uncertainty of the long-term value of DNI is found to be 2.9% for multiple years and 4.1% for single year.

For risk assessment of CSP projects, Meteorological Years representing P75, P90 and P95 values of DNI are derived based on the P50 value and the associated uncertainty related to multiple and single year uncertainty. For the demo site 1, ESPSA, it is found that the P90 values of DNI at this site considering uncertainty associated with inter-annual variability related to single-year and multiple-years differ by 3.8%. The multiple years P90 value of DNI at this site is estimated to be 3.5% below the long-term best estimate (P50). This leads to a long-term average P90 value of DNI, based on multiple years uncertainty of 244 W/m^2 or 2135 kWh/m^2 per year or 5.84 kWh/m^2 per day. The single year P90 value of DNI at this site is estimated to be 7.1% below the long-term best estimate (P50). This leads to a long-term average P90 value of DNI, based on single year uncertainty of 234 W/m^2 or 2054 kWh/m^2 per year or 5.62 kWh/m^2 per day. For the demo site 2, DZTAM, it is found that the P90 values of DNI at this site considering uncertainty associated with inter-annual variability related to single-year and multiple-years differ by 3.6%. The multiple years P90 value of DNI at this site is estimated to be 3.2% below the long-term best estimate (P50). This leads to a long-term average P90 value of DNI, based on multiple years uncertainty of 264 W/m^2 or 2318 kWh/m^2 per year or 6.35 kWh/m^2 per day. The single year P90 value of DNI at this site is estimated to be 6.6% below the long-term best estimate (P50). This leads to a long-term average P90 value of DNI, based on single year uncertainty of 255 W/m^2 or 2235 kWh/m^2 per year or 6.12 kWh/m^2 per day. For the demo site 3, SASOV, it is found that the P90 values of DNI at this site considering uncertainty associated with inter-annual variability related to single-year and multiple-years differ by 3.3%. The multiple years P90 value of DNI at this site is estimated to be 3.9% below the long-term best estimate (P50). This leads to a long-term average P90 value of DNI, based on multiple years uncertainty of 249 W/m^2 or 2187 kWh/m^2 per year or 5.99 kWh/m^2 per day. The single year P90 value of DNI at this site is estimated to be 7.1% below the long-term best estimate (P50). This leads to a long-term average P90 value of DNI, based on single year uncertainty of 241 W/m^2 or 2114 kWh/m^2 per year or 5.79 kWh/m^2 per day. For the demo site 4, ZADAA, it is found that the P90 values of DNI at this site considering uncertainty associated with inter-annual variability related to single-year and multiple-years differ by 1.6%. The multiple years P90 value of DNI at this site is estimated to be 3.7% below the long-term best estimate (P50). This leads to a long-term average P90 value of DNI, based on multiple years uncertainty of 298 W/m^2 or 2614 kWh/m^2 per year or 7.16 kWh/m^2 per day. The single year P90 value of DNI at this site is estimated to be 5.2% below the long-term best estimate (P50). This leads to a long-term average P90 value of DNI, based on single year uncertainty of 294 W/m^2 or 2573 kWh/m^2 per year or 7.05 kWh/m^2 per day.

Site-specific auxiliary meteorological data like wind speed and direction, relative humidity, pressure, etc. are obtained from the on-site measurements or from MERRA-2 and included in the TMY, MY75, MY90 and MY95.

7. References

Al-Abbadi, Naif (2016): Basic measurements of radiation at station Solar Village (1998-09 to 2002-12), reference list of 52 datasets. King Abdulaziz City for Science and Technology. doi:10.1594/PANGAEA.860279

Betcke, J. et al. (2006), Energy-Specific Solar Radiation Data from Meteosat Second Generation (MSG): The Heliosat-3 Project, HELIOSAT-3.

Bird, R. E., and R. L. Hulstrom. 1981. «Simplified Clear Sky Model for Direct and Diffuse Insolation on Horizontal Surfaces». SERI/TR-642-761.

Carsten Hoyer-Klick, Richard Meyer, y Stefan Wilbert. 2016. «MET_IEC Data format 1.0 - DRAFT». IEA SHC [TASK 46].

Esterhuyse, Danie (2008): Basic measurements of radiation at station De Aar (2000-06 to 2000-12 and 2001-07 to 2004-12), reference list of 48 datasets. South African Weather Service, Pretoria. doi:10.1594/PANGAEA.860278

IEC TC117. 2016. «IEC/TS 62862-1-2 Draft Ed. 1.0 Solar Thermal Electric Plants - Part 1-2: Creation of Annual Solar Radiation Data Set for Solar Thermal Electric Plant Simulation». International Electrotechnical Commission (IEC).

Long, Chuck N., y E.G. Dutton. 2002. «BSRN Global Network recommended QC tests V2.0». Baseline Surface Radiation Network (BSRN).

Long, Chuck N., y Y Shi. 2008. «An Automated Quality Assessment and Control Algorithm for Surface Radiation Measurements». *The Open Atmospheric Science Journal* 2: 23-27.

Meyer, Richard, Hans Georg Beyer, J Fanslau, Norbert Geuder, Annette Hammer, Tobias Hirsch, Carsten Hoyer-Click, N. Schmidt, y Marko Schwandt. 2009. «Towards standardization of CSP yield assessments». En *Proceedings of SolarPACES 2009*, 8. Berlin, Germany. http://solarpaces2009.org.

Meyer, Richard, Jesús Torres Butron, Gunnar Marquardt, Marko Schwandt, Norbert Geuder, Carsten Hoyer-Klick, Elke Lorenz, y Annette Hammer. 2008. «Combining solar irradiance measurements and various satellite-derived products to a site specific best estimate». En *Proceedings of SolarPACES 2008*. Las Vegas, USA.

Mimouni, Mohamed (2016): Basic measurements of radiation at station Tamanrasset (2001-01 to 2015-06), reference list of 174 datasets. National Meteorological Office of Algeria. doi:10.1594/PANGAEA.859963

Mieslinger, Theresa, Felix Ament, Kaushal Chhatbar, y Richard Meyer. 2014. «A new method for fusion of measured and model-derived solar radiation time-series». *Energy Procedia* 48: 1617-26. doi:http://dx.doi.org/10.1016/j.egypro.2014.02.182.

NREL. 1993. «Quality Assessment with SERI_QC».

Philippe Blanc, Lucien Wald. 2012. «The SG2 algorithm for a fast and accurate computation of the position of the Sun for multi-decadal time period». *Solar Energy*, n.º 86: 3072-83.

Schillings, C., H. Mannstein, and R. Meyer (2004a), Operational method for deriving high resolution direct normal irradiance from satellite data, Solar Energy, 76(4), 475–484.

Schillings, C., R. Meyer, and H. Mannstein (2004b), Validation of a method for deriving high resolution solar direct irradiation from satellites and application for the Saudi Arabian peninsula., Solar Energy, 76(4), 485–497.